The cell division protein FtsL of *Bacillus subtilis* and its proteolysis

Inaugural-Dissertation
zur
Erlangung des Doktorgrades
der mathematisch-naturwissenschaftlichen Fakultät
der Universität Köln

vorgelegt von
Inga Wadenpohl
aus Leverkusen

Köln, August 2010

Berichterstatter:	Prof. Dr. Reinhard Krämer Prof. Dr. Ulrich Baumann
Tag der mündlichen Prüfung:	12. Oktober 2010

Index

I **Abstract** IV

II **Zusammenfassung** V

III **Abbreviations** VI

1 Introduction

1.1 **Cell division in *Bacillus subtilis*** 1

1.2 **The division protein FtsL** 2

1.2.1 Localisation and stability depending on other cell division proteins 3

1.2.2 FtsL proteolysis by RasP 6

1.3 **Intra-membrane proteolysis** 7

1.3.1 Intra-membrane proteases 7

1.3.2 The S2P family 8

1.3.3 Substrate recognition by Rhomboid proteases 9

1.3.4 The protease RasP 10

1.4 **Aim of research** 11

2 Materials and Methods

2.1 **Oligonucleotides, plasmids and bacterial strains** 12

2.2 **Bacterial growth conditions** 21

2.2.1 Growth of *Bacillus subtilis* 21

2.2.2 Growth of *E. coli* 22

2.3 **Molecular biology** 23

2.3.1 Preparation of competent *E. coli* cells 23

2.3.2 Transformation of *E. coli* cells 24

2.3.3 Transformation of *Bacillus subtilis* cells 24

2.3.4 Preparation of genomic DNA 25

2.3.5 Amplification of DNA 26

2.3.6 Agarose gel electrophoresis 26

2.3.7 Plasmid construction 27
2.3.8 Slot-Lysis 28
2.3.9 Colony PCR 28

2.4 Protein biochemistry 29
2.4.1 Polyacrylamide gel electrophoresis (PAGE) 29
2.4.2 Preparation of protein samples for PAGE by precipitation 30
2.4.3 Staining of polyacrylamide gels 30
2.4.4 Immuno-blotting 32
2.4.5 Determination of protein concentrations 33
2.4.6 Purification of FtsL 34
2.4.7 Purification of MBP-FtsL 35
2.4.8 Purification of RasP 37
2.4.9 Purification of RsiW* 39
2.4.10 Preparation of liposomes 40
2.4.11 Reconstitution of membrane proteins into liposomes 41
2.4.12 MBP-FtsL proteolysis assay in liposomes 42

2.5 Fluorescence microscopy of *Bacillus subtilis* 42
2.5.1 General microscopy techniques 42

2.6 Other methods 43
2.6.1 Co-expression experiments in *E. coli* BL21 43
2.6.2 Bacterial Adenylate Cyclase Two-Hybrid Assay 43

3 Results

3.1 The putative N-terminal cleavage product of FtsL 45
3.1.1 Overexpression and of the putative cleavage product 45
3.1.2 Localisation and stability of the putative cleavage product 48

3.2 In vitro proteolysis of FtsL by RasP 50
3.2.1 Purification of FtsL 50
3.2.2 Purification of MBP-FtsL/MBP-FtsL$^{\Delta C}$ 56
3.2.3 Purification of RasP 57
3.2.4 In vitro proteolysis assays 58
3.2.5 Proteolysis assay with RsiW* 66

3.3 Heterologous co-expression of RasP, FtsL and FtsL interaction partners 67
3.3.1 Co-expression of FtsL, DivIC and DivIB 68
3.3.2 Co-expression of FtsL, DivIC and RasP 71
3.3.3 Influence of the putative recognition motif on FtsL proteolysis 72
3.3.4 Influence of the N-terminal domains of FtsL and DivIC on the protein-protein interactions 74
3.3.5 Co-expression of FtsL, DivIC$^{\Delta N}$ and RasP 77

4 Discussion

4.1 FtsL provides a scaffold for cytokinesis 79
4.2 A possible function of FtsL oligomerisation during complex assembly 82
4.3 The role of FtsL protolysis by RasP during cell division 83
4.3.1 The intramembrane protease RasP is inactive in vitro 84
4.3.2 Substrate recognition is essential for FtsL cleavage by RasP 86
4.3.3 RasP is involved in preventing divisome re-assembly 86
4.3.4 RasP seems to degrade FtsL without prior site-1-cleavage 88
4.4 A new model for FtsL proteolysis by RasP 90

5 References 91

6 Acknowledgements 97

7 Addendum 99

8 Affirmation 103

9 Curriculum vitae 104

I Abstract

Cell division in *Bacillus subtilis* is a highly regulated process. Division takes place precisely at midcell resulting in two equally sized daughter cells. It is important that the divisome is disassembled after division is completed and does not directly re-assemble. Otherwise a new cycle of division is initiated close to the new formed cell pole, resulting in non viable, DNA-less mini cells. This study analyses the role of the intramembrane protease RasP in preventing divisome re-assembly.

RasP degrades the late cell division protein FtsL in vivo. We tried to establish an in vitro assay to investigate this proteolysis. Both proteins were purified, but RasP seems to be partly unfolded after solubilisation. Therefore a heterolous co-expression system in *E. coli* was established instead.

It is shown here that the division protein DivIC can protect FtsL against RasP cleavage. This stabilisation is achieved by inhibiting substrate recognition. It could be shown that a recognition motif within the cytosolic N-terminal domain of FtsL is essential for degradation by RasP. FtsL and DivIC tightly interact with each other. Direct interaction of the N-terminal domains blocks accessibility of the FtsL substrate recognition motif. Hence, as long as FtsL is incorporated in the divisome, RasP cleavage is impaired. After the division complex disassembles RasP is able to degrade FtsL. This cleavage removes FtsL from the membrane. Using fluorescence microscopy it was shown that the cytosolic cleavage product is then rapidly degraded by general proteolysis.

A complex network of the late division proteins FtsL, DivIC and DivIB most likely provides a scaffold for cytokinesis. Since these proteins are strongly interdependent on each other for correct assembly, complete degradation of FtsL should efficiently prevent re-assembly of the divisome close to the new cell pole.

II Zusammenfassung

Zellteilung in *Bacillus subtilis* ist ein exakt regulierter Prozess. Die Teilung erfolgt präzise in der Zellmitte, so dass zwei gleich große Tochterzellen gebildet werden. Es ist wichtig, dass der Zellteilungapparat anschließend vollständig disassembliert und sich nicht direkt wieder zusammenlagert. Andernfalls wird eine erneute Zellteilung nahe des neu gebildeten Zellpols eingeleitet, die zu nicht lebensfähigen, DNS-freien Minizellen führt. In dieser Arbeit wurde untersucht, welche Rolle die Intramembran-Protease RasP bei der Verhinderung einer solchen Re-Assemblierung spielt.

In vivo kann RasP das Zellteilungsprotein FtsL abbauen. Zur näheren Untersuchung dieser Proteolyse sollte ein in vitro Assay etabliert werden. Beide Proteine konnten gereinigt werden, jedoch scheint RasP nach der Solubilisierung teilweise entfaltet vorzuliegen. Daher wurde stattdessen ein heterologes Co-Expressionssystem in *E. coli* etabliert.

Es wurde gezeigt, dass das Zellteilungsprotein DivIC FtsL vor diesem Abbau durch RasP schützen kann. Diese geschieht, indem die Substraterkennung durch die Protease verhindert wird. Es konnte gezeigt werden, dass ein Substraterkennungsmotif in der cytosolischen, N-terminalen Domäne von FtsL für die Proteolyse essentiell ist. FtsL und DivIC interagiren stark miteinander. Dabei führt direkte Interaktion der N-terminalen Domänen dazu, dass das Substraterkennungsmotif nicht zugänglich ist. Daher kann RasP FtsL nicht abbauen, solange das Protein noch in den Zellteilungsapparat eingebunden ist. Erst nachdem der Komplex nach der Zellteilung zerfällt, kann FtsL von RasP hydrolisiert werden. Dadurch wird FtsL aus der Membran entfernt. Mittels Fluoreszenzmikroskopie wurde gezeigt, dass das cytosolische Fragment danach sehr schnell durch generelle Proteolyse abgebaut wird.

Ein komplexes Netzwerk der Zellteilungsproteine FtsL, DivIC und DivIB bildet ein strukturelles Gerüst für die Cytokinese. Da die Komplexbildung dieser Proteine stark voneinander abhängig ist, sollte der vollständige Abbau von FtsL eine Re-Assemblierung des Zellteilungsapparates und die Bildung von Minizellen verhindern.

III Abbreviations

AAA-proteins	ATPases associated with a various cellular activities
ABC transporter	ATP-binding cassette transporters
APS	Ammoniumperoxodisulfate
ATP	Adenosine-5'-triphosphate
BACTH	Bacterial Adenylate Cyclase Two-Hybrid Assay
BCA	Bicinchoninic acid (assay)
BCIP	5-Bromo-4-chloro-3-indolyl phosphate
BSA	Bovine serum albumin
CAA	Casamino acids
DAPI	4'-6-diamidino-2-phenylindole
DDM	n-Dodecyl-β-D-maltoside
DMSO	Dimethyl sulfoxide
DNA	Deoxyribonucleic acid
dNTPs	Deoxyribonucleotides
DTT	Dithiothreitol
E. coli	*Escherichia coli*
EDTA	Ethylenediaminetetraacetic acid
GFP	Green fluorescent protein
GTP	Guanosine-5'-triphosphate
IPTG	Isopropyl β-D-1-thiogalactopyranoside
kb	Kilo base pairs
kDa	Kilo Dalton
LAPAO	Laurylamidodimethylpropylaminoxide
LB	Luria Bertani-Medium
MBP	Maltose binding protein
MCS	Multiple cloning site
MES	2-(N-morpholino)-ethanesulfonic acid
NBT	Nitro blue tetrazolium chloride
NEB	New England Biolabs
OD_{600}	Optical density at 600nm
PAGE	Polyacrylamide gel electrophoresis
PCR	Polymerase chain reaction
PVDF	Polyvinylidene fluoride
RT	Room temperature
TAE	Tris-Acetat/EDTA-Buffer
S1P	Site-1-protease
S2P	Site-2-protease
SDS	Sodium dodecylsulfate
SREBPs	Sterol regulatory element binding proteins
TCA	Trichloroacetic acid
TEMED	*N*,*N*,*N'*,*N'*-Tetramethylethan-1,2-diamin
TEV protease	Protease found in tobacco etch virus
Tris	Tris-(hydroxymethyl)-aminomethane
w/v	weight per volume
w/w	weight per weight
X-Gal	5-Bromo-4-chloro-3-indolyl-β-D-galactopyranoside

1 Introduction

1.1 Cell division in *Bacillus subtilis*

Bacillus subtilis is a Gram-positive soil bacterium. It is often used as a model organism as it is naturally competent and its genome has been completely sequenced. Under normal growth conditions *Bacillus subtilis* cells grow along their axis. Reproduction is achieved by dividing a parental cell into two equally sized daughter cells both containing a copy of the bacterial chromosome. This mechanism requires a multi-protein machinery, termed the divisome, and is tightly regulated. The first step of divisome assembly is the localisation of FtsZ to the new division site at mid cell [Bi and Lutkenhaus, 1991], [Beall and Lutkenhaus, 1991]. FtsZ is a GTPase and a bacterial tubulin homologue. It polymerises into a ring like structure, the so called Z-ring. Other cytosolic proteins are recruited to this ring, including the actin homologue FtsA, ZapA and SepF [Bork et al., 1992; Din et al., 1998], [Gueiros-Filho and Losick, 2002], [Hamoen et al., 2006]. All of them can promote and stabilise the Z-ring assembly. For efficient cell division the cytosolic part of the divisome has to be tethered to the membrane. The membrane integrated protein EzrA has been suggested as an anchor, because of its large cytosolic domain interacting with FtsZ [Levin et al., 1999]. However, EzrA is a negative regulator of FtsZ polymerisation and is also localized throughout the whole cytoplasmatic membrane [Kawai and Ogaswara, 2006], [Levin et al., 1999]. It has been suggested, that instead FtsA might tether the ring to the membrane by a C-terminal amphipatic helix [Pichoff and Lutkenhaus, 2005].

The divisome is then completed by several membrane spanning proteins. Among these is the protein MinJ, which is part of the Min system [Bramkamp et al., 2008], [Patrick and Kearns, 2008]. The Min system is involved in division site selection and seems to play in role in divisome assembly and disassembly as well [van Baarle and Bramkamp, 2010]. In the later stages of assembly the proteins DivIB, DivIC, FtsL, FtsW and the penicillin binding protein Pbp2B localise to the division site. In *E. coli* these so called late division proteins are recruited in a linear dependence pathway [Goehring et al., 2006]. However, in *Bacillus subtilis* the proteins seem to be interdependent for correct localization at the division site [Errington and Daniel, 2001], [Daniel et al., 2006] or at least for correct and stable assembly [Foster and Popham, 2001]. The function of many membrane spanning division proteins is unknown. However, for Pbp2B a clear biochemical function has been shown. It is involved in synthesising peptidoglycan for the new cell wall by catalysing the transpeptidation, [Nguyen-

Distèche, 1998]. For FtsW a function has been suggested that is linked to Pbp2B. Studies of the *E. coli* FtsW show that it targets the transpeptidase FtsI to the division site [Mercer and Weiss, 2002]. FtsI is the *E. coli* homologue to Pbp2B. Also it was suggested, that FtsW could translocate lipid-linked precursors for peptidoglycan synthesis and delivery to peptidoglycan synthesis machinery [Lara et al., 2005]. In contrast FstL, DivIB and DivIC seem to play more of a structural and/or regulatory role. A schematic overview of divisome assembly is shown in Fig. 1.1. When the assembly is completed the Z-ring starts constricting and synchronously a new cross-wall is synthesised. Division results in a pair of sister cells that are joined by this layer of cell wall material. They are later separated through cell wall autolysis [Blackman et al., 1998].

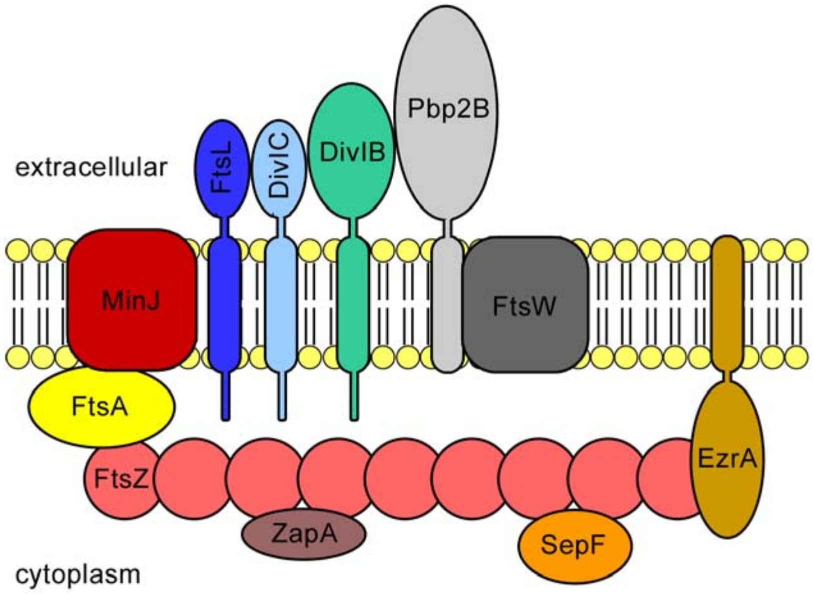

Figure 1.1: Schematic view of divisome assembly in *Bacillus subtilis*. The tubulin homologue FtsZ polymerises into the so called FtsZ ring, which is stabilised by cytosolic factors. The actin homologue FtsA most likely tethers the FtsZ ring to the membrane. In the late stages of assembly the membrane spanning proteins FtsL, DivIC, DivIB and Pbp2B are recruited interdependently.

1.2 The division protein FtsL

FtsL of *Bacillus subtilis* is a small membrane integral protein, belonging to the late division proteins. It consists of 117 amino acids and has a molecular mass of 12.9 kDa. FtsL has a cytoplasmatic domain, one transmembrane domain and an extracellular predicted leucine zipper domain. FtsL transcription is cell cycle dependent, it is controlled by DnaA [Goranov et al., 2005]. The protein is essential for cell division, a *ftsL* knock out is lethal. A conditional mutant can be constructed with the only copy of *ftsL* under the control of a xylose inducible promoter. When these cells are brought into a medium without xylose they continue growing, but fail to divide, resulting in abnormally long cells [Daniel et al., 1998]. Overexpression of FtsL in *Bacillus subtilis* leads to shorter cell length compared to a wild type control. Apparently the cells are able to divide more often when the FtsL concentration is increased, resulting in shorter length. FtsL seems to be a rate limiting factor for division.

1.2.1 Localisation and stability depending on other cell division proteins

The late cell division proteins seem to be all interdependent in their recruitment to the division site (see chapter 1.1). DivIC and DivIB have been suggested as primary interaction partners of FtsL. The predicted DivIC structure shows strong similarity to FtsL and the protein is essential for cell division as well [Daniel et al., 2006]. The predicted structure of DivIB shows a similiar N-terminal cytosolic domain and a transmembrane domain, but its extracellular domain is considerably bigger than the ones of FtsL and DivIC. The protein is not essential, though DivIB deficient cells are temperature sensitive [Rowland et al., 1997].

FtsL is intrinsically unstable. When transcription in the conditional mutant is shut down, the protein rapidly disappears. How FtsL stability is influenced by other cell division proteins has been previously studied by measuring protein levels in vivo [Daniel et al., 2006]. FtsL is dependent on DivIC in its stability and vice versa. DivIB overexpression has no effect on FtsL levels at 37°C. However, at higher temperatures a DivIB null mutant shows a division phenotype, which can be overcome by overexpression of FtsL. This suggests that DivIB might play a role in stabilising FtsL at high temperatures. Interestingly in the absence of FtsL, DivIC is destabilised by DivIB overexpression. Apparently DivIB is somehow involved in DivIC turnover when FtsL is absent.

Direct protein-protein interactions of FtsL, DivIC and DivIB have previously been discussed controversially [Sievers and Errington, 2000], [Robson et al., 2002], [Daniel et al., 2006]. Because of the strong interdependency of these proteins in vivo their direct interactions were mostly studied in heterologous systems. This enables analysis of only two possible interaction partners without other *Bacillus subtilis* division proteins present. Controls showed that none of the *Bacillus subtilis* proteins is interfering with the *E. coli* division proteins or is recruited to the division site by them [Robichon et al., 2008]. The broadest approach to investigate the interaction network of the late division proteins of *Bacillus subtilis* was done by utilising an *E. coli* based bacterial two-hybrid and a yeast three-hybrid system [Daniel et al., 2006]. In the bacterial two-hybrid system FtsL showed direct interactions with all other late cell division proteins and self-interaction. The most prominent interaction was the FtsL-DivIC interaction. DivIC itself only seems to interact with FtsL, while DivIB can interact with FtsL and Pbp2B. This would hint towards an indirect effect of DivIB on DivIC turnover in the absence of FtsL as mentioned above. Further experiments with the yeast three-hybrid system showed a ternary complex of FtsL, DivIC and DivIB. This led to a model supposing that FtsL and DivIC form stable heterodimers. DivIB can then interact with these dimers for further stabilisation.

Apart from in vivo stabilisation studies and bacterial two-hybrid assays the interactions of FtsL, DivIC, DivIB and Pbp2B have also been analysed in *E. coli* by a method called artificial septal targeting [Robichon et al., 2008]. One of the proteins was fused to ZapA from *E. coli* and by that targeted to midcell. The second protein was fused to GFP and its localisation was checked using fluorescence microscopy. It was determined which interactions of were strong enough to recruit the GFP fused protein to midcell. Only two pairs of protein-protein interactions resulted in recruitment of the GFP-fused “prey” protein. Those were FtsL-DivIC interaction and DivIB-Pbp2B interaction. This was in accordance to the previous bacterial two-hybrid assays which revealed these pairs to be the strongest interactions. Interestingly other interactions, that were observed in the bacterial two-hybrid studies and indicated by the in vivo data (such as FtsL-Pbp2B or FtsL-DivIB), were not sufficient to result in protein recruitment. However, these findings cannot explain the actual recruitment mechanisms in *Bacillus subtilis*. As mentioned above all of the four proteins are interdependent for localisation. Obviously the interaction network between them is more complex and not only regulated by each proteins primary interaction partners.

While this interdependency makes it relatively difficult to study the late division proteins of *Bacillus subtilis*, their homologues in *E. coli* have been analysed in a bit more detail. In *E. coli* the localisation of the membrane spanning cell division proteins follows more a sequential pattern. After localisation of the protein ZipA, which serves as a kind of linker between the cytosolic part of the divisome and the membrane part, the DNA translocase FtsK is recruited [Hale and Boer, 2002]. This is the *E. coli* homologue of the *Bacillus subtilis* protein SpoIIIE which is involved in DNA translocation during sporulation [Burton et al., 2007]. The protein FtsQ, the *E. coli* homologue of DivIB, is dependent on FtsK for its localisation [Chen and Beckwith , 2001]. It has been shown that a trimeric FtsQ/FtsL/FtsB complex can assemble in the absence of other cell division proteins [Buddelmeijer and Beckwith, 2004]. This led to the idea that such complexes pre-assemble and are then recruited to the division site by FtsB interaction with FtsQ. However this model cannot be applied to the situation in *Bacillus subtilis,* as there DivIB is not essential at normal growth conditions. For the *E. coli* proteins a lot of information has been gained, how different domains interact with each other and how those interactions influence recruitment of FtsL, FtsB and FtsQ themselves as well as other downstream division proteins. The N-terminal half of FtsB is necessary for interaction with FtsL and in complex with FtsL sufficient to recruit downstream proteins [Gonzales and Beckwith, 2009]. The C-terminal part of FtsB seems to be required for interaction with FtsQ [Gonzales and Beckwith, 2009]. In accordance to that the C-terminal part of FtsQ is important for interaction with FtsL and FtsB [Goehring et al., 2007], [van den Ent et al., 2008]. The direct interactions patterns for the FtsL domains were also analysed [Gonzales et al., 2010]. It seems the interaction of FtsQ and FtsL is not only mediated by FtsB. The C-terminal part of FtsL is necessary for interaction with FtsQ, but not for interaction with FtsB. The main function of the N-terminal part of FtsL appears to be the recruitment of downstream proteins.

In addition the extracellular domain of FtsL is not only important for interaction with FtsQ, but for self interaction of FtsL as well. In vitro *E. coli* FtsL can form SDS resistant dimers [Ghigo and Beckwith, 2000]. The reason for such stable folding is most likely the predicted coiled-coil conformation of the C-terminal domain. In accordance to that mutation of the leucine zipper like heptad repeat motif impairs FtsL dimerisation. The mutation also affects FtsL function and localisation. Probably the localisation defect is due to impaired interaction with FtsQ. Surprisingly, mutation of the heptad repeat motif had no effect on the function of FtsL in *Bacillus subtilis*.

It is very interesting that such a consistent interaction network of FtsL, FtsB and FtsQ could be shown for the *E. coli* proteins, but it is apparently not completely conserved in *Bacillus subtilis*. While some interactions seem to be similiar, the general influence of FtsL, DivIC and DivIB on each other and their localisation pattern differs in *Bacillus subtilis.*

1.2.2 FtsL proteolysis by RasP

FtsL has been shown to be a substrate of the intra-membrane protease RasP [Bramkamp et al., 2006]. In a RasP mutant strain FtsL is significantly stabilised and cells are shorter compared to a wild type control. This phenotype can be complemented by insertion of *yluC* (the gene encoding RasP) into the *amyE* locus under the control of a xylose inducible promoter. In an *E. coli* BL21 co-expression system RasP was able to degrade FtsL, while the active site mutant RasP-E21A did not hydrolise FtsL.

Another known substrate of RasP is the anti-sigma factor RsiW of *Bacillus subtilis* [Schöbel et al., 2004]. Sequence alignment of FtsL and RsiW shows conserved two conserved boxes. One putative substrate recognition motif in the N-terminal cytoplasmic domain (25-KKRAS-29) and one putative cleavage site within the transmembrane domain (39-VLFAAAV-45). When the N-terminus of FtsL is successively truncated by five amino acids from Δ10-FtsL to Δ30-FtsL protein stability is increasing, especially in the case of the 30 amino acid truncation [Bramkamp et al., 2006]. This truncation completely lacks the putative recognition motif. The same stabilising effect can be observed when altering the motif from 25-KKRAS-29 to 25-AVAVA-29 (FtsL-25A) or 25-KKAVA-29 (FtsL-25B). This shows that the cytoplasmic domain and the putative substrate recognition are indeed important for FtsL turnover.

RasP belongs to the site-2-protease family. These proteases usually cleave their substrates after an initial cut by a site-1-protease has been performed. However, for FtsL no such site-1-protease has been identified yet. The site-1-protease PrsW is involved in cleaving RsiW prior to RasP cleavage [Heinrich and Wiegert, 2006], [Ellermeier and Losick, 2006], but is not able to degrade FtsL [Wiegert, personal communication].

So far no cleavage products of FtsL have been identified. This might be due to the small size of the protein and unspecific degradation of the resulting peptides. In most cases an intra-membrane cleavage releases a biologically active protein or peptide into the cytosol. This is the case for RsiW, where the anti-sigma factor is released from the membrane by RasP cleavage and then further degraded to activate the sigma-factor σ^W. If the conserved motif within the transmembrane domain of FtsL is interpreted as the cleavage site, the predicted proteolysis product shows no resemblance to any known protein class. There are no obvious motifs or structures that point towards a function of this small 5 kDa peptide. Is seems possible, that the main function of FtsL proteolysis might not be the release of an effector into the cytosol, but to remove the protein from the membrane. This could either be a regulatory mechanism for temporal control of cell division or to prevent re-assembly after division is completed. It has been shown, that spontaneous re-assembly of a division close to a new cell pole [Gregory et al., 2008] or reduced disassembly [van Baarle and Bramkamp, 2010] can lead to mini cell formation in *Bacillus subtilis*,. Removing essential division proteins from the membrane could provide an effective mechanism to prevent re-assembly.

1.3 Intra-membrane proteolysis

1.3.1 Intra-membrane proteases

Proteases catalyse the hydrolysis of amide bonds that link amino acids into peptides and proteins. There are four general types of proteases known so far. Serine/threonine proteases, cysteine proteases, aspartyl proteases and metalloproteases. Hundreds of examples from all kind of organisms have been identified for each class. Most of them are soluble proteins, which are either freely distributed within an aqueous environment or the soluble part of the protease is linked to a membrane via an anchor. Intra-membrane proteases or intra-membrane cleaving proteases (I-CLiPs) are membrane spanning proteases that are able to hydrolise their transmembrane substrates within the hydrophobic environment of a lipid bilayer [Wolfe et al., 1999]. The substrates are unusual, too. They are typically folded into an α-helix. In this conformation the backbone amide bonds are not accessible for a nucleophilic attack, because the amino side chains will provide a steric block. This means that intra-membrane proteases must be able to create a hydrophilic micro environment as well as partly bend or unfold their substrates. It is therefore not very surprising, that a lot of substrates contain helix-breaking residues near the cleavage site. Three types of intra-membrane proteases have been identified so far. The S2P family, the Rhomboid family and the intra-membrane proteases Presenilin and SPP, which all can be sorted into the general protease classes known from soluble proteases. The S2P proteases are metalloproteases [Rawson et al., 1997], Rhomboid proteins are serine proteases [Urban et al., 2001] Presenilin and SPP belong to the aspartyl proteases [Wolfe et al., 1999], [Weihofen et al., 2002]. Apparently these enzymes are able to create a special environment and prepare their substrates for cleavage, but the hydrolysis of the amide bond itself follows the principles well known from soluble proteases.

1.3.2 The S2P family

The first discovery of an intra-membrane protease was linked to regulation of sterol and fatty acid metabolism [Brown and Goldstein, 1997]. Sterol regulatory element binding proteins (SREBPs) are proteins with two transmembrane domains and a cytosolic transcription factor domain. At reduced cholesterol levels SREBP is transported to the Golgi apparatus [Nohturfft et al., 1999]. There it is cleaved in two steps to release the transcription factor, which will be translocated to the nucleus. First the luminal loop between the two transmembrane domains of SREBP is cleaved by the membrane-tethered Site-1-protease (S1P) [Sakai et al., 1998]. The second step is the hydrolysis of a bond predicted to lie three residues within the transmembrane helix. This degradation step is carried out by the Site-2-protease (S2P) [Duncan et al., 1998]. Most intra-membrane proteases are part of proteolytic cascades like this and require initial cleavage of their substrates by other proteases.

Complementation studies have revealed that S2P contains a conserved HEXXH motif, characteristic for zinc metalloproteases [Rawson et al., 1997]. In agreement with data from soluble zinc metalloproteases both histidines and the glutamate are essential for proteolytic activity of S2P. The two histidines most likely coordinate the zinc, while the glutamate interacts with a water molecule. About 300 residues from the HEXXH motif another essential amino acid was identified. It is a conserved aspartate that in involved in the zinc coordination [Zelenski et al., 1999], [Feng et al., 2007].

Several members of the S2P family are known in different organisms. Among them are S2P in *Methanocaldococcus jannaschii*, SpoIVFB and RasP in *Bacillus subtilis* as well as the *E. coli*. RasP homologue RseP (YaeL). SpoIVFB is involved in sporulation, processing the membrane bound transcription factor σ^k [Campo and Rudner, 2006]. After engulfment of the forespore σ^k is cleaved and released into the mother cell. Interestingly SREBP and σ^k have an opposite membrane orientation, which correlates with the opposite orientation of the proteases S2P and SpoIVFB [Rudner et al., 1999]. This suggests that the catalytic region must align with the substrate in a matching directionality. Some insights into the mechanism of S2P family proteases come from structural data. S2P from *Methanocaldococcus jannaschii* has been crystalised and a 3.3 Å resolution structure was solved [Feng et al., 2007]. It contains six transmembrane domains TM1-6 with TM2-4 building the core structure. The zinc atom is located about 14 Å within the lipid bilayer. It is coordinated by the two Histidines of the HEXXH motif in TM2 and the conserved aspartate in TM3. The protein was present in two different conformations. The conformations of the core domains are identical, but TM1 and TM6 are 10-12 Å farer apart in one conformation. Only in this conformation the active site would be accessible, suggesting that this is an open state of the protease. In the closed state a hydrophilic channel is formed which opens into the cytoplasm. Water molecules could access the zinc through this channel. The sequence of the core domains is relatively similar in all S2P proteases, suggesting that its structure might be similar as well and the active site position would be conserved. However, different members of the family cleave their respective substrates at different positions of the transmembrane helices. If the active site position is conserved, this means that the protease must be able to recognise a certain motif of the substrate for appropriate positioning of the cleavage site. Upon changing from closed to open position a number of buried amino acids become exposed, that might be involved in substrate recognition. So far relatively little is known about specific substrate recognition by S2P proteases. However, recently substrate recognition by Rhomboid proteases has been investigated and the results support the idea of choosing the cleavage side by substrate recognition (see chapter 1.3.3).

1.3.3 Substrate recognition by Rhomboid proteases

The name giving member of the Rhomboid family is Rhomboid-1 found in *Drosophila*. Rhomboid-1 is the protease required for cleavage of the protein Spitz [Lee et al., 2001]. Spitz is the Drosophila ortholog of the epidermal growth factor (EGF). Full-length Spitz is located in the ER until Star ushers it to the Golgi apparatus. There it is cleaved by Rhomboid-1 and the product is secreted for intercellular communication. Rhomboid-1 requires three conserved residues for proteolytic activity, a serine, a histidine and an asparagine [Urban et al., 2001] which form a catalytic triad as known from soluble serine proteases. Rhomboid-1 can cleave Spitz without prior processing by other proteases. This is an exception among the intra-membrane proteases. Apparently regulation is achieved mainly by the Star-mediated translocation of Spitz. The yeast Rhomboid RBD1 cleaves two mitochondrial membrane proteins [Esser et al., 2002], [Herlan et al., 2003]. The human ortholog of RBD1 is PARL and it could restore proteolysis, growth rates and mitochondrial morphology in a RBD1 mutant [McQuibban et al., 2003]. Obviously the role of these Rhomboids in mitochondrial function has been evolutionary conserved. Rhomboids are also present in Bacteria and surprisingly bacterial Rhomboids are capable of cleaving *Drosophila* Rhomboid substrates [Urban et al., 2002]. Obviously not only specific functions but also substrate recognition by Rhomboids is widely conserved. This led to an intensive search for specific recognition motifs. In the case of Spitz most of the transmembrane domain could be swapped with that of a non-substrate protein without affecting cleavage. Only the N-terminal quarter of this domain turned out to be sufficient for recognition [Urban and Freeman, 2003]. Inserting this motif into the Notch ligand Delta converted it into a Rhomboid-1 substrate. As two critical residues a gylcine and an alanine were identified. Apparently Rhomboid-1 requires helix-destabilising residues for substrate cleavage like S2P and SPP. However, recently it has been discovered that while Rhomboids do require helix-destabilisation they primary recognise their substrates by a specific sequence near the cleavage site [Strisovsky et al., 2009]. This sequence specificity seems to be widely conserved among Rhomboids. The recognition motif is found among many different Rhomboid substrates. Further studies with a model substrate showed that not only its natural protease, but also several bacterial Rhomboids react sensitive to mutation of the recognition motif. Moreover the position of this recognition motif determined the site of cleavage.

1.3.4 The protease RasP

RasP is an intra-membrane protease from *Bacillus subtilis*. It belongs to the S2P family. RasP contains the conserved HEXXH motif and a mutation of the glutamate to alanine abolishes activity [Bramkamp et al., 2006]. The predicted structure of RasP shows four transmembrane domains and a PDZ domain. Both termini are facing the outside of the cell.

So far two substrates of RasP have been identified. As mentioned before it cleaves the anti-sigma factor RsiW [Schöbel et al., 2006] and the cell division protein FtsL [Bramkamp et al., 2006]. While its role in cell division is unclear, its involvement in RsiW processing has been investigated in more detail. RsiW is a membrane integrated anti-sigma factor. The corresponding sigma factor σ^W belongs to the ECF sigma factors. ECF sigma factors regulate genes linked to extracytoplasmic functions [Lonetto et al., 1994]. In *Bacillus subtilis* σ^W is needed for a cellular response to alkaline shock. The first step in RsiW degradation is cleavage by the site-1-protease PrsW [Heinrich and Wiegert, 2006]. RasP can afterwards cleave within the transmembrane domain and release a part of the anti-sigma factor into the cytosol. This fragment needs to be further degraded by ClpXP to release σ^W [Zellmeier et al., 2006]. ClpX is an AAA-protein that interacts with the peptidase ClpP to form ClpXP. This process represents a typical proteolytic cascade as known from other S2P proteases. Interestingly though, recent studies revealed that RsiW seems not to be degraded in a simple two-step fashion by PrsW and RasP. PrsW cleaves RsiW site specific, but it has been shown that other peptidases must be involved in further degradation before RasP cleavage occurs [Heinrich et al., 2009].

This is in contrast to the findings for the *E. coli* RasP homologue RseP. RseP cleaves the anti-sigma factor RseA [Kanehara et al., 2002]. Site-1-proteolysis of RseA is carried out by the protease DegS [Alba et al., 2002]. After DegS degradation the newly exposed C-terminal residue is a valine. If this position is mutated, RseP cleavage is impaired [Li et al., 2009]. Structural analysis of RseP showed that most likely its second PDZ domain binds this single hydrophobic acid. Site-specific cleavage of RseA by DegS therefore is sufficient to trigger further degradation by RseP.

1.4 Aim of research

The aim of research was to investigate a possible role of RasP in regulating cell division and to gain more insight about the mechanism of FtsL cleavage.

So far, regulation of cell division in *Bacillus subtilis* has mainly been analysed under the aspect of spatial control. The fact that the rate limiting factor FtsL is degraded by the intramembrane protease RasP lend support to the notion that proteolysis might be part of temporal control of cell division. The complex interaction network of the late division proteins suggests that degradation of FtsL might lead to divisome disassembly and termination of cytokinesis. However, this would only be possible if the protease is able to cleave FtsL within the assembled divisome. Therefore, an important goal of this study was to test if FtsL is degraded by RasP in the presence of its divisomal interaction partners DivIC and/or DivIB.

To investigate FtsL proteolysis by RasP on a mechanistic level we wanted to establish an in vitro assay. This would provide a tool to determine the FtsL cleavage site and study the influence of the putative substrate recognition motif. A functional in vitro assay could also be used to study site-1-cleavage of FtsL. Possible candidates for site-1-proteases could be purified and tested for their ability to directly cleave FtsL.

2 Materials and Methods

2.1 Oligonucleotides, plasmids and bacterial strains

Table 2.1: Oligonucleotides

Primer name	**Sequence (5’-3’)**
ftsl-1-43-for	CGCTCTAGACGCAAAATTAAAAGGAGG
ftsl-1-43-rev	GCTCGGCCGTCATTACGCAGCAAAGAGGAC
ftsl-1-43dd-rev	GCTCGGCCGTCATTAGTCGTCAAAGAGGACAAGAAG
gfpftsl-1-43-for	CCCCTCGAGATGAGCAATTTAGCTTACC
gfpftsl-1-43-rev	GCTGAATTCTCATTACGCAGCAAAGAGGAC
gfpftsl-1-43dd-rev	GCTGAATTCTCATTAGTCGTCAAAGAGGACAAGAAG
ftsl-61-117-for	GGGGGGCATATGCAAACCAATATTGAGGTG
ftsl-61-117-rev	CCCGGATCCTTCCTGTATGTTTTTCAC
ybbm-1-107-for	GGGCTCGAGATGAGCTGTCCTGAACAA
ybbm-1-107-rev	GAGGGATCCGCTGTTAAAAAAACCCCCGCCCATC
ylucduet-for	GATCATATGTTCGTGAATAC
ylucduet-rev	CATGGTACCCAAAAACAGCC
ylucE21Aduet-for	TTTCGGAACGCTCGTTTTCTTCCAT**GCA**CTGGGCCATTTATTGC

ftslduet-for	CATGGATCCATGAGCAATTTAGC
ftslduet-rev	CATGCGGCCGCTTCCTGTATGTTTTTCAC
ΔN-ftslduet-for	CGGGAATTCGACTCTCGGAGAAAAAGTG
ΔC-ftslduet-rev	CGGAAGCTTTCAATTGGTTTGATATGCCGC
divICduet-for	GGGGGGCATATGTTGAATTTTTCCAGGGAACG
divICduet-rev	CCCCTCGAGCTTGCTCTTCTTCTCCAC
ΔN-divICduet-for	GGGGGGCATATGCGCAAAGGGCTGTACAGA
divIBduet-for	CGGGAATTCGATGAACCCGGGTCAAGAC
divIBduet-rev	CGGAAGCTTTCAATTTTCATCTTCCTTTTTAGC
ftslB2H-for	GGGTCTAGAGATGAGCAATTTAGCTTAC
ΔN-ftslB2H-for	GGGTCTAGAGACTCTCGGAGAAAAAGTG
ftslB2H-rev	GCGGGTACCCTATTCCTGTATGTTTTTCAC
divICB2H-for	GGGTCTAGAGTTGAATTTTTCCAGGGAACG
ΔN-divICB2H-for	GGGTCTAGAGCGCAAAGGGCTGTACAGA
divICB2H-rev	GCGGGTACCCTACTTGCTCTTCTTCTCCAC

Table 2.2: Plasmids

Plasmid	**Characteristic trait**	**Source**
pJPR1	*bla amyE3' cat* P_{xyl} *amyE5'*	Rawlings, Errington, unpublished
pWB20	*bla amyE3' cat* P_{xyl}*-ftsL1-43 amyE5'*	this study
pWB21	*bla amyE3' cat* P_{xyl}*-ftsL1-43dd amyE5'*	this study
pSG1729	*bla amyE3' cat* P_{xyl}*-gfpmut1 amyE5'*	Lewis and Marston, 1999
pWB22	*bla amyE3' cat* P_{xyl}*-gfpmut1-ftsL1-43 amyE5'*	this study
pWB22	*bla amyE3' cat* P_{xyl}*-gfpmut1-ftsL1-43dd amyE5'*	this study
pET16b	*bla* P_{T7lac}*-10his lacI*	Novagen
pWB23	*bla* P_{T7lac}*-10his-ftsL lacI*	Bramkamp, unpublished
pWB24	*bla* P_{T7lac}*-10his-ftsL61-117 lacI*	this study
pWB25	*bla* P_{T7lac}*-10his-ybbM1-107 lacI*	this study
pOPTM-FtsL	*bla* P_{T7lac}*-mbp-ftsL-10his lacI*	Löwe, unpublished
pOPTM-FtsLCT	*bla* P_{T7lac}*-mbp-ftsLCT-10his lacI*	Löwe, unpublished
pHis17-RasP	*bla* P_{T7lac}*-yluC-10his lacI*	Löwe, unpublished
pHis17-RasPE21A	*bla* P_{T7lac}*-yluCE21A-10his lacI*	Löwe, unpublished
pACYCDuet-1	*cat* P_{T7lac}- P_{T7} *lacI*	Novagen

pETDuet-1	*bla* P_{T7lac}- P_{T7} *lacI*	Novagen
pWB1	*cat* P_{T7lac}-*6his-ftsL lacI*	this study
pWB2	*cat* P_{T7lac}-*6his-ftsL* P_{T7}-*yluC-S lacI*	this study
pWB2	*cat* P_{T7lac}-*6his-ftsL* P_{T7}-*yluC-E21A-S lacI*	this study
pWB5	*cat* P_{T7lac}-*6his-ΔN-ftsL lacI*	this study
pWB6	*cat* P_{T7lac}-*6his-ΔN-ftsL* P_{T7}-*yluC-S lacI*	this study
pWB7	*cat* P_{T7lac}-*6his-ΔN-ftsL* P_{T7}-*yluC-E21A-S lacI*	this study
pWB26	*cat* P_{T7lac}-*6his-ΔC-ftsL lacI*	this study
pWB17	*cat* P_{T7lac}-*6his-ftsL25B lacI*	this study
pWB18	*cat* P_{T7lac}-*6his-ftsL25B* P_{T7}-*yluC-S lacI*	this study
pWB19	*cat* P_{T7lac}-*6his-ftsL25B* P_{T7}-*yluC-E21A-S lacI*	this study
pWB4	*bla* P_{T7}-*divIC-S lacI*	this study
pWB8	*bla* P_{T7}-*ΔN-divIC-S lacI*	this study
pWB27	*bla* P_{T7lac}-*6his-divIB lacI*	this study
pWB28	*bla* P_{T7lac}-*6his-divIB* P_{T7}-*divIC-S lacI*	this study
pUT18C	*bla* P_{lac}-*cya*$^{675-1197}$	Euromedex
pKT25	*aphA* P_{lac}-*cya*$^{1-675}$	Euromedex

pUT18C-zip	*bla* P_{lac}-*cya*$^{675-1197}$-*zip* (construct encoding leucine zipper from GCN4)	Euromedex
pKT25-zip	*aphA* P_{lac}-*cya*$^{1-675}$-*zip* (construct encoding leucine zipper from GCN4)	Euromedex
pWB9	*bla* P_{lac}-*cya*$^{675-1197}$-*ftsL*	this study
pWB10	*aphA* P_{lac}-*cya*$^{1-675}$-*ftsL*	this study
pWB11	*bla* P_{lac}-*cya*$^{675-1197}$-*divIC*	this study
pWB12	*aphA* P_{lac}-*cya*$^{1-675}$-*divIC*	this study
pWB13	*bla* P_{lac}-*cya*$^{675-1197}$-*ΔN-ftsL*	this study
pWB14	*aphA* P_{lac}-*cya*$^{1-675}$-*ΔN-ftsL*	this study
pWB15	*bla* P_{lac}-*cya*$^{675-1197}$-*ΔN-divIC*	this study
pWB16	*aphA* P_{lac}-*cya*$^{1-675}$-*ΔN-divIC*	this study

Table 2.3 Bacterial strains

Strain	**Relevant genotype/characteristic trait**	**Source**
Bacillus subtilis		
168	*trypC2*	
WB01	*trypC2, amyE::spec Pxyl-ftsL1-43*	this study
WB02	*trypC2, amyE::spec Pxyl-ftsL1-43dd*	this study
WB03	*trypC2, clpX::XXX*	this study
WB04	*trypC2, clpX::XXX, amyE::spec Pxyl-ftsL1-43*	this study
WB05	*trypC2, amyE::spec Pxyl-gfpmut1-ftsL1-43*	this study
WB06	*trypC2, amyE::spec Pxyl-gfpmut1-ftsL1-43dd*	this study
WB07	*trypC2, clpX::XXX, amyE::spec Pxyl-gfpmut1-ftsL1-43*	this study
E. coli		
DH5α	*supE*44, Δ*lac*U169(φ80*lacZ*ΔM15), *hsdR*17, *recA*1, *endA*1, *gyrA*96, *thi*-1, *relA*1	Invitrogen
BL21(DE3)	F^- *ompT* [*lon*] $hsdS_B$ ($r_B^-m_B^-$) λ(DE3) *pol*(T7)	Novagen
BL21(DE3)/pWB23	FtsL$^+$	this study
BL21(DE3)/pWB24	FtsL61-117$^+$	this study
BL21(DE3)/pWB25	YbbM1-107$^+$	this study

BL21(DE3)/pOPTM-FtsL	MBP- FtsL^{+}	this study
BL21(DE3)/ pOPTM-FtsLCT	MBP- FtsL$^{\Delta C+}$	this study
BL21(DE3)/pHis17-RasP	RasP^{+}	this study
BL21(DE3) /pHis17-RasPE21A	RasP-E21A^{+}	this study
BL21(DE3)/pWB1/ pETDuet-1	FtsL^{+}	this study
BL21(DE3)/pWB2/ pETDuet-1	FtsL^{+}, RasP^{+}	this study
BL21(DE3)/pWB3/ pETDuet-1	FtsL^{+}, RasP-E21A^{+}	this study
BL21(DE3)/pWB5	ΔN-FtsL^{+}	this study
BL21(DE3)/pWB6	ΔN-FtsL^{+}, RasP^{+}	this study
BL21(DE3)/pWB7	ΔN-FtsL^{+}, RasP-E21A^{+}	this study
BL21(DE3)/pWB26	ΔC-FtsL^{+}	this study
BL21(DE3)/pWB17	FtsL25B^{+}	this study
BL21(DE3)/pWB18	FtsL25B^{+}, RasP^{+}	this study
BL21(DE3)/pWB19	FtsL25B^{+}, RasP-E21A^{+}	this study
BL21(DE3)/pWB4	DivIC^{+}	this study
BL21(DE3)/pWB8	ΔN-DivIC^{+}	this study
BL21(DE3)/pWB1/pWB4	FtsL^{+}, DivIC^{+}	this study

BL21(DE3)/pWB2/pWB4	FtsL^{+}, RasP^{+}, DivIC^{+}	this study
BL21(DE3)/pWB3/pWB4	FtsL^{+}, RasP-E21A^{+}, DivIC^{+}	this study
BL21(DE3)/pWB1/pWB8	FtsL^{+}, ΔN-DivIC^{+}	this study
BL21(DE3)/pWB2/pWB8	FtsL^{+}, RasP^{+}, ΔN-DivIC^{+}	this study
BL21(DE3)/pWB3/pWB8	FtsL^{+}, RasP-E21A^{+}, ΔN-DivIC^{+}	this study
BL21(DE3)/pWB8/pWB17	FtsL25B^{+}, ΔN-DivIC^{+}	this study
BL21(DE3)/pWB8/pWB18	FtsL25B^{+}, ΔN-DivIC^{+}, RasP^{+}	this study
BL21(DE3)/pWB8/pWB19	FtsL25B^{+}, ΔN-DivIC^{+}, RasP-E21A^{+}	this study
BL21(DE3)/pWB5/pWB8	ΔN-FtsL^{+}, ΔN-DivIC^{+}	this study
BHT101	F^{-}, *cya-99*, *araD139*, *galE15*, *galK16*, *rpsL1 (Str^{r})*, *hsdR2*, *mcrA1*, *mcrB1*	Euromedex
BHT101/pKT25/pUT18C	CyaA-T18^{+}, CyaA-T25^{+}	this study
BHT101/pKT25-zip/ pUT18C-zip	CyaA-T18-zip^{+}, CyaA-T25-zip^{+}	this study
BHT101/pWB9/pWB10	CyaA-T18-FtsL^{+}, CyaA-T25-FtsL^{+}	this study
BHT101/pWB9/pWB14	CyaA-T18-FtsL^{+}, CyaA-T25-ΔN-FtsL^{+}	this study
BHT101/pWB10/pWB13	CyaA-T18-ΔN-FtsL^{+}, CyaA-T25-FtsL^{+}	this study
BHT101/pWB13/pWB14	CyaA-T18-ΔN-FtsL^{+}, CyaA-T25-ΔN-FtsL^{+}	this study
BHT101/pWB11/pWB12	CyaA-T18-DivIC^{+}, CyaA-T25-DivIC^{+}	this study

BHT101/pWB11/pWB16	CyaA-T18-DivIC$^+$, CyaA-T25-ΔN-DivIC$^+$	this study
BHT101/pWB12/pWB15	CyaA-T18-ΔN-DivIC$^+$, CyaA-T25-DivIC$^+$	this study
BHT101/pWB15/pWB16	CyaA-T18-ΔN-DivIC$^+$, CyaA-T25-ΔN-DivIC$^+$	this study
BHT101/pWB9/pWB12	CyaA-T18-FtsL$^+$, CyaA-T25-DivIC$^+$	this study
BHT101/pWB10/pWB11	CyaA-T18-DivIC$^+$, CyaA-T25-FtsL$^+$	this study
BHT101/pWB9/pWB16	CyaA-T18-FtsL$^+$, CyaA-T25-ΔN-DivIC$^+$	this study
BHT101/pWB10/pWB15	CyaA-T18-ΔN-DivIC$^+$, CyaA-T25-FtsL$^+$	this study
BHT101/pWB12/pWB13	CyaA-T18-ΔN-FtsL$^+$, CyaA-T25-DivIC$^+$	this study
BHT101/pWB11/pWB14	CyaA-T18-DivIC$^+$, CyaA-T25-ΔN-FtsL$^+$	this study
BHT101/pWB13/pWB16	CyaA-T18-ΔN-FtsL$^+$, CyaA-T25-ΔN-DivIC$^+$	this study
BHT101/pWB14/pWB15	CyaA-T18-ΔN-DivIC$^+$, CyaA-T25-ΔN-FtsL$^+$	this study

2.2 Bacterial growth conditions

2.2.1 Growth of *Bacillus subtilis*

Solution G, 2.5 l

25 g Casein hydrolysate (Oxoid)
9.2 g L-glutamic acid
3.13 g L-alanine
3.48 g L-asparagine
3.4 g KH_2PO_4
1.34 g NH_4Cl
0.27 g Na_2SO_4
0.24 g NH_4NO_3
2.45 mg $FeCl_3 \cdot 6\ H_2O$
2.35 l distilled H_2O

Adjust pH to 7.0 with 10 N NaOH and autoclave.

Solution D

0.1 M $CaCl_2 \cdot 2\ H_2O$
Autoclave

Solution F

1 M $MgSO_4 \cdot 7\ H_2O$
Autoclave

Solution H, 500 ml

5.5 g $MnSO_4 \cdot 5\ H_2O$
Add distilled H_2O
Autoclave

CH Medium, 1 l

1 l Solution G
1.0 ml Solution D
0.4 ml Solution F
2.0 ml Solution H
10 ml L-Tryptophan

L-Tryptophan

2 mg/ml distilled H_2O
Sterile filter.

Bacillus subtilis was grown on nutrient agar plates made with 13 grams nutrient broth (Oxoid) and 15 grams agar per one litre of distilled water. The plate medium was sterilised for 20 minutes at 121°C.

If not otherwise noted liquid cultures of *Bacillus subtilis* were done in 10 ml CH medium and incubated in a 100 ml shaking flask at 37°C. Overnight cultures were grown in 5 ml CH medium in a test-tube at 37°C. When necessary media were supplemented with antibiotics and other additives according to table 2.4.

For growth experiments fresh CH medium was inoculated with an overnight liquid culture to result in a start OD_{600} of 0.1. Samples were taken every 30 minutes.

Table 2.4: Concentrations of antibiotics and other medium additives for *Bacillus subtilis*

Compound	**Final concentration**
Chloramphenicol	5 µg/ml
Kanamycin	5 µg/ml
Spectinomycin	50 µg/ml
Erythromycin	1 µg/ml
Lincomycin	25 µg/ml
Tetracyclin	12 µg/ml
IPTG	1 mM
Starch	0.1 %
Xylose	0.5 %

2.2.2 Growth of *E. coli*

LB Medium, 1 l

10 g Bacto-Trypton
5 g Bacto-Yeast extract
10 g NaCl
1 l distilled H_2O
Autoclave

E. coli was grown on LB (Luria Bertani) agar plates made with 15 grams agar per one litre of LB medium. The plate medium was sterilised for 20 minutes at 121°C.

Liquid cultures were done in LB medium at 37°C. Overnight cultures were done in 5 ml LB medium in test-tubes. When necessary media were supplemented with antibiotics and other additives according to table 2.5.

Table 2.5: Concentrations of antibiotics and other medium additives for *E. coli*

Compound	**Final concentration**
Chloramphenicol	50-100 µg/ml
Kanamycin	50 µg/ml
Carbenicillin	50-100 µg/ml
IPTG	1 mM
X-gal	120-160 µg/ml

2.3 Molecular biology

2.3.1 Preparation of competent *E. coli* cells

SOB Medium, 250 ml

5 g Bacto-Trypton
1.25 g Bacto-Yeast extract
0.125 g NaCl
625 µl 1M KCl solution
Add distilled H_2O

Autoclave and add 1.25 ml of 2M $MgCl_2$ solution afterwards.

TB buffer, 200 ml

605 mg Pipes
333 mg $CaCl_2$
3.725 g KCl
Add distilled H_2O

Adjust pH to 6.7 (with KOH) and afterwards add 1.39 g $MnCl_2$.
Sterile filter.

E. coli cells were freshly streaked out on LB plates. An overnight culture of 10 ml was inoculated and incubated in a 100 ml shaking flask at room temperature. In the morning the main culture was done in SOB medium. The medium was inoculated resulting in a start OD_{600} of approximately 0.05. The cells were incubated at room temperature in a shaking flask. The volume of the shaking flask should be about ten times bigger than the culture volume. When an OD_{600} between 0.3-0.6 was reached, the cells were incubated on ice for 10 minutes and afterwards harvested by centrifugation (10 minutes, 3220 g, 4°C). The supernatant was discarded and the pellet was resuspended in 80 ml of ice-cold TB buffer per 250 ml of main culture. After incubation on ice for 10 minutes the cells were spun down again and resuspended in 20 ml of ice-cold TB buffer per 250 ml of main culture. 0.7 ml of DMSO per 10 ml were added drop by drop and the cells were again left on ice for 10 minutes. The suspension was divided into 100-200 µl aliquots using pre-cooled reaction tubes. The aliquots were flash frozen in liquid nitrogen and stored at -80°C.

2.3.2 Transformation of *E. coli* cells

Competent *E. coli* cells were thawed on ice. DNA was added to 50 µl of cells and the suspension was incubated on ice for at least 30 minutes. The cells were heat shocked for 30 seconds at 42°C and afterwards incubated on ice for five more minutes. 400 µl of LB medium were added and the cells were shaken at 37°C for one hour. For selection the cells were harvested by centrifugation and resuspended in the backflow of the supernatant. Finally the culture was plated on LB agar plates supplemented with the appropriate antibiotic.

2.3.3 Transformation of *Bacillus subtilis* cells

Solution E

40% (w/v) glucose
Autoclave

Solution F

1 M $MgSO_4 \cdot 7\ H_2O$
Autoclave

L-Aspartate

50mg/ml distilled H_2O
Adjust pH to 7.0 and sterile filter.

10 x PC buffer, 1l

107 g K_2HPO_4 (anhydrous)
60 g KH_2PO_4 (anhydrous)
10 g Na_3 citrate· 5 H_2O
Add distilled H_2O

Autoclave

L-Tryptophan

2 mg/ml distilled H_2O
Sterile filter.

Ferric ammonium citrate

2.2 mg/ml distilled H_2O
Sterile filter.

MD medium, 50 ml

5 ml 10 x PC buffer
2.5 ml Solution E
2.5 ml L-Aspartate
1.25 ml L-Tryptophan
250 µl Ferric ammonium citrate
150 µl Solution F
Add sterile H_2O.

Casamino acids

20% (w/v) in distilled H_2O
Sterile filter.

The night previous to transformation *Bacillus subtilis* cells were streaked out on nutrient agar plates. In the morning MD medium was prepared. 10 ml of MD medium were supplemented with 50 µl of casamino acids and inoculated with the freshly grown cells. The rest of the MD medium was kept at 37°C. The cell culture was incubated at 37°C in a 100 ml shaking flask. When an OD_{600} between 1.0-1.5 was reached, 10 ml of warm MD medium lacking casamino acids were added. After one more hour of shaking at 37°C the cells became competent. 800 µl of the culture were added to the DNA in a pre-warmed 15 ml plastic centrifuge tube and were again shaken at 37°C. 20 minutes later 25 µl of casamino acids were added. For antibiotic resistance the cells were incubated for at least one hour longer (80 minutes for Erythromycin). Finally the cells were harvested by centrifugation, resuspended in the backflow of the supernatant and plated on nutrient agar plates with the appropriate antibiotic.

2.3.4 Preparation of genomic DNA

For preparation genomic DNA from either *Bacillus subtilis* or *E. coli* strains a 5 ml LB culture was done over night at 37°C. In the morning 3 ml of the culture were centrifuged to harvest the cells. The pellet was resuspended in 200 µl distilled H_2O. 200 µl of phenol were added. The suspension was mixed well and incubated for at least 10 minutes at 65°C followed by incubation on ice for two minutes. To remove the phenol 200 µl of cold chloroform were added. The dispersion was then mixed well and centrifuged (5 minutes, 15,000 g, 4°C). This resulted in three phases. The top phase was the aqueous phase containing the DNA. The middle phase consisted of precipitated proteins and the bottom phase was a phenol-chloroform mixture. The aqueous phase was removed and again extracted with 200 µl of cold chloroform. This step was repeated at least once until all phenol was removed from the aqueous DNA solution.

For DNA amplification by PCR this solution was usually diluted 10 times and 1 µl of the resulting solution was used as template (see chapter 2.3.5).

2.3.5 Amplification of DNA

PCR mix, 50 µl

10 µl 5x HF buffer (15mM $MgCl_2$)
1 µl dNTP mix (10 mM each dNTP)
2.5 µl Forward primer
2.5 µl Reverse primer
1 µl Template DNA
0.5 µl Phusion polymerase (5 U/µl)
Add sterile H_2O.

Amplification of DNA fragments for cloning was done by polymerase chain reaction (PCR). As template either chromosomal DNA or plasmid DNA was used. Primers were synthesised by Eurofins MWG Operon. The 100 µM stock solutions were diluted to 10 µM with sterile H_2O. The PCR reaction was carried out with Phusion polymerase enzyme (New England Biolabs). The reaction was started with a denaturing step at 95°C for 5-10 minutes. Then a cycle of denaturing at 95°C, primer annealing usually between 45°C and 65°C and elongation at 72°C (1 min/1 kb) was done 30 times. This was followed by one final elongation step (72°C, 10 min) and samples were afterwards cooled to 4°C.

For further usage the PCR result was controlled via agarose gel electrophoresis. The rest of the DNA was purified using the Nucleospin Extract II kit from Machery & Nagel.

2.3.6 Agarose gel electrophoresis

50x TAE buffer, 1 l

242 g Tris
57.1 ml Acetic acid
100 ml of 0.5 M EDTA solution (pH 8.0)
Add distilled H_2O.

If not otherwise noted for DNA gel electrophoresis a 1% agarose gel in 1x TAE buffer was used. In case the samples needed to be prepared with loading buffer, Fermentas 6x Loading buffer was added. Seperation was carried out in 1x TAE buffer at 105 volts for 30-50 minutes. Determination of fragment sizes was done by comparison to a DNA ladder, either GeneRuler

1kb or GeneRuler 1kb plus (both Fermentas). Gel staining was done by incubation in ethidium bromide solution.

2.3.7 Plasmid construction

DNA double digest, 30 µl
(NEB enzymes)

1.5 µl Enzyme 1
1.5 µl Enzyme 2
1.5 µl BSA
3 µl 10x NEB buffer
22.5 µl DNA in sterile H_2O

Plasmid DNA fast digest, 20 µl
(Fermantas FD enzymes)

1 µl Enzyme 1
1 µl Enzyme 2
2 µl 10x FD buffer
16 µl DNA in sterile H_2O

DNA ligation, 20 µl

5 µl Plasmid DNA solution
11 µl Insert DNA solution
2 µl 10x T4 ligase buffer
2 µl T4 DNA ligase

PCR product fast digest, 30 µl
(Fermentas FD enzymes)

1 µl Enzyme 1
1 µl Enzyme 2
3 µl 10x Digest buffer
25 µl DNA in sterile H_2O

For plasmid construction the designated insert was amplified by PCR and purified (see chapter 2.3.5). Plasmid stock concentrations were usually about 50 µg/ml, insert concentrations were ranging within 30-50 µg/ml. The digestions were done with NEB restriction enzymes for 1-1.5 hours or with Fermentas fast digest enzymes (times according to the Fermentas FD enzyme manuals). In both cases 5 µl of plasmid stock solution and 22.5 µl of insert solution were digested. In case of lower DNA concentrations the volumes were adjusted accordingly. Afterwards the DNA was purified using the Nucleospin Extract II kit from Machery & Nagel. Note that elution was not done in buffer, but in 30 µl of sterile H_2O. If a double digestion with NEB enzymes was not possible, sequential digestion was done. In this case the first digestion step was upscaled toa total volume of 40 µl to compensate DNA loss during purification.

The insert was then ligated into the vector using T4 DNA ligase (Fermentas). The reaction was carried out for at least one hour at room temperature. As a plasmid re-ligation control one reaction as done without insert DNA. 10 µl of the ligation mixture were directly transformed into *E. coli* DH5α or *E. coli* XL1 Blue cells and correct clones were selected by growth on antibiotic LB agar plates, followed by controls such as slot lysis or colony PCR (see chapter

2.3.8 and 2.3.9). Clones with positive control results were used to inoculate LB overnight cultures. The next day 3 ml of each culture were used to extract the plasmid with the Nucleospin Plasmid kit from Machery & Nagel. Afterwards plasmid sequencing was done by GATC Biotech or the Center of Molucular Medicine in Cologne.

2.3.8 Slot-Lysis

Protoplasting buffer

30 mM Tris
5 mM EDTA
50 mM NaCl
20% sucrose
50 µg/ml RNAse
50 µg/ml Lyzozyme

Adjust pH to 8.0 with HCl.

Lysis buffer

89 mM Tris
89 mM Boric acid
2.5 mM EDTA
2% SDS
5% sucrose
0.04% Bromphenolblue

Adjust pH to 8.0 with HCl.

Slot-Lysis was carried out to check *E. coli* clones for plasmids containing a DNA insert of 500bp or more. A small amount of cells was taken from a LB agar plate, resuspended in 10 µl protoplasting buffer and incubated at room temperature for approximately 10 minutes. The slots of an agarose gel were preloaded with 4 µl of lysis buffer. The protoplast solution was then loaded under the lysis buffer. For the first 20 minutes the gel was run at 30 volts to completely lyse the cells. Afterwards voltage was increased to 105 volts. As a size control the original plasmid without the insert was used.

2.3.9 Colony PCR

Colony PCR mix, 10 µl

5 µl 2x Mastermix
1 µl Forward primer
1 µl Reverse primer
3 µl sterile H_2O

To check transformed *E. coli* or *Bacillus subtilis* cells for plasmids or plasmid insertions with a DNA insert a colony PCR with specific primer combinations was carried out. A small amount of cells was taken from a plate and added to the colony PCR reaction mixture. The commercial mastermix EconoTaq PLUS GREEN contained buffer, Taq polymerase enzyme and dNTPs. Whenever possible, one plasmid specific primer and one insert specific primer were combined. If no plasmid specific primers were available only insert specific primers were used. The PCR results were analysed by agarose gel electrophoresis.

2.4 Protein biochemistry

2.4.1 Polyacrylamide gel electrophoresis (PAGE)

10x Anode buffer

2 M Tris

Adjust pH to 8.9 with HCl.

10x Kathode buffer

1 M Tris
1 M Tricine
1 % SDS

SDS gel buffer

3 M Tris
1 M HCl
0.3 % SDS

10% Separation gel (for 2 gels)

5.4 g Urea
5 ml SDS gel buffer
4 ml Acrylamide/Bisacrylamide
1 ml distilled H_2O
50 µl 10 % APS
5 µl TEMED

4x Sample buffer

150 mM Tris
12 % SDS
6 % β-Mercaptoethanol
30 % Glycerol
0.05 % Coomassie G-250

Adjust pH to 7.0 with HCl.

Stacking gel (for 2 gels)

1.55 ml SDS gel buffer
0.5 ml Acrylamide/Bisacrylamide
4 ml distilled H_2O
50 µl 10 % APS
5 µl TEMED

To analyse protein samples usually a polyacrylamide gel electrophoresis under denaturing conditions was carried out. A 10% Schaegger gel with SDS and urea was used for separation. The ratio of acrylamide to bisacrylamide was 37.5:1 (Roth, Rotiphorese Gel 30). Samples were treated with 4x sample buffer and incubated at 95°C for 15-15 minutes before loading them onto the gel. Gels run in a BioRad Mini-PROTEAN chamber at 50 volts for focussing and 150 volts for separation.

2.4.2 Preparation of protein samples for PAGE by precipitation

To concentrate protein samples and remove lipids, the protein was precipitated with either ethanol or TCA. Cold ethanol was added to a final concentration of 70% and precipitation was done over night at -20°C. TCA was added to a final concentration of 10% and precipitation was done for at least one hour on ice. Afterwards the samples were centrifuged (10 minutes, 10,000 g, 4°C) and the protein pellet was resuspended in 1x sample buffer for SDS PAGE (see chapter 2.4.1) and incubated at 95°C.

2.4.3 Staining of polyacrylamide gels

2.4.3.1 Staining with Coomassie

Coomassie staining solution

45 % Methanol
10 % Acetic acid
0.1 % Coomassie Blue G-250

Polyacrylamide gels were gently shaken in Coomassie staining solution for at least one hour. The staining solution was removed and gels were washed in 10 % acetic acid. They were then left shaking in 10 % actetic acids until all blue background colour was removed and clear protein bands could be seen.

2.4.3.2 Staining with silver

Fixing solution, 1 l

500 ml Methanol
120 ml Acetic acid
Add distilled H_2O.

Add 0.5 µl/ml formaldehyde (37 %) freshly before use.

Developing solution, 250 ml

7.5 g Na_2CO_3
200 µl Sodium thiosulfate solution
Add distilled H_2O.

Add 0.5 µl/ml formaldehyde (37 %) freshly before use.

Sodium thiosulfate solution, 250 ml

0.05 g $Na_2S_2O_3$
Add distilled H_2O.

Silver nitrate solution, 250 ml

0.25 g $AgNO_3$
Add distilled H_2O.

Stopping solution, 1 l

23 g EDTA (sodium salt)
Add distilled H_2O.

Gels were gently shaken in fixing solution for 10 minutes. Afterwards two washing steps with distilled H_2O were done for 5 minutes each. The gels were soaked in sodium thiosulfate solution for one minute, briefly (~ 30 seconds) washed with distilled H_2O two times and then gently shaken in silver nitrate solution for 10 minutes. To develop the gels they were rinsed with distilled H_2O and a small portion of developing solution. They were soaked in developing solution until the band intensities were adequate (usually 1-5 minutes). Developing was stopped by quickly discarding the developing solution and shaking the gels in stopping solution for 10 minutes. Afterwards the gels were washed and kept in distilled H_2O.

2.4.4 Immuno-blotting

Blot buffer

25 mM Tris
192 mM Glycin
20 % (v/v) Methanol

Adjust pH to 8.3 with HCl.

Washing buffer

50 mM Tris
0.9 % (w/v) NaCl

Adjust pH to 7.5 with HCl.

Blocking buffer

50 mM Tris
0.9 % (w/v) NaCl
5 % (w/v) low fat milk powder

Adjust pH to 7.5 with HCl.

NBT solution, 20 ml

1 g NBT
8 ml Dimethylformamide
12 ml sterile H_2O

BCIP solution, 40 ml

1 g BCIP
40 ml Dimethylformamide

Incubation buffer

100 mM Tris
100 mM NaCl
5 mM $MgCl_2$
0.01 % NaN_3

Adjust pH to 9.5 with HCl.
Freshly add 66 µl NBT solution and 66 µl BCIP solution per 10 ml buffer.

For immuno-blotting polyacrylamid gels were soaked in blot buffer. For blotting a wet blot chamber of the electrophoresis blotting systems by C.B.S. was used. The transfer membrane was a PVDF membrane (Immobilon-P, Millipore) with 0.45 µm pore size. To ensure optimal transfer, gel and membrane were stacked between two pieces of buffer soaked Whatman paper on each side. Blotting was done over night at 75 mA.

The next morning the blots were gently shaken in blocking buffer for one hour. Afterwards the solution was exchanged to blocking buffer containing the first antibody. For appropriate antibodies concentrations see table 2.6. After one hour unbound first antibody was washed away by shaking the blots three times in washing buffer for 10-15 minutes. Blocking buffer with the second antibody was then added and blots were shaken for 30 minutes. After washing three times again the blots were soaked in incubation buffer until the band intensities were adequate. Note: For S-tag detection the Novagen S-tag western blot kit was used as described in the kit manual.

Table 2.6: Antibody concentrations for immuno-blotting

Antibody	Stock solution	Final dilution
α-PentaHis	0.2 µg/µl, Qiagen	1:2,000
α-DivIC	Rabbit blood serum[1]	1:5,000
α-DivIB	Rabbit blood serum[1]	1:5,000
α-Mouse IgG-AP	Commercial solution, Sigma	1:10,000
α-Rabbit IgG-AP	Commercial solution, Sigma	1:10,000

[1] Provided by Richard Daniel, Centre for Bacterial Cell Biology, Newcastle University

2.4.5 Determination of protein concentrations

2.4.5.1 Determination by Bradford assay

The Bradford reagent Roti-Nanoquant by Roth was diluted with four volumes of distilled H_2O. A small volume of the protein sample was diluted with H_2O to an end volume of 200 µl. These 200 µl of the diluted sample were mixed with 800 µl of diluted reagent solution. The mixture was incubated for 5-10 minutes at room temperature before absorbance at 590 nm and 450 nm was measured. The protein concentration was determined by comparison with a calibration curve that was done with BSA solutions.

2.4.5.2 Determination by BCA assay

For the assay the Pierce BCA Protein Assay Kit by Thermo Scientific was used. 50 volumes of BCA reagent A were mixed with one volume of BCA reagent B to prepare the working reagent. A small volume of the protein sample was diluted with H_2O to an end volume of 100 µl. These 100 µl of the diluted sample were mixed with 2 ml of the working reagent. The mixture was incubated at 37°C for 30 minutes. Absorbance at 562 nm was measured. The protein concentration was determined by comparison with a calibration curve that was done with BSA solutions.

2.4.6 Purification of FtsL

FtsL buffer

50 mM Tris
500 mM NaCl
10 mM $MgCl_2$
10 % Glycerin

Adjust pH to 7.5 with HCl

Elution buffer

50 mM NaH2PO4
300 mM NaCl
250 mM imidazole

Adjust pH to 8.0 with NaOH

LEW buffer

50 mM NaH_2PO_4
300 mM NaCl

Adjust pH to 8.0 with NaOH

To purify FtsL an overexpression culture was done in *E. coli* BL21. FtsL was expressed from plasmid pET16b. Cells were grown in 500 ml LB medium in 2 l shaking flasks at 37°C. For purification a total volume of 4 l was inoculated. When the OD_{600} reached about 1.0 expression was induced by addition of IPTG to a final concentration of 0.5 mM. After two hours cells were harvested by centrifugation (15 minutes, 3,000 g, 4°C) and resuspended in FtsL buffer. Complete EDTA-free Protease Inhibitor Cocktail Tablets (Roche) and a small amount of DNase I were added. The cells were disrupted by two passes through a French Press (SLM Aminco) at 1,200 psi. Cell debris and not disrupted cells were spun down (45 minutes, 3220 g, 4°C). The supernatant was then ultra-centrifuged (60 minutes, 223,000 g, 4°C) to harvest the cell membranes. The membrane pellets were resuspended in FtsL buffer and spun down again. For solubilisation the washed membranes were resuspended in 10 ml FtsL buffer per 1g of membranes. LAPAO in FtsL buffer was added drop wise to a final concentration of 1 % (w/v). The solution was gently stirred for one hour at 4°C. To remove larger membrane parts the solution was again ultra-centrifuged (60 minutes, 223,000 g, 4°C). From the supernatant FtsL was precipitated by addition of NH_4SO_4. The volume of the supernatant was measured and saturated NH_4SO_4 solution was added drop by drop at 4°C until a final concentration of 70% (v/v) NH_4SO_4 solution was reached. The mixture was stirred over night at 4°C. The precipitate was spun down (15 minutes, 9,900 g, 4°C) and the pellet was resuspended in FtsL buffer with 0.05 % LAPAO.

For affinity chromatography a pre-packed Protino Ni-IDA 1000 column by Machery & Nagel was used. To all kit buffers 0.05 % (w/v) LAPAO was added. The column was equilibrated with 2 ml LEW buffer. After protein binding the column was washed with 4 ml LEW buffer. Afterwards two 500 µl washing steps with 20 mM imidazole and 50 mM imidazole were carried out. To this purpose LEW buffer and elution buffer were mixed to obtain LEW buffer with the appropriate imidazole concentrations. Elution was done with 4.5 ml of elution buffer. Fraction sizes were chosen as described in table 2.7. The elution fractions were flash frozen in liquid nitrogen and stored at -80°C.

Table 2.7: Fraction sizes for FtsL purification

Step	**Fraction size**
Equilibration	2 ml
Sample loading	1 ml
Washing	1 ml
Washing with imidazole	500 µl
Elution	1 ml

2.4.7 Purification of MBP-FtsL

FtsL Ni-A buffer

50 mM Tris
300 mM NaCl

Adjust pH to 7.0 with HCl and sterile filter. Add 0.05 % DDM where necessary.

FtsL Ni-B buffer

50 mM Tris
1 M Imidazole

Adjust pH to 7.0 with HCl and sterile filter. Add 0.05 % DDM.

The major problem during purification of FtsL was protein aggregation. To prevent aggregation the group of Jan Löwe (MCR Laboratory of Molecular Biology, Cambridge) has developed a purification protocol for FtsL N-terminally fused with maltose-binding protein (MBP) as a soluble tag. The group provided us with two pOPTM plasmids for overexpression of MBP-FtsL and a C-terminally truncated version MBP-FtsLΔCT in *E. coli* BL21. Cells were grown in 500 ml SOB medium in 2 l shaking flasks. A total volume of 4 l of cell culture was used. Overexpression was induced at OD_{600} of 0.7-0.8 by addition of IPTG to a final concentration of 1 mM. After three hours the cells were harvested by centrifugation (15 minutes, 3,000 g, 4°C). The cell pellets were resuspended in FtsL Ni-A buffer and a small amount of DNase I was added. The cells were disrupted by two passes through a French Press (SLM Aminco) at 1,200 psi. Cell debris and not disrupted cells were spun down (120 minutes, 30,000 g, 4°C). The supernatant was then ultra-centrifuged (120 minutes, 223,000 g, 4°C) to harvest the cell membranes. The membrane pellets were resuspended in 10 ml FtsL Ni-A buffer per 1 g of membranes. DDM in FtsL Ni-A buffer was added drop by drop to a final concentration of 1 % (w/v). The solution was gently stirred for one hour at 4°C. Afterwards the solution was directly loaded on an affinity purification column.

For affinity chromatography a HisTrap FF Crude 1 ml column by GE Healthcare was used. The purification was carried out at an Äkta purifier system. All buffers contained 0.05 % DDM. The column was equilibrated with FtsL Ni-A buffer until the baseline was stable. After protein binding the column was washed with 20 CV of 95 % FtsL Ni-A buffer and 5 % FtsL Ni-B buffer. Elution was done with 70 % FtsL Ni-A buffer and 30 % FtsL Ni-B buffer. Fraction sizes were chosen as described in table 2.8. Peak fractions were used for direct reconstitution into liposomes (see chapter 2.4.11) or flash frozen in liquid nitrogen and stored at -80°C.

Table 2.8: Fraction sizes for MBP-FtsL purification

Step	**Fraction size**
Equilibration	Fractions were not collected
Sample loading	45 ml
Washing	45 ml
Elution	1 ml
Peak fractions	0.5 ml

2.4.8 Purification of RasP

RasP Ni-A buffer

100 mM MES
300 mM NaCl

Adjust pH to 6.0 with NaOH and sterile filter. Add 0.05 % DDM where necessary.

RasP Ni-B buffer

100 mM MES
300 mM NaCl
1 M imidazole

Adjust pH to 6.0 with NaOH and sterile filter. Add 0.05 % DDM.

RasP Q-A buffer

20 mM MES
100 µM $ZnCl_2$

Adjust pH to 6.0 with NaOH and sterile filter. Add 0.05 % DDM.

RasP Q-B buffer

20 mM MES
100 µM $ZnCl_2$
1 M NaCl

Adjust pH to 6.0 with NaOH and sterile filter. Add 0.05 % DDM.

For overexpression of RasP and an inactive mutant RasP-E21A in *E. coli* the group of Jan Löwe provided us with the L-(+)-arabinose inducible strain *E. coli* BL21 A1 and appropriate plasmids. A cell culture in 100 l LB medium was done at the Institute of Microbiology of the University Osnabrück. Cells were grown in a fermenter to an OD_{600} of about 3.0. Expression was then induced by addition of L-(+)-arabinose to a final concentration of 0.25 % (w/v). After two hors the culture was cooled to 20°C and concentrated. The cells were harvested by centrifugation (15 minutes, 3,000 g, 4°C). The cell pellets were flash frozen in liquid nitrogen and stored at -80°C.

Approximately 80g of cell pellet were used for a RasP or RasP-E21A purification. The cells were resuspended in RasP Ni-A buffer and a small amount of DNase I was added. Cell disruption was done by three passes through an EmulsiFlex-C5 (Avestin) at 1,500-2,000 psi. Cell debris and not disrupted cells were spun down (120 minutes, 30,000 g, 4°C). The supernatant was then ultra-centrifuged (120 minutes, 223,000 g, 4°C) to harvest the cell membranes. The membrane pellets were resuspended in 10 ml RasP Ni-A buffer per 1 g of membranes. DDM in RasP Ni-A buffer was added drop by drop to a final concentration of 1 % (w/v). The solution was gently stirred for one hour at 4°C. Afterwards the solution was directly loaded on an affinity purification column.

For affinity chromatography a HisTrap FF Crude 1 ml column by GE Healthcare was used. The purification was carried out at an Äkta purifier system. All buffers contained 0.05 % DDM. The column was equilibrated with RasP Ni-A buffer until the baseline was stable. After protein binding the column was washed with 100 CV of 80 % RasP Ni-A buffer and 20% RasP Ni-B buffer. Elution was done with 100 % RasP Ni-B. Fraction sizes were chosen as described in table 2.9. Peak fractions were pooled for the second chromatography step. The protein solution was diluted with nine volumes of buffer RasP Q-A and then loaded onto a HiTrap Q HP 1 ml column by GE Healthcare. Unbound protein was washed away with RasP Q-A buffer until the baseline was stable. Elution was done with 40% buffer RasP Q-B and 60% buffer RasP Q-A. For fraction sizes see table 2.9. Peak fractions were used for direct reconstitution into liposomes (see chapter 2.4.11).

Table 2.9: Fraction sizes for RasP purification

Step	**Fraction size**
Equilibration	Fractions were not collected
Sample loading	45 ml
Washing HisTrap FF Crude	45 ml
Elution HisTrap FF Crude	1 ml
Washing HiTrap Q HP	10 ml
Elution HiTrap Q HP	1 ml

2.4.9 Purification of RsiW*

RsiW* resuspension buffer

50 mM Tris
Adjust pH to 8.0 with HCl.

Denaturing solution

8 M Guanidinium chloride
50 mM DTT

RsiW* refolding buffer

50 mM Tris
100 mM NaCl
10 mM KCl

Adjust pH to 8.0 with HCl.
Add 0.05 % DDM.

RsiW* washing buffer

50 mM Tris
100 mM NaCl
10 mM KCl

Adjust pH to 7.5 with HCl.
Sterile filter and add 0.05 % DDM

RsiW* elution buffer

50 mM Tris
100 mM NaCl
10 mM KCl
1 M imidazole

Adjust pH to 7.5 with HCl.
Sterile filter and add 0.05 % DDM

A truncated form of RsiW (RsiW*) was purified from inclusion bodies. Overexpression was done in *E. coli* BL21 from plasmid pET16b. A 250 ml LB liquid culture in a 1 l shaking flask was inoculated in the morning and grown at 37°C. When the OD$_{600}$ reached about 1.0 overexpression was induced by addition of IPTG to a final concentration of 1 mM. After three hours the cells were harvested by centrifugation (15 minutes, 3,000 g, 4°C) and resuspended in RsiW* resuspension buffer. The cells were disrupted by sonification with a Branson Sonifier 250. Duty cycle was set to constant, the micro tip limit was set to 5. Cells were sonificated four times for 30 seconds. Between each sonfification the suspension was cooled on ice for a few minutes to avoid overheating. Cell debris and the inclusion bodies were spun down (20 minutes, 8,000 g, 4°C) and washed once each with RsiW* resuspension buffer and H_2O. To remove cell debris and membrane particles the pellet was finally resuspended in a 2 % (w/v) Triton X-100 solution. The inclusion bodies were spun down again and resuspended in 5 ml sterile H_2O. This suspension was added drop by drop to 20 ml of denaturing solution. The solution was stirred gently over night at 4°C. In the morning it was centrifuged (20 minutes, 8,000 g, 4°C) and stored at 4°C.

For refolding 2.5 ml of the protein solution was added drop wise to 200 ml refolding buffer and stirred over night at 4°C. The next morning it was loaded onto a HisTrap FF Crude 1 ml column by GE Healthcare. The purification was carried out at an Äkta purifier system. All buffers contained 0.05 % DDM. The column was equilibrated with RsiW* washing buffer until the baseline was stable. Unbound protein was washed away with 92 % RsiW* washing buffer and 8 % RsiW* elution buffer until the baseline was stable. Elution was done in two steps of 10 CV 40 % RsiW* washing buffer and 60 % RsiW* elution buffer and 10 CV 100 % RsiW* elution buffer. For fraction sizes see table 2.10. The elution fractions were pooled and then either directly reconstituted into liposomes or stored. For storage glycerin was added up to 10 % (v/v) and the samples were flash-frozen in liquid nitrogen before stored at -80°C.

Table 2.10: Fraction sizes for RsiW* purification

Step	**Fraction size**
Equilibration	Fractions were not collected
Sample loading	45 ml
Washing	10 ml
Elution	1 ml

2.4.10 Preparation of liposomes

Liposome buffer

20 mM MES
100 µM $ZnCl_2$
150 mM NaCl

Adjust pH to 6.0 with NaOH
and sterile filter.

For the preparation of liposomes *E. coli* total lipid extract (20 mg/ml) by Avanti Polar Lipids was used in all cases. To remove the chloroform of the stock solution 20 ml of the lipid solution were evaporated in a 250 ml round bottom flask at 20°C. Afterwards the lipids were dried over night at a lyophiliser. The next morning the lipids were thoroughly resuspended in 20 ml of liposome buffer by stirring. The suspension was aliquoted into 1.5 ml reaction tubes and put under nitrogen atmosphere. The aliquots were then flash-frozen in liquid nitrogen and stored at -80°C.

2.4.11 Reconstitution of membrane proteins into liposomes

An appropriate amount of frozen liposome aliquots were thawed at room temperature. The liposome suspension was extruded through a membrane with a pore size of 400 nm (15-20 passes) and afterwards diluted with 3 volumes of liposome buffer (see chapter 2.4.10). The suspension was filled into 1 ml cuvettes and absorbance at 540 nm was measured. In steps of 2µl a 20% (w/v) solution of Triton X-100 was added. The absorbance increased upon Triton X-100 addition. When the maximum has been reached and the absorbance started to decreased again, detergent addition was stopped. The suspension of all cuvettes was pooled into a 15 ml plastic tube. The protein solution was warmed to room temperature and added drop by drop to the liposomes. The tube was gently shaken on a rolling mixer (RM-5 by Assistent) for 15 minutes.

The detergent was removed by addition of BIO-RAD Bio-Beads SM2 Adsorbent. The Bio-Beads were previously soaked in methanol for activation, extensively washed with sterile H_2O and stored in sterile H_2O at 4°C. The amount of Bio-Beads that needed to be added was calculated as follows:

1 mg per 1 µl Triton X-100 solution added +
10 mg per 1 µl protein solution x DDM concentration

The beads were added and the plastic tube was shaken for one hour at room temperature. Afterwards the same amount of fresh beads was added and again the solution was shaken for one hour at room temperature. Then a double amount of beads was added and the tube was shaken over night at 4°C. In the morning fresh beads were added one more time and the tube was shaken 45 minutes longer at 4°C. To harvest the proteoliposomes the supernatant was removed carefully and ultra-centrifuged (20 minutes, 365,000 g, 4°C). The pellet was resuspended in cold liposome buffer and spun down again. This washing step was repeated one more time. Finally the proteoliposomes were resuspended in 600µl liposome buffer per 1 ml of original liposome suspension used. The suspension was aliquoted and put under nitrogen atmosphere. The aliquots were then flash-frozen in liquid nitrogen and stored at -80°C.

2.4.12 MBP-FtsL proteolysis assay in liposomes

As RasP has been shown to not be stable in detergent solution [Jan Löwe, personal communication] the MBP-FtsL proteolysis assay was done in liposomes. Either MBP-FtsL liposomes or MBP-FtsLΔCT liposomes were mixed with RasP and RasP* liposomes. As an additional control either EDTA or phenanthrolin was added to one sample. All samples were diluted with liposome buffer (see chapter 2.4.10) to a total volume of 200 µl.

To prepare mixed proteoliposomes containing MBP-FtsL and RasP the samples were flash-frozen in liquid nitrogen and thawed at 4°C. This should result in multi lamellar vesicles. Afterwards the samples were sonificated in a water bath for one minute and then flash-frozen again. This cycle was repeated three times. Finally the suspensions were passed through a membrane with a pore size of 400 nm 20 times. Those mixed proteoliposomes were incubated at 30°C for three hours. Samples for a SDS-PAGE were taken every hour. The suspensions were left at 30°C over night and a last sample was taken in the morning. All samples were run on an SDS-gel, which was stained with Coomassie (see chapters 2.4.1 and 2.4.3.1).

2.5 Fluorescence microscopy of *Bacillus subtilis*

2.5.1 General microscopy techniques

In the morning a 10 ml culture of CH medium (see chapter 1.1.1) in a 100 ml shaking flask was inoculated with *Bacillus subtilis* cells from an over night culture to result in a start OD_{600} of 0.1. Cells were shaken at 37°C until an OD_{600} of approximately 0.7 was reached. A 10 µl sample of the cell culture was taken and when necessary stained with fluorescent dyes according to table 2.11. Then 3 µl of the stained cells were pipetted onto a freshly prepared 76x26 mm microscopy slide, which was covered with a thin layer of 1 % agarose in sterile H_2O. The cells were then covered with a 20x20 mm cover slip. Microscopy was done on a Zeiss Axiolmager M1 equipped with a Zeiss AxioCam HRm camera. The objective was an EC Plan-Neofluar 100x/1.3 Oil objective used with Zeiss Immersol 518F oil. Table 2.8 shows which filters were used according to the fluorophor. Digital images were acquired and analysed with the AxioVision 4.6 software by Zeiss. Final image editing was done with Adobe Photoshop 6.0.

Table 2.11: Cell staining and filters for fluorescence microscopy of *Bacillus subtilis*

Fluorophor	**Stock solution**	**Final concentration**	**Filter**
NileRed	100 µg/ml in methanol	10 µg/ml	43 HE Cy3
DAPI	1 µg/ml in 50% glycerol	0.1 µg/ml	49
GFP	---	---	38 HE eGFP

2.6 Other methods

2.6.1 Co-expression experiments in *E. coli* BL21

For co-expression of up to four proteins in *E. coli* BL21 the Duet plasmids pACYCDuet and pETDuet by Novagen were used. The constructed co-expression plasmids were freshly transformed into competent *E. coli* BL21 cells. The next day over night cultures were done with a mixture of several clones of each plate to ensure average expression levels in the end. In the morning 10 ml LB medium in a 100 ml shaking flask were inoculated to a start OD_{600} of 0.1. Cells were shaken at 37°C until an OD_{600} of approximately 0.7 was reached. Overexpression was then induced by addition of 0.1 mM IPTG. After three hours the OD_{600} of each culture was measured and 1 ml of cells was spun down. The cell pellet was resuspended in LB medium to result in an OD_{600} of 10. Samples of these suspensions were taken and prepared for SDS-PAGE and immuno-blotting.

2.6.2 Bacterial Adenylate Cyclase Two-Hybrid Assay

To test interaction of bacterial membrane proteins the BACTH System Kit by Euromedex was used. Proteins of interest were fused to the T18 and the T25 part of the adenylate cyclase of *Bordetella pertussis*. For each combination 1.5 µl of the high copy plasmid with the T18 fusion product and 3 µl of the low copy plasmid with the T25 fusion product were transformed into competent *E. coli* BTH101 cells. 10 µl of each transformation culture were spotted on LB agar plates supplemented with 100 µg/ml Carbenicillin, 50 µg/ml Kanamycin, 1 mM IPTG and 160 µg/ml X-gal. The plates were incubated in the dark at 30°C for 20-30 hours. When round spots of bacteria were grown, a small amount of cells was taken from the plate and diluted in 1 ml of LB medium. 10 µl of this dilution were again spotted on supplemented LB agar plates and incubated in the dark at 30°C for 30 hours.

3 Results

3.1 The putative N-terminal cleavage product of FtsL

FtsL is cleaved within its transmembrane domain by the protease RasP [Bramkamp et al., 2006]. Proteases of the S2P family like RasP usually clip their substrates to release an effector into the cytosol [Wolfe and Kopan, 2004]. This was best demonstrated for the second known RasP substrate RsiW, where cleavage results in the release of the sigma-factor σ^W [Heinrich and Wiegert, 2009]. Sequence alignment of RsiW and FtsL led to the identification of a putative cleavage site [Bramkamp et al., 2006]. The putative N-terminal cleavage product shows no sequence similarity to any known class of peptides or proteins. It seems possible, that in the case of FtsL RasP cleavage simply removes the protein from the membrane instead of releasing an effector.

It has been shown that cleavage of the anti-sigma factor RseA by the *E. coli* RasP homologue RseP deliberates a protein with the C-terminal sequence VAA [Akiyama et al., 2004]. This sequence has similarity to the known SsrA tag, which is recognised by the ClpXP protease complex in *Bacillus subtilis* and leads to rapid proteolytic degradation [Griffith and Grossman, 2008]. The cytosolic RasP cleavage product of RsiW is further degraded by ClpXP as well [Zellmeier et al., 2006]. Two conserved alanine residues at the C-terminus are required for this degradation. Based the putative cleavage site motif within the transmembrane domain of FtsL, a cleavage product can be predicted. The C-terminus of this putative FtsL cleavage fragment has the amino acid sequence 39-VLFAA-43, suggesting that ClpXP might be involved in degrading FtsL.

3.1.1 Overexpression and of the putative cleavage product

If FtsL proteolysis by RasP would result in the release of an effector into the cytosol, overexpression of this putative FtsL fragment (FtsL1-43) might influence growth and/or cell length. In case the fragment is degraded by ClpXP mutating the C-terminus from 39-VLFAA-43 to 39-VLFDD-43 would likely stabilise the peptide and enhance the effect. Therefore two *Bacillus* strains were constructed. Strain WB01 expresses the FtsL1-43 fragment from the *amyE* locus under control of a xylose inducible promoter. The strain WB02 expresses the fragment with a mutated C-terminus 39-VLFDD-43 (FtsL1-43^{DD}). Cells were grown in CH medium containing 0.5 % xylose and growth was compared to the wild type *Bacillus subtilis* 168 (Fig. 3.1). Overexpression of the FtsL1-43 fragment showed no significant effect, expression of the mutated FtsL1-43^{DD} fragment led to slightly decreased growth rates. However, the OD_{600} value after 24 hours was comparable to the wild type culture.

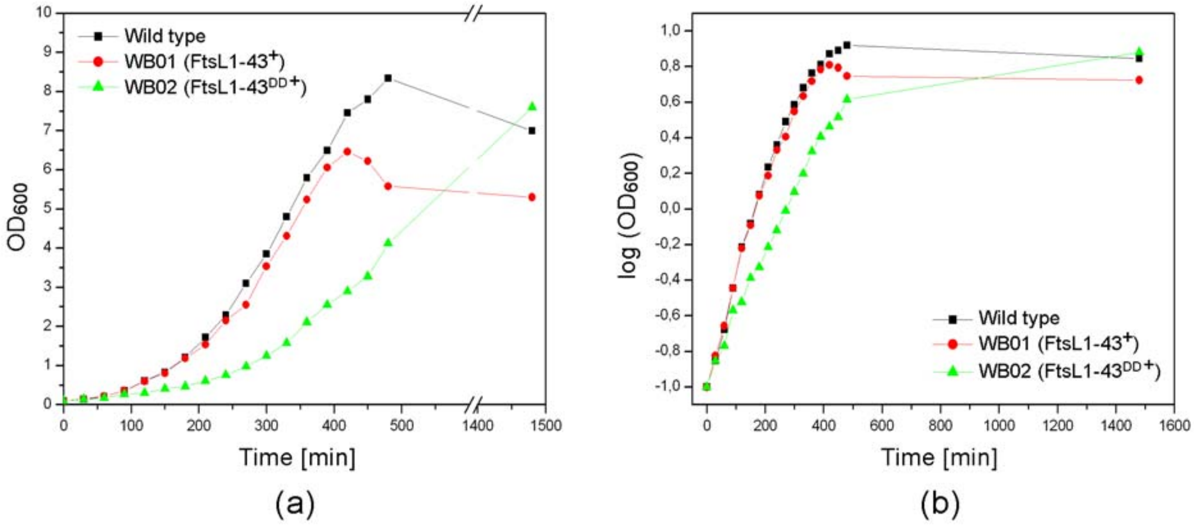

Figure 3.1: Influence of the FtsL fragment on cell growth in *Bacillus subtilis*. Strains overexpressing the putative cleavage fragment FtsL1-43 or a mutated fragment FtsL1-43^{DD} were compared to a wild type control. Shown are arithmetic (a) and logarithmic (b) growth curves in CH medium with 0.5 % xylose.

For further analysis two additional strains were constructed to investigate a possible degradation by ClpXP. Strain WB03 is a Δ*clpX* mutant and strain WB04 expresses the FtsL1-43 fragment in the Δ*clpX* background. The average cell length of these strains was measured by fluorescent microscopy. Cells were stained with DAPI and NileRed and length was measured using the AxioVision software. Between 400 and 700 cells were measured for each strain. No significant effect of the FtsL1-43 fragment or the mutated FtsL1-43^{DD} fragment was observed (Fig 3.2). The average cell length varied within a normal range and no obvious division phenotype was found. Expression of the FtsL1-43 fragment in a Δ*clpX* background had no effect either. The relatively high standard deviation is caused by the severe change of length a *Bacillus subtilis* cell undergoes during each cell cycle.

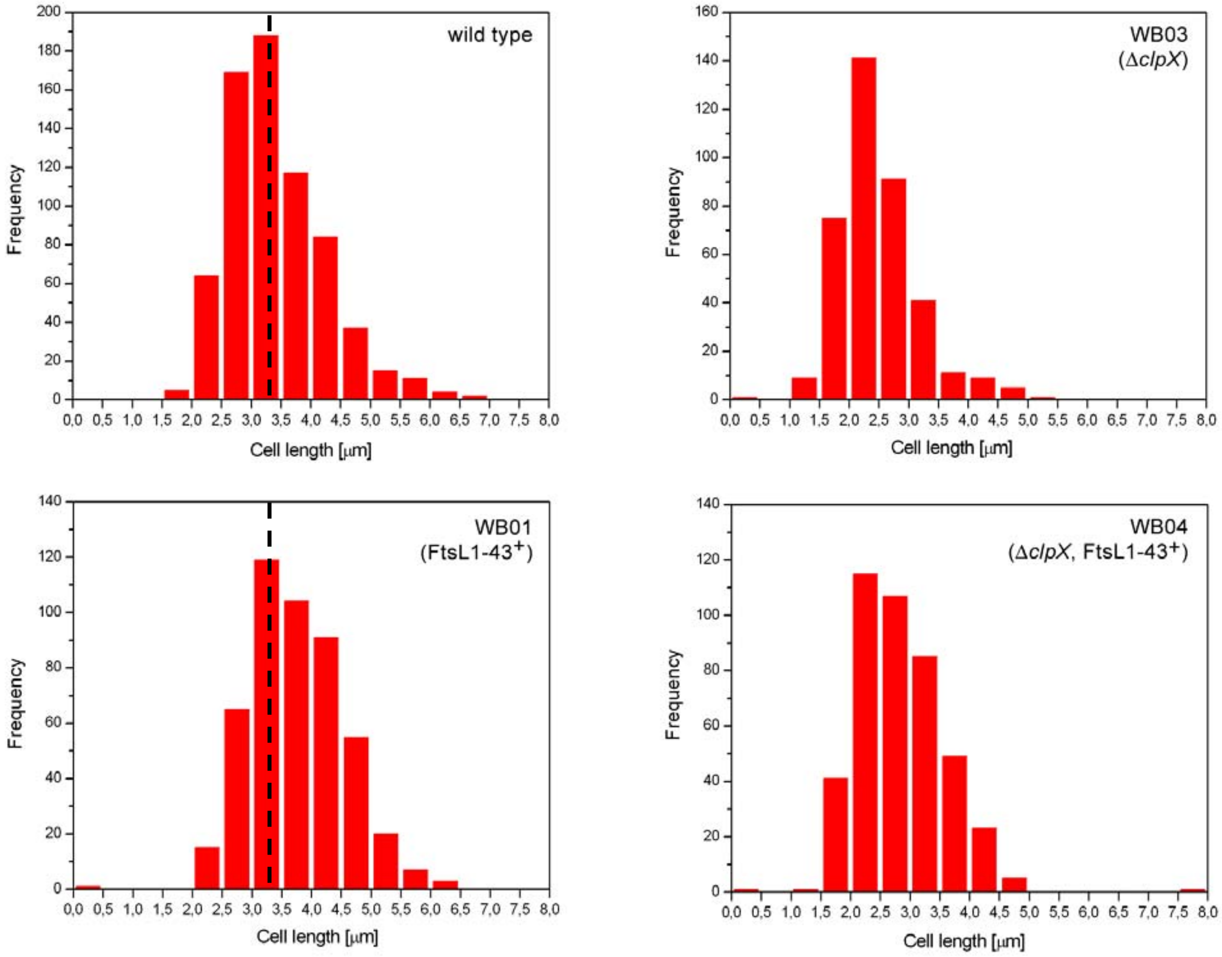

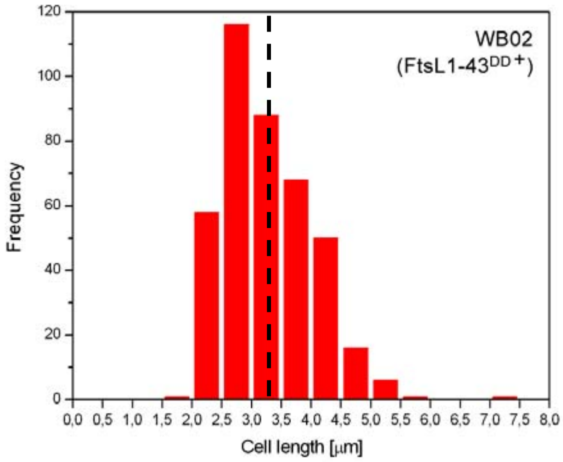

Mutant	**Average cell length**	**Standard deviation**
Wild type	3,4 µm	0,8 µm
WB01	3,7 µm	0,8 µm
WB02	3,3 µm	0,7 µm
WB03	2,5 µm	0,7 µm
WB04	2,8 µm	0,7 µm

Figure 3.2: Influence of the FtsL fragment on cell length in *Bacillus subtilis*. Strains overexpressing the putative cleavage fragment FtsL1-43 (WB01) or the mutated FtsL1-43^{DD} fragment (WB02) were compared to a wild type control. Additionally the influence of ClpXP degradation was shown. A strain overexpressing the FtsL1-43 fragment in a Δ*clpX* background (WB04) was compared to the Δ*clpX* strain (WB03). Average cell length of the wild type is indicated by dotted lines.

3.1.2 Localisation and stability of the putative cleavage product

A specific localisation of the putative FtsL cleavage product could hint to a cellular function of the fragment. To study this GFP was fused to the N-terminus of the FtsL1-43 fragment. *Bacillus subtilis* strains were constructed overexpressing the GFP fusion of the FtsL1-43 fragment (WB05) or the mutated FtsL1-43^{DD} fragment (WB06) from the *amyE* locus. In addition a strain was constructed, in which the GFP fusion of the FtsL1-43 fragment is expressed in a Δ*clpX* background (WB07).

Cells were prepared for fluorescence microscopy and the DNA was additionally stained with DAPI. Images were taken showing phase contrast, GFP fluorescence and DAPI fluorescence (Fig. 3.3). Wild type cells and the Δ*clpX* mutant as expected showed only background levels of GFP fluorescence. Overexpression of the GFP-FtsL1-43 fragment led to relatively weak GFP signals. Usually overexpression of a stable cytosolic protein fused to GFP results in strong fluorescence signals. It seems the GFP-FtsL1-43 fragment is rapidly degraded in vivo. The peptide was evenly dispersed throughout the cytosol and no specific localisation pattern was observed. Expression in a Δ*clpX* background or expression of the mutated GFP-FtsL43^{DD} fragment led to fluorescence signals as well, but the levels were still low. No obvious difference in fluorescence intensity was detected. However, the weak GFP fluorescence made it impossible to rule out a ClpXP specific effect.

To quantify the amount of the GFP-FtsL1-43 fragment present in these strains, the brightness of GFP fluorescence was measured for each cell and compared to the background brightness. For every strain an average brightness was calculated by measuring about 200 cells. To rule out possible differences caused by cultivation, three different cultures per strain were measured, one control culture without induction and two cultures induced with 0.5 % xylose. The results are shown in Fig. 3.4. As seen already in the microscopy pictures (Fig. 3.3) the GFP signals were very low. As expected, induction with xylose had no effect in the wild type. The uninduced cultures of WB05, WB06 and WB07 were comparable to the wild type control. Expression of GFP-FtsL1-43 resulted in a GFP brightness of ca. 140 % relative to background (WB05). Mutating the C-terminal sequence (WB06) or expressing the fragment in a Δ*clpX* background (WB07) did not increase the brightness of the GFP fluorescence. If the FtsL fragment is specifically degraded, this does not seem to involve ClpXP.

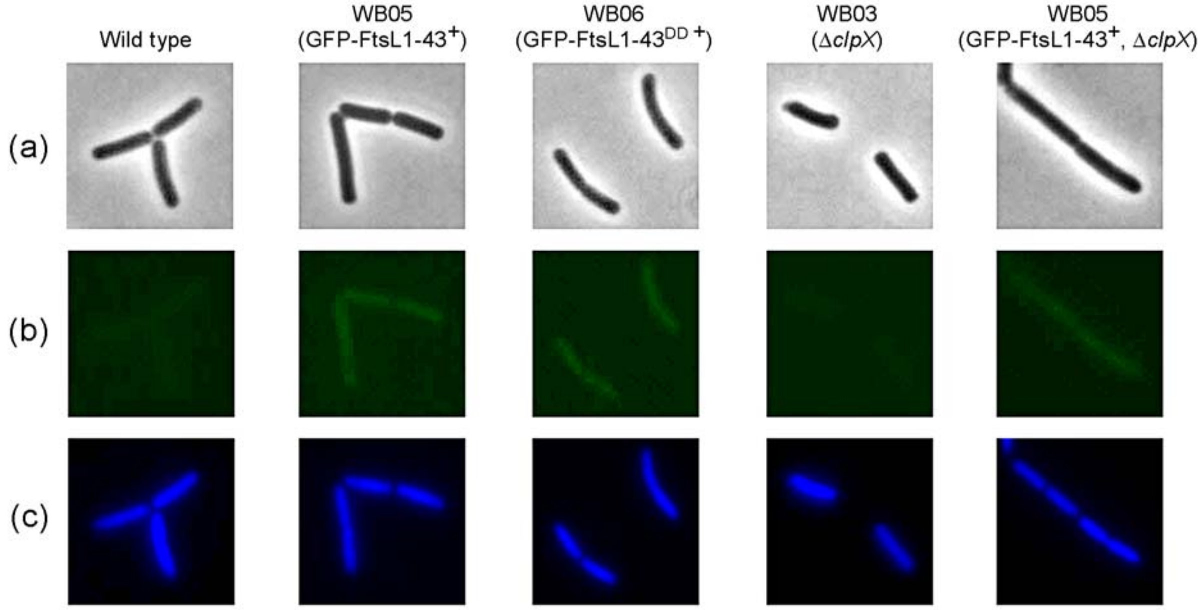

Figure 3.3: Localisation of the putative FtsL cleavage product. Shown are images of (a) phase contrast, (b) GFP fluorescence and (c) DAPI fluorescence of *Bacillus subtilis* cells. Strains overexpressing a GFP fusion of the FtsL fragment (WB05) or the mutated fragment (WB06) were compared to a wild type control. Additionally the influence of ClpXP on the fragment stability was shown. A strain overexpressing the GFP fused FtsL fragment in a Δ*clpX* background (WB07) was compared to the Δ*clpX* strain (WB03).

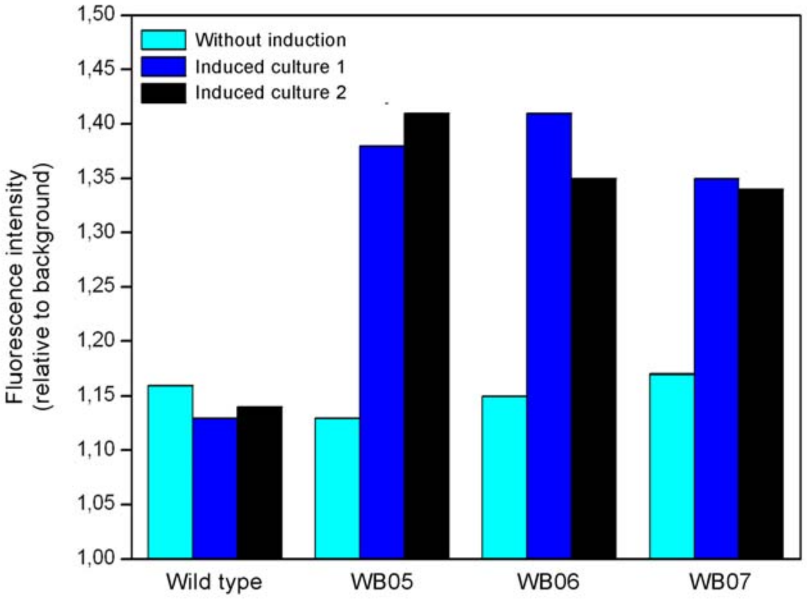

Figure 3.4: Stability of the putative FtsL cleavage product in vivo. Shown is the average brightness of GFP fluorescence relative to background for one not induced culture and two cultures induced with 0.5 % xylose. Strains overexpressing a GFP-FtsL1-43 fragment (WB05) or the mutated GFP-FtsL1-43^{DD} fragment (WB06) were compared to a wild type control. Additionally the influence of ClpXP on the fragment stability was shown with a strain overexpressing the GFP-FtsL1-43 fragment in a Δ*clpX* background (WB07).

Taken together all data indicate that the putative FtsL fragment does not have a cell cycle related function. Instead it seems possible, that RasP cleavage is only required to remove FtsL from the membrane. After cleavage the cytosolic fragment seems to be rapidly degraded. However, a final proof that RasP results in exactly this N-terminal FtsL1-43 fragment is lacking. Therefore it cannot be completely ruled out that an effector is released upon cleavage.

3.2 In vitro proteolysis of FtsL by RasP

The degradation of FtsL by RasP had previously been studied in vivo [Bramkamp et al., 2006]. However, to determine the cleavage site and mechanism an in vitro assay is necessary. To establish such an assay FtsL as well as protease needed to be purified. The group of Dr. Jan Löwe (MCR Cambridge) had already established a purification protocol for RasP.

3.2.1 Purification of FtsL

For purification FtsL was heterologously expressed in *E. coli* BL21 (DE3). The pET16b plasmid was used, that fuses a 10x His-tag to the N-terminus of the protein. An expression test showed a maximum yield of FtsL two hours after induction with 1mM IPTG (Fig. 3.5).

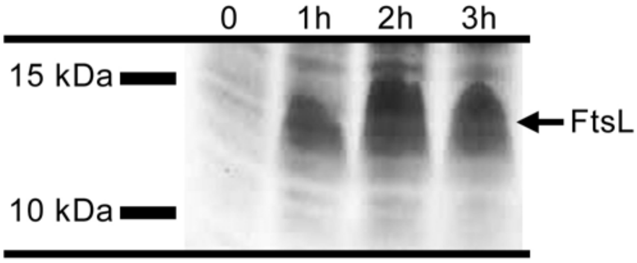

Figure 3.5: Overexpression of FtsL in *E. coli* BL21 (DE3). Induction was done by addition of IPTG to a final concentration of 1 mM. Shown are total cell lysates on a 10 % Schaegger gel stained with Coomassie. Samples were taken before induction and 1, 2 and 3 hours after addition of IPTG.

One major issue during FtsL purification was the solubilisation of the protein. Only a small amount of FtsL was solubilised using 1 % DDM. To optimise the solubilisation several non-ionic detergents were tested (Fig 3.6). *E. coli* membranes were treated with 1 % of each detergent and afterwards spun down to compare the FtsL amount in the soluble and in the membrane fraction. LAPAO was able to solubilise most of the protein, according to the FtsL signal in the membrane fraction after LAPAO treatment. It also showed the highest FtsL amount in the soluble fraction. However, when the solubilisation was upscaled to greater amounts of cell membranes, most of FtsL still stayed in the membrane fraction (data not shown). Therefore, the conditions for solubilisation with LAPAO were further optimised. The influence of detergent concentration, pH and salt concentration was tested. Increasing the LAPAO concentration over 1 % did not have a significant effect on solubilistion (data not shown).

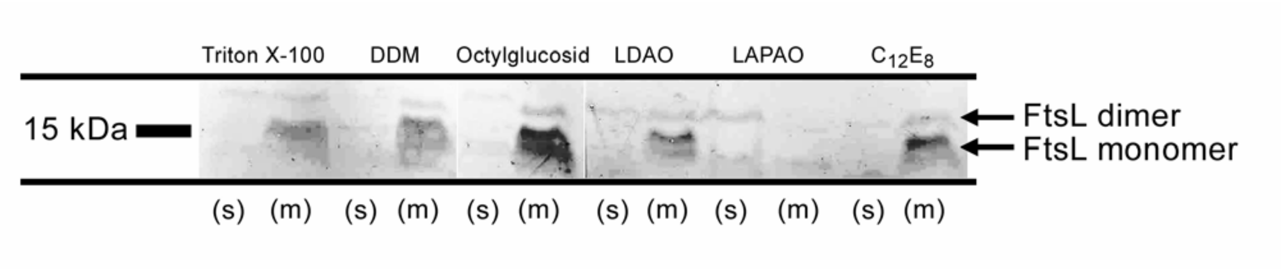

Figure 3.6: Testing of different detergents for FtsL solubilisation. Shown are Western blots of 10 % Schaegger gels treated with α-PentaHis and α-Mouse IgG-AP for FtsL detection in the soluble fraction (s) and the membrane fraction (m) after treatment with 1 % detergent.

To test the influence of the pH value the solubilisation was carried out with 1 % LAPAO with varying pH from 6.0 to 9.0 in steps of 0.5 pH. In all cases most of FtsL remained in the membrane fraction (Fig. 3.7). The significant protein overload in the membrane fraction samples led to broad bands, smearing from the height of a monomer band to the height of a dimer band and higher. The highest amount of solubilised FtsL was observed at pH 7.5, though overall the effect of the pH value was rather low.

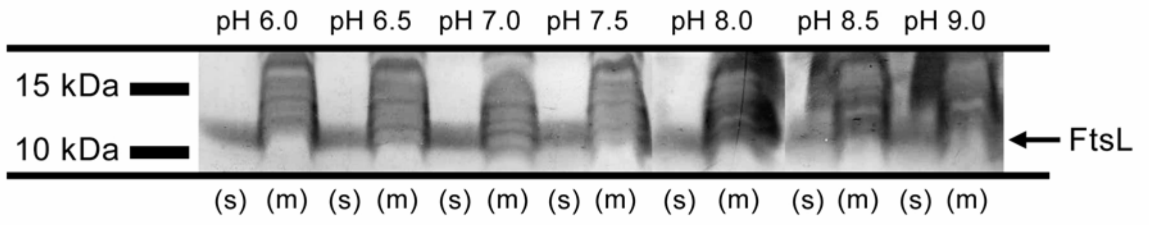

Figure 3.7: Influence of the pH value on FtsL solubilisation with LAPAO. Shown are Western blots of 10 % Schaegger gels treated with α-PentaHis and α-Mouse IgG-AP for FtsL detection in the soluble fraction (s) and the membrane fraction (m).

When non ionic detergents are used for solubilisation, optimising the salt concentration can make a significant difference [Too and Hanley, 1988], [Little et al., 1994], [Arnold and Linke, 2008]. Therefore solubilisation was carried out at different NaCl concentration ranging from 10 mM to 500 mM (Fig. 3.8 a). An increase in NaCl concentration led to an increased efficiency of the solubilisation. In the presence of 500 mM NaCl the highest amount of FtsL was detected in the soluble fraction. To test whether the solubilisation could be further optimised at even higher salt concentrations, the experiment was repeated with NaCl concentration between 500 mM and 2 M. In addition the effect of KCl compared to NaCl was tested. The results showed that NaCl had a stronger effect than KCl (Fig. 3.8 b). The solubilisation efficiency was further increased at high salt concentration compared to 500 mM. The best solubilisation efficiency was obtained at 1.5 M NaCl. Yet for FtsL purification the solubilisation was done with 1 % LAPAO and 500 mM NaCl. Higher salt concentrations would cause problems during binding to affinity columns.

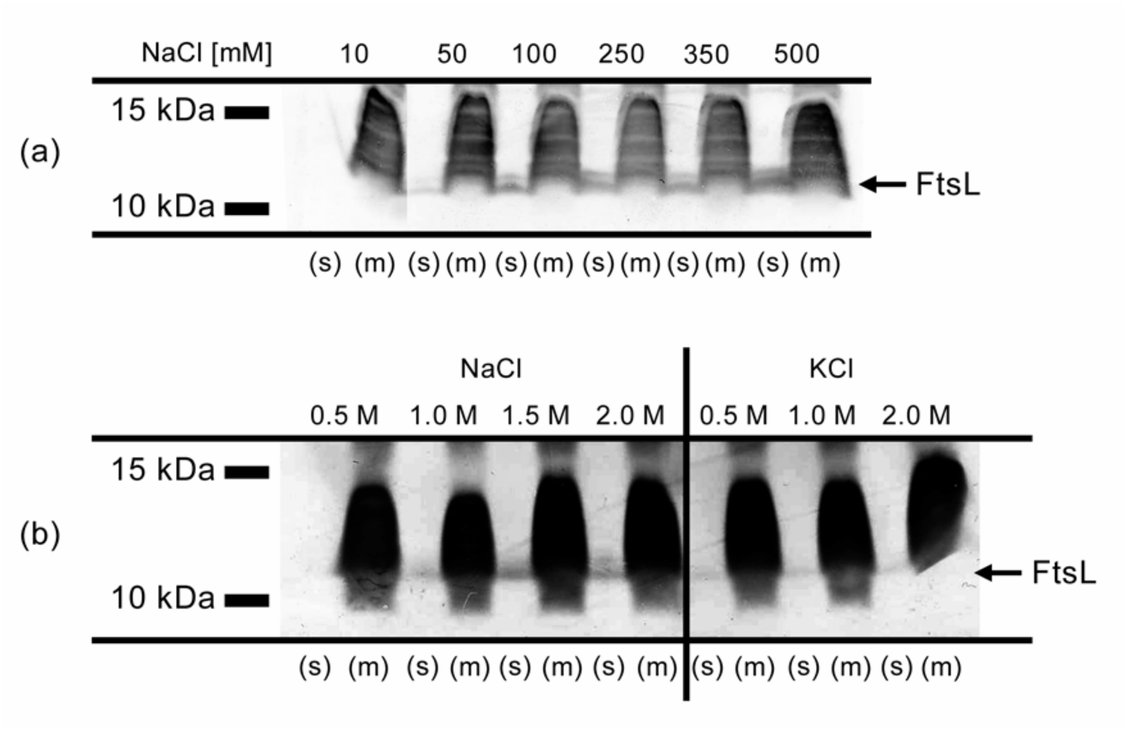

Figure 3.8: Influence of the salt concentration on FtsL solubilisation with LAPAO. Shown are Western blots of 10 % Schaegger gels treated with α-PentaHis and α-Mouse IgG-AP for FtsL detection in the soluble fraction (s) and the membrane fraction (m). (a) Solubilisation in the presence of different NaCl concentrations. (b) Solubilisation at high concentrations of of NaCl or KCl.

Even after optimisation only a very low amount of protein could be solubilised from the *E. coli* membranes. This is surprising as FtsL is a small protein with only one transmembrane domain and it is not extremely hydrophobic compared to other membrane integral proteins.

The difficulties solubilising FtsL could indicate direct binding to lipids. This might also explain why FtsL bands in SDS gels are usually rather diffuse and blot poorly to PVDF membranes. Another possibility is that FtsL forms complexes, which could then be difficult to solubilise.

In the past affinity purification of FtsL was unsuccessful. His-tagged FtsL did not bind to affinity columns, neither under native nor under denaturing conditions. GST or Strep affinity tagging did not solve the problem [Errington, personal communication]. The previous results from the solubilisation experiments suggested the possibility of lipid binding to FtsL. This could negatively influence the binding of FtsL to a column matix. Protein precipitation with ammonium sulfate might reduce the lipid content of the FtsL samples. To test whether precipitation could increase binding to a Ni-affinity column, solubilised FtsL was either directly applied to a Protino Ni-IDA 1000 column or first precipitated with ammonium sulfate and afterwards loaded to the column.

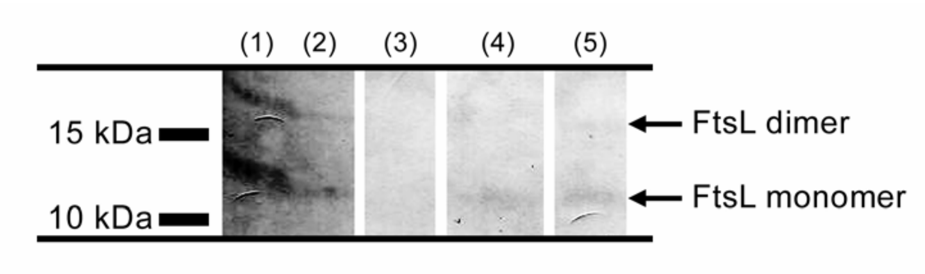

Figure 3.9: Ni-affinity purification of FtsL after ammonium sulfate precipitation. Western blot of a 10 % Schaegger gels treated with α-PentaHis and α-Mouse IgG-AP for FtsL detection. Lanes show flowtrough (1 and 2), washing (3), elution with 50 mM imidazole (4) and elution with 1 M imidazole (5).

Without prior precipitation no FtsL bound to the column (data not shown). When the precipitated and resuspended FtsL was loaded to the column, most of the protein was still found in the flowthrough fractions (Fig 3.9, lanes 1 and 2). However, a small amount of FtsL could be eluted with imidazole (Fig. 3.9, lanes 4 and 5). Apparently lipid impurities were indeed decreased by the precipitation and this enables a small portion of the protein to bind to the column. Unfortunately, upscaling of ammonium sulfate precipitation did not result in increased amounts of protein precipitate. In a lot of cases too much lipid remained in the precipitate. Several times a proteinaceous lipid mass was floating on the buffer surface and could not be spun down.

During the experiments with ammonium sulfate precipitation another effect became notable. To run FtsL samples after precipitation on SDS gels, the ammonium sulfate had to be removed. This was done by precipitation with TCA and resuspension in sample buffer. After that treatment FtsL bands in Schaegger gels seemed more focused (Fig. 3.10). This raised the question, whether the effect was due to the precipitation with TCA or the prior ammonium sulfate precipitation. TCA precipitation was repeated with solubilised FtsL, which was not precipitated with ammonium sulfate before. Interestingly, the effect was also observed for these samples (Fig. 3.10). To test whether the effect was due to precipitation in general or a specific effect of TCA treatment, solubilised FtsL was precipitated with TCA or ethanol. In addition the membrane fractions after solubilisation were treated with TCA or ethanol as well, to obtain samples with a high FtsL concentration.

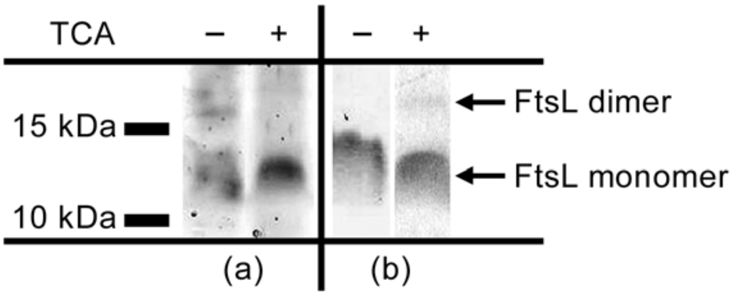

Figure 3.10: FtsL precipitation with TCA. Western blot of a 10 % Schaegger gels treated with α-PentaHis and α-Mouse IgG-AP for FtsL detection. (a) Bands of solubilised FtsL without prior ammonium sulfate precipiation. (b) Bands of solubilised FtsL previously precipitated with ammonium sulfate.

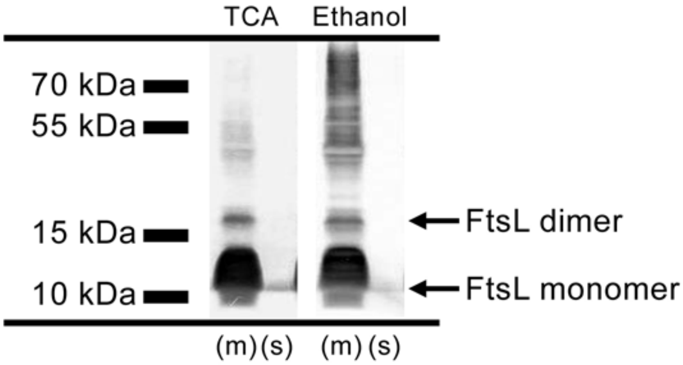

Figure 3.11: FtsL precipitation with TCA and ethanol. Western blot of a 10 % Schaegger gels treated with α-PentaHis and α-Mouse IgG-AP for FtsL detection. Shown are FtsL solubilisation samples of membrane fractions (m) and soluble fractions (s) after precipitation with TCA or ethanol.

Both precipitation methods resulted in relatively clear and focused FtsL bands (Fig. 3.11). This supports the idea that lipid impurities might cause unfocussed FtsL bands. A very surprising effect was observed after ethanol precipitation. The highly concentrated FtsL in the membrane fraction was not only present as monomers and dimers, but also showed a lot of higher molecular complexes. To a much lesser extent these complexes were observed in the TCA treated membrane fraction as well. Apparently their assembly is concentration dependent as such complexes were not detected in blot of previous membrane fractions. By precipitating FtsL the concentration was increased and it seems likely that this promotes assembly of such complexes. It seems that precipitation with TCA was able to destroy most of the complexes while precipitation with ethanol did not. This indicates some sort of ionic interaction between the FtsL molecules. Ethanol would probably not influence these interaction to the same extent as TCA. The existence of high molecular FtsL complexes could explain the low solubilisation efficiency.

For the FtsL protein from *E. coli* it has been shown that formation of detergent resistant dimers is likely mediated by the C-terminal leucine zipper domain [Ghigo and Beckwith, 2000]. Therefore it was tested whether the C-terminal domain of *Bacillus subtilis* FtsL alone is able to form higher complexes. The extracellular domain of FtsL (AS 61-117) was cloned into the plasmid pET16b by which a 10x His-tag was fused to the N-terminus of the protein. It was expressed in *E. coli* BL21 (DE3) and purified according to the protocol for full-length FtsL (see chapter 1.3.6). The elution fractions after Ni-affinity chromatography were analysed by SDS-PAGE (Fig. 3.12).

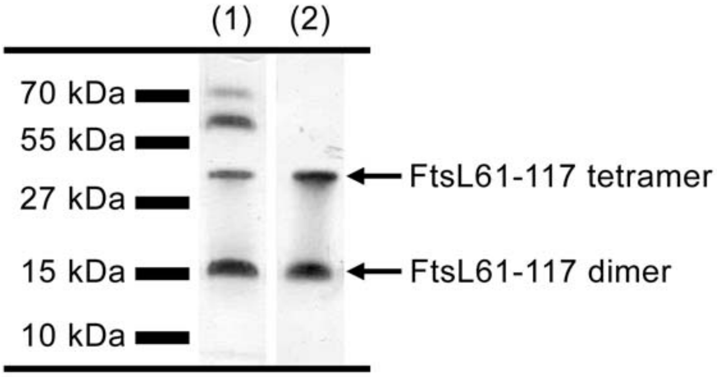

Figure 3.12: Oligomerisation of the C-terminal leucine zipper domain of FtsL. Shown are elution fractions after Ni-affinity chromatography. (1) 10% Schaegger SDS-Gel stained with Coomassie-Blue. (2) Blot of a 10% Schaegger SDS-Gel treated with α-PentaHis and α-Mouse IgG-AP.

Comparison of the Coomassie stained SDS-gel (Fig. 3.12, lane 1) and the immuno-blot (Fig. 3.12, lane 2) showed two protein impurities of higher molecular weight and two bands of FtsL61-117 detectable with α-PentaHis and α-Mouse IgG-AP. The molecular weight of the protein is ca 6.5 kDa. Therefore the height of the FtsL61-117 bands corresponded approximately to the molecular weight of dimers and tetramers. Obviously FtsL oligomer formation can be mediated by the C-terminal domain. The fact that tetramers were detectable indicates that more than one interaction site exists within this domain. This further supports the idea of high molecular FtsL complexes.

In order to overcome the problems due to aggregation and complex formation, we got plasmids and a different protocol for FtsL purification (Jan Löwe, MCR, personal communication). The C-terminus of FtsL was fused with a His-tag for affinity chromatography and the N-terminus of FtsL was fused to a maltose-binding protein (MBP). In this case MBP served as a big, soluble tag to prevent aggregation. Further purifications were therefore done with MBP-FtsL.

3.2.2 Purification of MBP-FtsL/MBP-FtsL$^{\Delta C}$

MBP-FtsL was expressed in *E. coli* BL21 (DE3) cells and purified according to the protocol described in chapter 2.4.7. The solubilisation efficiency was dramatically enhanced using the MBP-fusion protein. Also most of the protein was able to bind to a Ni-affinity column. The original protocol from the group of Jan Löwe included a second chromatography step using gel filtration. Purifying MBP-FtsL on a Superdex200 gel filtration column significantly increased the purity, but also led to loss of 60-80 % of the protein (data not shown). Therefore only Ni-affinity chromatography was carried out (Fig. 3.13). The MBP-FtsL was then directly reconstituted into liposomes from *E. coli* lipids.

As mentioned before it is not known whether RasP can cleave full-length FtsL or requires initial processing of FtsL by an unknown site-1-protease. To mimic a possible site-1-cleavage a truncated form of FtsL was purified (MBP-FtsL$^{\Delta C}$). This construct contained an N-terminally MBP-fused FtsL, which was truncated at the C-terminus and fused to His-tag. Unfortunately the exact site of truncation was not communicated. Overexpression of MBP-FtsL$^{\Delta C}$ in *E. coli* BL21 (DE3) resulted in significantly higher protein levels compared to the full length MBP-FtsL. The eluted protein samples after Ni-affinity chromatography were in general of high purity (Fig. 3.14).

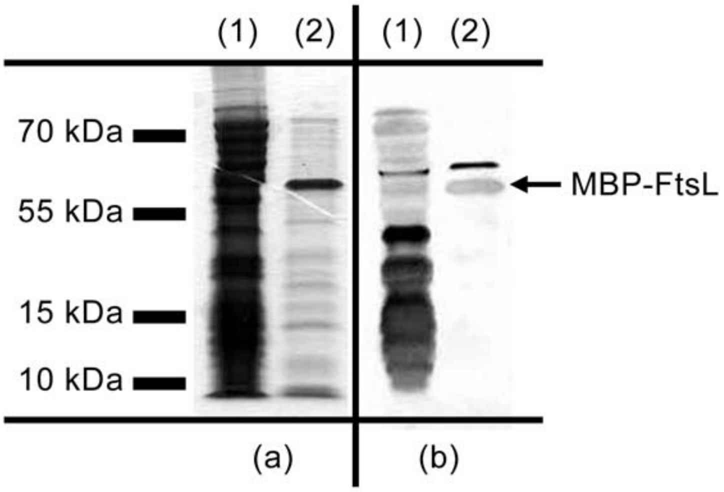

Figure 3.13: Ni-affinity chromatography of MBP-FtsL showing total *E. coli* BL21 (DE3) membranes (1) and elution fraction (2). (a) 10% Schaegger SDS-Gel stained with Coomassie-Blue. (b) Blot of a 10% Schaegger SDS-Gel treated with α-PentaHis and α-Mouse IgG-AP.

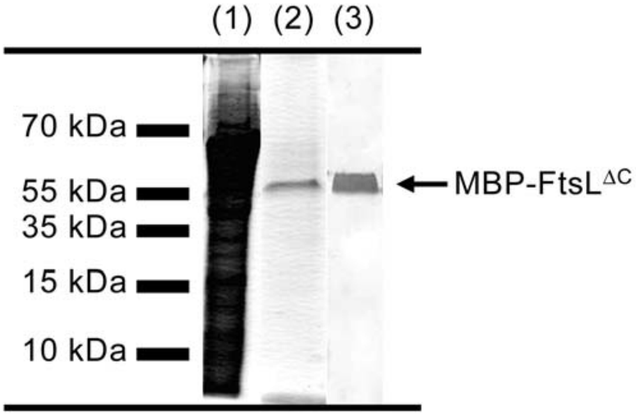

Figure 3.14: Ni-affinity chromatography of MBP-FtsL$^{\Delta C}$. (1) + (2) Samples of total *E. coli* BL21 (DE3) membranes and elution fraction run on a 10% Schaegger SDS-Gel stained with Coomassie-Blue. (3) Blot of the elution fraction treated with α-PentaHis and α-Mouse IgG-AP.

3.2.3 Purification of RasP

Expression of N-terminally His-tagged RasP in *E. coli* BL21 (DE3) is toxic and leads to cell lysis even at low induction levels [Bürmann, 2007]. To overexpress RasP for purification, a His-tag was fused to the C-terminus of the protein and it was expressed in *E. coli* BL21 A1 cells. Unfortunately, the expression levels were very low. Therefore cells were induced at a relatively high optical density (OD_{600} 3.0) and cultivation was done in a 100 litre fermenter to obtain a sufficient amount of cell pellet. For each purification attempt at least 70-80 g of cell pellet were used. Another problem was that RasP seemed to be rather unstable in detergent solution [Löwe, personal communication]. This implied that a proteolysis assay in solution could be a problem. Also it was not clear, whether RasP as an intramembrane protease would require a insertion into a lipid bilayer to effectively cleave its substrate. Therefore an assay carried out in artificial liposomes containing FtsL and RasP might be more successful. To this end the proteins were purified and then reconstituted into liposomes made from *E. coli* lipids (see chapter 2.4.10 and 2.4.10).

RasP was purified by two chromatography steps. First the solubilised protein was applied to a Ni-affinity column. The second step was an anion exchange chromatography after which the protein was directly reconstituted into liposomes (Fig. 3.15). There were still impurities visible in the proteoliposome samples. Unfortunately, a third chromatography step is not possible, due to the mentioned instablity of RasP in detergent solution. After an additional purification step the protein would be denatured and inactive.

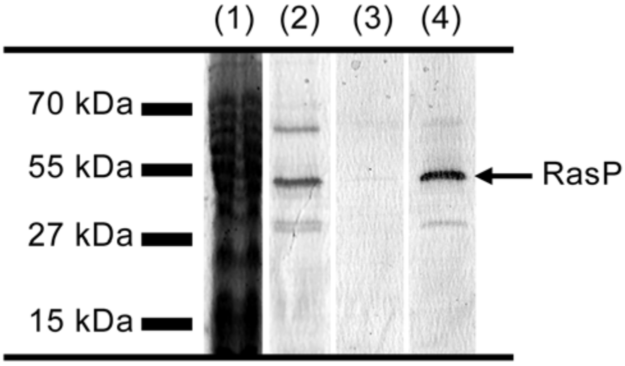

Figure 3.15: Example of a RasP purification. 10% Schaegger SDS-Gel stained with Coomassie-Blue. Shown are samples of (1) total *E. coli* BL21 A1 membranes, (2) elution fraction after Ni-affinity chromatography, (3) elution fraction after gel filtration and (4) proteoliposomes

3.2.4 In vitro proteolysis assays

To bring MBP-FtsL or MBP-FtsL$^{\Delta C}$ and RasP together in a lipid bilayer, the previously prepared proteoliposomes were mixed. New proteoliposomes containing FtsL as substrate and the protease were created by the method described under 2.4.12. As RasP is a zinc-metallo protease a sample with 1 mM EDTA was used as a preliminary negative control. The first experiment compared proteolysis of the full length MBP-FtsL and MBP-FtsL$^{\Delta C}$ after 3h at 30°C (Fig. 3.15). While *Bacillus subtilis* shows a growth optimum at 37°C a lower temperature was used to avoid problems with the liposomes such a flipping of lipids and proteins. No degradation could be seen in the MBP-FtsL sample (Fig. 3.16, lane 3). In contrast a small amount of the MBP-FtsL$^{\Delta C}$ seemed to be degraded, resulting in a weak degradation band with a size of ca. 45 kDa (Fig. 3.16, lane 6). As only a very small percentage of the protein was cleaved, it is possible that the MBP-FtsL concentration was simply not high enough to detect degradation. But as MBP-FtsL$^{\Delta C}$ seemed to be a substrate of RasP the experiments were continued using this protein.

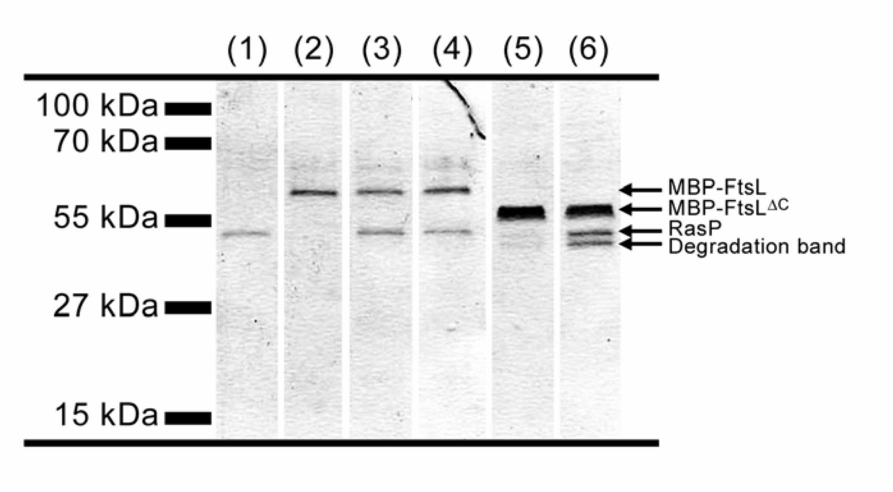

Figure 3.16: Degradation of MBP-FtsL and MBP-FtsL$^{\Delta C}$ by RasP purification. 10% Schaegger SDS-Gel stained with Coomassie-Blue. Shown are samples of liposomes containing (1) RasP, (2) MBP-FtsL, (3) MBP-FtsL and RasP, (4) MBP-FtsL, RasP and 1mM EDTA, (5) MBP-FtsL$^{\Delta C}$ and (6) MBP-FtsL$^{\Delta C}$ and RasP.

The small amount of cleaved MBP-FtsL$^{\Delta C}$ raised the question whether this was due to a very low turnover. Usually specific proteolysis should lead to high turnover rates. However, in an in vitro assay in detergent described for RseP, the *E. coli* homologue of RasP, a very low turnover was observed as well [Li et al., 2009]. To further investigate this, another proteolysis assay with MBP-FtsL$^{\Delta C}$ was carried out and samples for SDS-PAGE were taken between 30 minutes and three hours and additionally one overnight sample (Fig. 3.17). The time series showed that the amount of degraded MBP-FtsL$^{\Delta C}$ significantly increased between three hours and the overnight sample, suggesting that the turnover is indeed low. It has been shown, that in vivo RasP activity is influenced by the ABC transporter EcsAB [Heinrich et al., 2008]. In an EcsAB mutant strain no RasP activity was observed. Although it is not clear if this is a direct or indirect effect, it shows that in vivo RasP activity is affected by other factors. Therefore, it seems possible that in an in vitro system the proteolytic activity is drastically decreased.

In the negative control samples treated with 1mM EDTA there was still degradation detectable, though the turnover was clearly lower than without EDTA. This showed that MBP-FtsL$^{\Delta C}$ was degraded by a metallo-protease which could not be completely inactivated by addition of EDTA.

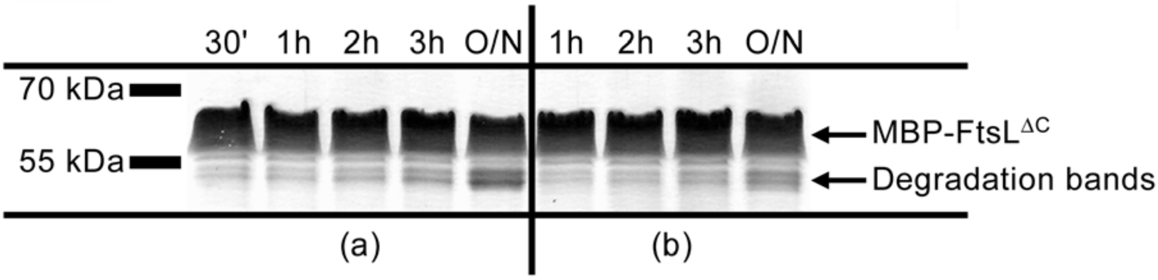

Figure 3.17: Time series of MBP-FtsL$^{\Delta C}$ proteolysis by RasP purification. 10% Schaegger SDS-Gel stained with Coomassie-Blue. Shown are samples of mixed liposomes containing MBP-FtsL$^{\Delta C}$ and RasP taken up to three hours after of incubation at 30°C and one overnight sample. (a) Proteolysis assay without EDTA. (b) Proteolysis assay with 1 mM EDTA as negative control.

The time series experiment revealed another interesting fact about the MBP-FtsL$^{\Delta C}$ proteolysis. Degradation of the substrate does not lead to one degradation band, but a double band. This was not detectable in the beginning, as the higher degradation band co-migrates with the RasP band in the SDS gels. In the overnight sample it became very clear, that the intensity of this band is increasing meaning it is most likely a second degradation band. Both bands correspond to sizes indicating that the maltose binding protein must still be fused to this degradation product. In accordance to this both degradation bands were not visible on a Western blot treated with α-Penta His and α-Mouse IgG-AP (data not shown). As the His-tag was fused to the C-terminus of MBP-FtsL$^{\Delta C}$ both bands must represent N-terminal cleavage products containing MBP. The other cleavage product of the MBP-FtsL$^{\Delta C}$ protein should have a size of ca. 5 kDa. It was neither detected on the Coomasssie stained SDS-gels nor on the Western blot. This could be a problem of the resolution of the small SDS-gels. Though Schaegger gels were used to enhance the separation of small peptides for detection of these cleavage products gradient gels will likely be necessary.

As this assay was done in liposomes several factors had to be optimised. Ideally the mixed liposomes should contain several molecules of MBP-FtsL$^{\Delta C}$ per RasP molecule. To obtain such liposomes the best ratio of MBP-FtsL$^{\Delta C}$ proteoliposomes to RasP proteoliposomes needed to be determined. To this end 50 µl of MBP-FtsL$^{\Delta C}$ proteoliposomes were mixed with 10-50 µl of RasP containing liposomes according to the protocol described under 2.4.12 and incubated at 30°C for several hours. The substrate degradation was analysed by SDS-PAGE (Fig. 3.18).

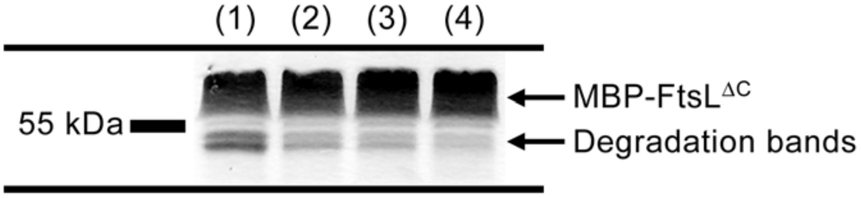

Figure 3.18: MBP-FtsL$^{\Delta C}$ proteolysis with different RasP concentrations. 10% Schaegger SDS-Gel stained with Coomassie-Blue. Shown are samples of 50 µl MBP-FtsL$^{\Delta C}$ proteoliposomes mixed with (1) 10 µl RasP proteoliposomes, (2) 30 µl RasP proteoliposomes, (3) 50 µl RasP proteoliposomes and (4) 50 µl RasP proteoliposomes and EDTA as a negative control.

Surprisingly an increasing addition of RasP proteoliposomes to the assay decreased MBP-FtsL$^{\Delta C}$ proteolysis. The strongest degradation bands were observed upon addition of 10 µl RasP proteoliposomes. There are different possible explanations for this effect. As the protein concentration in the MBP-FtsL$^{\Delta C}$ containing liposomes was significantly higher than in the RasP proteoliposomes, this might be a dilution effect. However, there was almost no difference in degradation efficiency between the samples containing 30 µl or 50 RasP µl proteoliposomes. In case of a dilution effect of MBP-FtsL$^{\Delta C}$ a difference should still be visible. A more likely possibility is that the liposome concentration during extrusion influenced the result. For the samples containing less than 50 µl RasP proteoliposomes the final volume was adjusted with buffer. As the MBP-FtsL$^{\Delta C}$ proteoliposome solution was very concentrated, this could have an effect. The extrusion of the liposome mixture is the critical point to ensure an even dispersion of both proteins in the final proteoliposomes. A to concentrated liposome solution could cause blocking of the membrane pores and a less efficient extrusion. To ensure comparable liposome concentrations in each sample for all further experiments the sample volumes were adjusted with liposomes containing no proteins. Therefore the proteoliposome mixture was diluted with buffer prior to extrusion.

To further analyse the degradation products the assay was carried out again and samples were run on a 10% Schaegger gel and 10-20 % gradient gel by BioRad (Fig. 3.19). As the EDTA treated samples showed degradation by endogenous *E. coli* metallo-proteases, an active site mutant RasP-E21A was purified and used for negative controls.

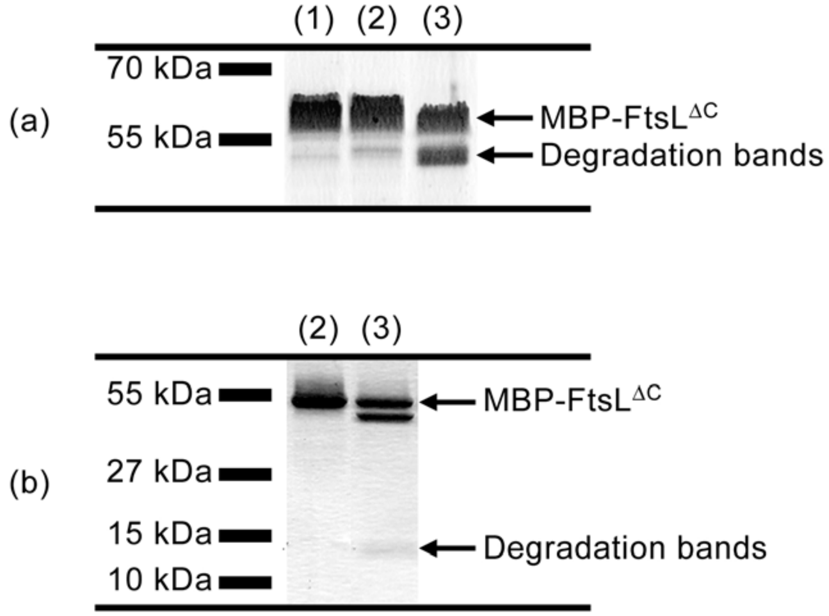

Figure 3.19: MBP-FtsL$^{\Delta C}$ proteolysis assay. (a) 10% Schaegger SDS-Gel stained with Coomassie-Blue. (b) 10-20% Gradient SDS-Gel stained with Coomassie-Blue. Shown are samples of (1) MBP-FtsL$^{\Delta C}$ proteoliposomes, (2) mixed proteoliposomes containing MBP-FtsL$^{\Delta C}$ and RasP-E21A and (3) mixed proteoliposomes containing MBP-FtsL$^{\Delta C}$ and RasP.

The degradation bands were again detected in the samples containing RasP, but not in the samples containing RasP-E21E. The SDS-PAGE using the gradient gel revealed a weak double band at ca. 13 kDa. This would correspond to the size of FtsL$^{\Delta C}$ without the maltose binding protein. The amount of degraded MBP-FtsL$^{\Delta C}$ proetolysis was increased compared to previous experiments, but still relatively low. To test if MBP-FtsL$^{\Delta C}$ proetolysis can be increased by a higher RasP concentration, a five fold higher amount of the protease containing liposomes were added. However, MBP-FtsL$^{\Delta C}$ proetolysis was not significantly increased (data not shown). This did not seem to be a liposome concentration effect as observed before. One explanation might be the orientation of MBP-FtsL$^{\Delta C}$ in the liposomes. Examples from other intramembrane proteases suggest that substrate and protease most likely need to be orientated in the same direction to allow proteolysis (see chapters 1.3.2 and 1.3.3). The fusion of the big soluble MBP-tag to the cytosolic N-terminus of FtsL$^{\Delta C}$ could lead to mostly inside-out orientation. The RasP protease only contains an extracellular PDZ domain as a soluble domain. It is questionable though, whether this would be sufficient to enhance an inside-in orientation. RasP might as well be statistically inserted in both orientations. Yet, it was possible, that only a small portion of the MBP-FtsL$^{\Delta C}$ was present in an orientation matching the protease and therefore degradation was not increased by addition of more protease liposomes.

As mentioned above four degradation bands were detected (Fig. 3.19). The corresponding sizes of the fragments were approximately 12 kDa, 14 kDa, 42 kDa and 45 kDa. Apparently two different cleavage events took place. Most likely resulting in two degradation products containing MBP (42 kDa and 45 kDa) and two cleavage products containing the remaining FtsL$^{\Delta C}$ fragments (12 kDa and 14 kDa). All four bands were cut from the gels and send to a service lab (Prof. Dr. Hanisch, Center for Molecular Medicine, University of Cologne) for peptide mass fingerprint analysis. For the complete analysis of the mass spectrometry data see supplement, Fig. S1-S4.

The results showed that indeed the bands at 42 kDa and 45 kDa both contained MBP. However, no additional part of fused FtsL$^{\Delta C}$ was detectable. Considering the analytic method this might simply be due to the MBP making up most the mass. In addition peptide mass fingerprint usually rarely leads to 100 % sequence coverage for membrane proteins. RasP was identified in the 45 kDa product band showing that this cleavage product co-migrated with the protease. Analysis of the 12 kDa and 13 kDa bands only led to a result for the 14 kDa band. The protein could be identified as FtsL$^{\Delta C}$. From the sequence coverage it seemed FtsL$^{\Delta C}$ was not truncated except that the MBP-tag was removed. This was in accordance with the migration in the SDS gel (Fig. 3.19 b), as a band of complete FtsL$^{\Delta C}$ should be detected around this height. It therefore seemed likely that endogenous *E. coli* membrane proteases cleaved the MBP-FtsL$^{\Delta C}$ protein and the band at 42 kDa contained the removed MBP-tag. This cleavage is visualised in Figure 3.20 a.

The question was which products were produced by the second cleavage event. Based on the putative cleavage site identified by sequence alignment of FtsL and RsiW, intramembrane cleavage by RasP should result in a ca. 8 kDa C-terminal FtsL fragment. The corresponding 5 kDa FtsL fragment should still be fused to MBP, resulting in a band of ca. 47 kDa. This is not in accordance with the detected bands in the gradient gel (see Fig. 3.19b). The second degradation band clearly did not correspond to molecular weight below 10 kDa. A FtsL fragment with a size of ca. 12 kDa would be produced if the protein was cut within its cytosolic domain, close to the N-terminus as visualised in Figure 3.20 b. It seems unlikely that RasP would cleave FtsL at such a site, though it cannot be completely ruled out. As the protein of the 12 kDa band unfortunately was not identified by peptide mass fingerprint, all interpretations must remain purely speculative. Still, taken together the results rather indicated that MBP-FtsL$^{\Delta C}$ was degraded by endogenous *E. coli* membrane proteases.

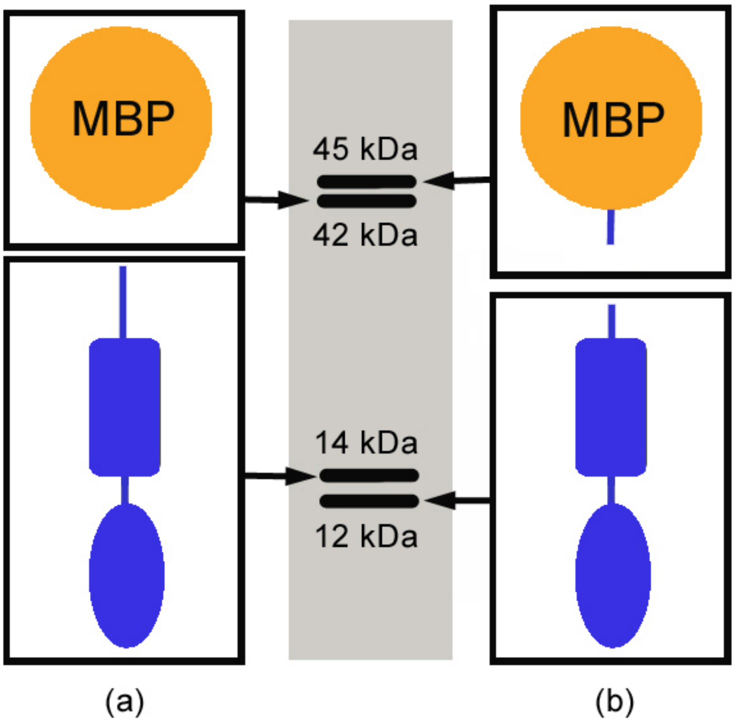

Figure 3.20: Scheme of the possible MBP-FtsL$^{\Delta C}$ degradation band pattern. Shown are degradation products of to possible cleavage events. (a) Removal of the MBP-tag resulting in two bands corresponding to sizes of ca. 42 kDa and 14 kDa. (b) Cleavage within the N-terminal FtsL$^{\Delta C}$ domain resulting in two bands corresponding to sizes of ca. 45 kDa and 12 kDa. The maltose binding protein tag is illustrated in orange, the FtsL$^{\Delta C}$ protein in blue.

This raised the question why no obvious RasP cleavage was observed. As mentioned above the orientation of FtsL might prevent degradation by RasP. To test how much of the MBP-FtsL$^{\Delta C}$ protein was orientated inside-out a specific digestion with TEV-protease was carried out. The protein displays a TEV cleavage side in the linker region between MBP and FtsL$^{\Delta C}$ designed to remove the tag when necessary. As TEV should not be able to diffuse across the membrane into the proteoliposomes, it could only cleave outside orientated MBP from the FtsL$^{\Delta C}$ N-terminus. MBP-FtsL$^{\Delta C}$ proteoliposomes were treated with TEV for two hours at 30°C. Then they were spun down to separate the soluble MBP from the proteoliposomes. To avoid a loss of liposomes no additional washing step was carried out. Samples of the total proteoliposome mixture after TEV treatment as well as the soluble and the proteoliposome fraction were seperated on a 10 % Schaegger gel (Fig. 3.21).

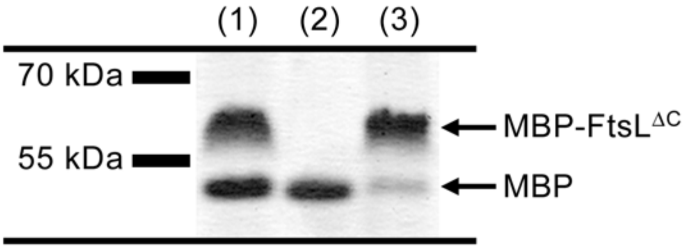

Figure 3.21: TEV cleavage of reconstituted MBP-FtsL$^{\Delta C}$. 10% Schaegger SDS-Gel stained with Coomassie-Blue. Shown are samples of (1) complete proteoliposome mixture after TEV cleavage, (2) soluble fraction and (3) proteoliposome fraction.

The sample of total proteoliposome mixture after TEV treatment shows two bands. The size of the upper band correlates to MBP-FtsL$^{\Delta C}$ and the size of the lower bands corresponds to the size of MBP. After separating the proteoliposomes from the soluble fraction the lower band was indeed found in the soluble fraction. Some free MBP could be detected in the proteoliposomes fraction as well together with all of the remaining MBP-FtsL$^{\Delta C}$. This is probably due to the fact that the proteoliposomes were not washed after centrifugation. In total less than 50 % percent of the MBP-FtsL$^{\Delta C}$ was cleaved by TEV. This indicated a statistic insertion of the protein in both directions and ruled out protein orientation as the main problem of the proteolysis assay. It was more likely that the purified protease was not active. This idea was further supported by the fact that all attempts failed to reproduce the results of the MBP-FtsL$^{\Delta C}$ proteolysis assay. No degradation bands of were observed (data not shown). As mentioned before the group of Jan Löwe suggested that RasP is prone to instability after 24-30 hours of purification procedure. It was hoped that reconstitution of RasP into liposomes would have a stabilising effect. However, reconstitution also requires incubation at room temperature for more than two hours in total. To test whether this and/or storage of the proteoliposomes led to inactivation of the protease, the proteolysis assay was repeated in detergent solution directly after the RasP purification. Unfortunately, still no degradation of MBP-FtsL$^{\Delta C}$ was detectable (data not shown).

It had been shown before, that in an *E. coli* co-expression system full-length FtsL seems to be a substrate of RasP [Bramkamp et al., 2006]. However, site-1-cleavage by an *E. coli* protease could not re ruled out. It was therefore not clear whether the purified MBP-FtsL and MBP-FtsL$^{\Delta C}$ really were substrates of RasP. To test if the protease was active in the proteolysis assay the second known substrate of RasP, the anti-sigma factor RsiW, was used as a control. In contrast to FtsL for RsiW the site-1-protease is known [Heinrich and Wiegert, 2006], [Ellermeier and Losick, 2006] and a truncated form of RsiW could be expressed in *E. coli* to mimic this cleavage.

3.2.5 Proteolysis assay with RsiW*

Previous studies showed that a truncated form of RsiW missing the complete C-terminal, extracellular domain (RsiW1-107, in the following abbreviated to RsiW*) was degraded in a *Bacillus subtilis* wildtype control, but stabilized in an *yluC::tet* background [Schöbel et al., 2004]. Apparently RasP is able to degrade this construct in vivo. Therefore RsiW* was chosen as a control substrate for RasP. For purification RsiW* was expressed in *E. coli* BL21 (DE3). Unfortunately most of the protein was present in inclusion bodies. As RsiW* is a relatively small protein of ca. 12 kDa it is reasonable that the protein is able to refold after denaturing of the inclusion bodies. Therefore, a His-tagged form of RsiW* was overexpressed and purified from inclusion bodies. After testing various refolding conditions, the protein was refolded in detergent containing solution as described under 2.4.9. Subsequently it was purified by Ni-affinity cromatography and directly reconstituted into liposomes made from *E. coli* lipids. Mixed proteliposomes containing RasP and RsiW* were created (see chapter 2.4.12). As a negative control liposomes containing RsiW* and RasP were treated with phenanthrolin, which is a metallo-protease inhibitor. The mixed proteoliposomes were incubated at 30°C for three hours and afterwards samples were analysed by SDS-PAGE (Fig. 3.22).

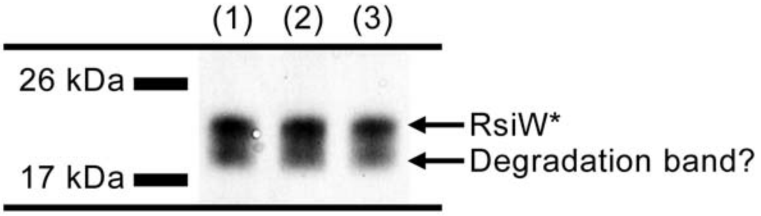

Figure 3.22: In vitro assay of RsiW* proteolysis by RasP. 10% Schaegger SDS-Gel stained with Coomassie-Blue. Shown are samples of (1) RsiW* proteoliposomes, (2) mixed proteoliposomes containing RsiW*, RasP and phenanthrolin as a negative control and (3) mixed proteoliposomes containing RsiW* and RasP.

There was no RasP specific degradation of RsiW* detectable, showing that most likely RasP was not active under this conditions. However, there seemed to be am unspecific degradation product present, resulting in a second band. The intensity of this band seemed reduced in the sample of the phenanthrolin negative control. It is possible that impurities of *E. coli* metalloproteases were present in this assay and led to degradation of RsiW*. Unfortunately the bands were rather diffuse, making it difficult to really judge this decrease in unspecific degradation. The proteolysis assay with RsiW* was repeated under different pH conditions as well as in detergent solution directly after RasP purification, but no RasP activity was observed. Taken together all data indicated that RasP was not active after purification. Optimising the purification protocol was extremely difficult due to the very low expression of RasP in *E. coli*. If less than 70g of cell pellet were used as starting material no RasP was detectable after the first chromatography step. Therefore, the proteolysis assay experiments in liposomes were not continued. Instead proteolysis of FtsL was studied in an *E. coli* co-expression system (see chapter 3.3).

3.3 Heterologous co-expression of RasP, FtsL and FtsL interaction partners

Because all attempts to establish a reproducible in vitro assay for FtsL degradation by RasP failed (see chapter 3.2) FtsL proteolysis was studied in an *E. coli* based co-expression system. It has been described before, that full length FtsL is degraded by RasP when co-expressed in *E. coli* [Bramkamp et al, 2006]. To reproduce this result *ftsL* and *yluC* were cloned into the co-expression vector pACYCDuet (Novagen). Overexpression *E. coli* BL21 (DE3) resulted in FtsL with a His-tag its N-terminus and RasP with an S-tag fused its C-terminus. As a negative control a pACYC vector with *ftsL* and *yluC-E21A* was constructed. The expression experiment was carried out according to the protocol described under 2.6.1. The FtsL concentration in the total cell lysate was analysed by SDS-PAGE and immuno-blotting (Fig. 3.23).

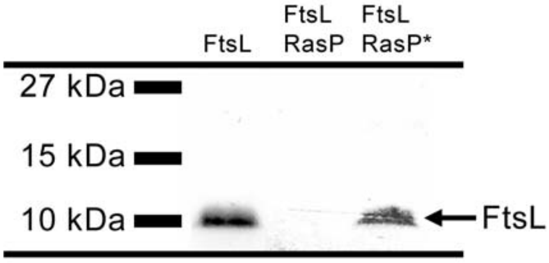

Figure 3.23: Co-expression of FtsL and RasP in *E. coli* BL21 (DE3). Shown are immuno-blots of 10% Schaegger SDS-gels. For FtsL detection blots were treated with α-PentaHis and α-Mouse IgG-AP. Proteins present in each strain after expression are noted on top. RasP-E21A was abbreviated to RasP*.

FtsL was expressed in the *E. coli* BL21 (DE3) cells. Co-expression of the catalytically inactive RasP-E21A (RasP*) led to accumulation of FtsL (Fig. 3.23, lane 3). The overall FtsL concentration was decreased compared to expression of FtsL alone. This was a general effect of RasP/RasP-E21A expression. Overexpression of S-tagged RasP in the Duet system did not lead to cell lysis as described before for N-terminally His-tagged RasP [Bürmann, 2007]. However, in all experiments co-expression of the protease lowered the overall protein expression, probably due to the burden of expressing multiple membrane proteins. As described before [Bramkamp et al, 2006] co-expression of active RasP resulted in FtsL degradation (Fig 3.23, lane 2). In addition to this simple substrate/protease assay, the influence of additional division proteins as DivIC and/or DivIB should be tested.

3.3.1 Co-expression of FtsL, DivIC and DivIB

Intramembrane proteases are often involved in regulatory proteolysis. This led to the suggestion of a model, that RasP might be able to cleave FtsL to regulate cell division [Bramkamp et al, 2006]. In this case RasP should most likely be able to degrade FtsL in the presence of its interaction partners. Although the late cell division proteins in *Bacillus subtilis* are interdependent in their recruitment to the division site [Errington and Daniel, 2001], [Daniel et al., 2006] DivIC and to a lesser extent DivIB have been suggested to interact tightly with FtsL within the divisome. They might even interact before recruitment to the divisome [Noirclerc-Savoye et al., 2005]. Co-expression of FtsL, DivIC and/or DivIB in *E. coli* should mimic the situation in the assembled divisome. It has already been shown, that FtsL and DivIC can interact in an *E. coli* system without interfering with *E. coli* cell division [Robichon et al., 2008]. Co-expression of DivIC and DivIB together with FtsL and RasP/RasP-E21A was achieved using a second co-expression plasmid. The genes *divIC* and *divIB* were cloned into pETDuet. DivIB was always expressed with a His-tag fused to its N-terminus, DivIC with am S-tag fused to its C-terminus. Table 3.1 shows an overview of all proteins with their respective tags and antibodies used for immuno-blotting.

Table 3.1: Overview of proteins expressed in the Duet co-expression system

Protein	**Expression plasmid**	**Tag**	**Antibody for immuno-blotting**
FtsL	pACYCDuet, MCS1	His-tag	α-PentaHis and α-Mouse IgG-AP
RasP/RasP-E21A	pACYCDuet, MCS2	S-tag	S-protein-AP conjugate
DivIB	pETDuet, MCS1	His-tag	α-PentaHis and α-Mouse IgG-AP
DivIC	pETDuet, MCS2	S-tag	S-protein-AP conjugate or α-DivIC and α-Rabbit IgG-AP

To first test the influence of DivIC and DivIB on each other and on FtsL combinations of the three proteins were co-expressed without RasP being present (Fig. 3.24). Co-expression of FtsL and DivIC led to increased concentrations of both proteins, suggesting that they generally stabilise each other, which supports earlier results [Robichon et al., 2008]. FtsL was mainly present as dimers. Such SDS-resistant dimers had already been observed for FtsL from *E. coli* [Ghigo and Beckwith, 2000]. It was not clear, whether this dimersation was an effect of the higher FtsL concentration or a DivIC specific effect. Co-expression of FtsL and DivIB had the same effect on oligomerisation. Only FtsL dimers were detected. As the overall concentration of FtsL was only slightly increased, it seem reasonable that this effect is DivIB specific.

Co-expression of DivIB and DivIC led to some interesting results. First off all, in contrast to the vivo data [Daniel et al., 2006] in the absence of FtsL the DivIC levels were not decreased by DivIB. On the contrary they seemed to be higher compared to DivIC expression alone. DivIB was degraded in the presence of DivIC. It seemed unlikely, that this was a DivIC specific effect. As both proteins were expressed to very high levels, DivIB degradation was more likely caused by the extremely high overall protein concentration in the membranes. Interestingly, most of the not degraded DivIB was slightly shifted to a band of a higher molecular weight. The size did not correspond to a DivIB dimer, but approximately to the size of a DivIB-DivIC heterodimer. However, this band was not observed on the blot detecting S-tagged DivIC. It might be possible, that the S-tag was not accessible in this dimer. The existence of a DivIB-DivIC heterodimer would contradict previous models that DivIC and DivIB do not directly interact in the absence of FtsL.

Additional co-expression of FtsL did not change the band patterns. FtsL was present as dimers, but DivIB was still shifted to a higher band and degraded. The DivIC levels were similar to the amount of DivIC when only DivIB was co-expressed.

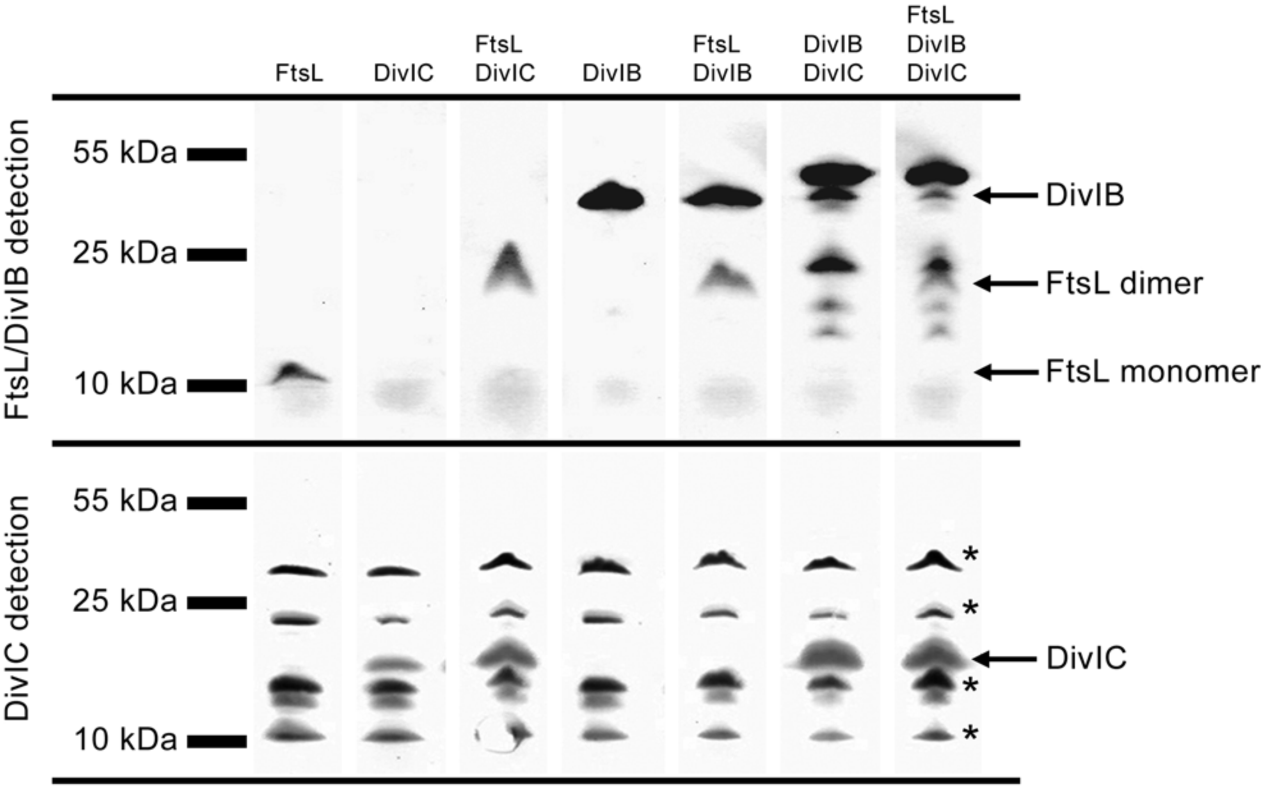
FtsL
DivIC
FtsL
DivIC
DivIB
FtsL
DivIB
DivIB
DivIC
FtsL
DivIB
DivIC
FtsL/DivIB detection
55 kDa
25 kDa
10 kDa
DivIB
FtsL dimer
FtsL monomer
DivIC detection
55 kDa
25 kDa
10 kDa
DivIC
*
*
*
*

Figure 3.24: Co-expression of FtsL, DivIB and DivIC in *E. coli* BL21 (DE3). Shown are immuno-blots of 10% Schaegger SDS-gels. For FtsL and DivIB detection blots were treated with α-PentaHis and α-Mouse IgG-AP and with S-protein-AP conjugate for DivIC detection. Unspecific bands were marked with asteriks. Proteins present in each strain after expression are noted on top.

These first results indicated that all of the proteins were able to directly interact with each other and that both DivIB and DivIC have an effect on FtsL dimerisation. In the case of DivIC this could be due to an increased FtsL concentration as well. To test this, co-expression of FtsL and DivIC was repeated at lower induction levels. *E. coli* BL21 (DE3) cultures were induced with 10 μM of IPTG instead of 100 μM of IPTG (Fig. 3.25).

The low induction still led to relatively good expression of DivIC, but the FtsL levels were significantly reduced. Co-expression of DivIC did not increase the FtsL concentration considerably. Most of the protein was present as monomers. A very weak dimer band was detectable when DivIC was co-expressed, which was not observed when FtsL was expressed alone. This indicated that the dimerisation of FtsL is concentration dependent, but is influenced specifically by DivIC as well. It is hard to judge, which influence is predominant at higher FtsL concentrations.

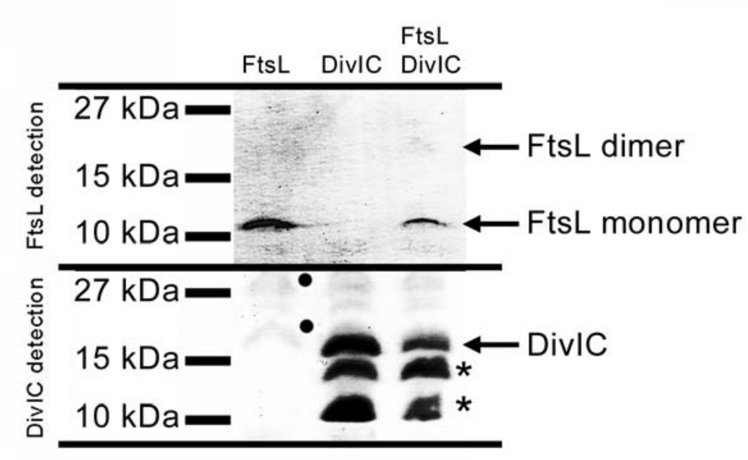

Figure 3.25: Co-expression of FtsL and DivIC in *E. coli* BL21 (DE3) after induction with 10 µM IPTG. Shown are immuno-blots of 10% Schaegger SDS-gels. For FtsL detection blots were treated with α-PentaHis and α-Mouse IgG-AP and for DivIC detection with α-DivIC and α-Rabbit IgG-AP. Unspecific bands were marked with circles, DivIC degradation bands were marked with asteriks. Proteins present in each strain after expression are noted on top.

It is also unclear, if FtsL is present as a dimer in vivo though its ability to form detergent resistant complexes in *E. coli* membranes would suggest that. Using α-DivIC for detection revealed general degradation of DivIC in the *E. coli* cells. Two distinct degradation bands were detected. As these bands were not visible on blots treated with S-protein-AP conjugate (see Fig. 3.24), DivIC is obviously degraded from the C-terminal end.

3.3.2 Co-expression of FtsL, DivIC and RasP

The experiments showed clearly that FtsL is able to interact with DivIC and DivIB in the Duet expression system. Both proteins can influence its oligomerisation and DivIC can furthermore stabilse FtsL against general proteolysis. To test whether DivIC and DivIB can stabilise FtsL against specific proteolysis by RasP strains were constructed co-expressing FtsL, RasP or RasP-E21A together with DivIC or DivIB. The protein concentrations in the total cell lysate were analysed by SDS-PAGE and immuno-blotting (Fig. 3.26). Unfortunately, it became clear, that co-expression of DivIB and the protease was toxic for the *E. coli* BL21 (DE3) cells. The overall protein concentration was very low and the OD_{600} values of these cultures were drastically lower compared to other RasP co-expression cultures. No FtsL was detectable even when only the inactive RasP-E21A mutant was co-expressed (data not shown). All future experiments were therefore carried out with DivIC as a FtsL interaction partner.

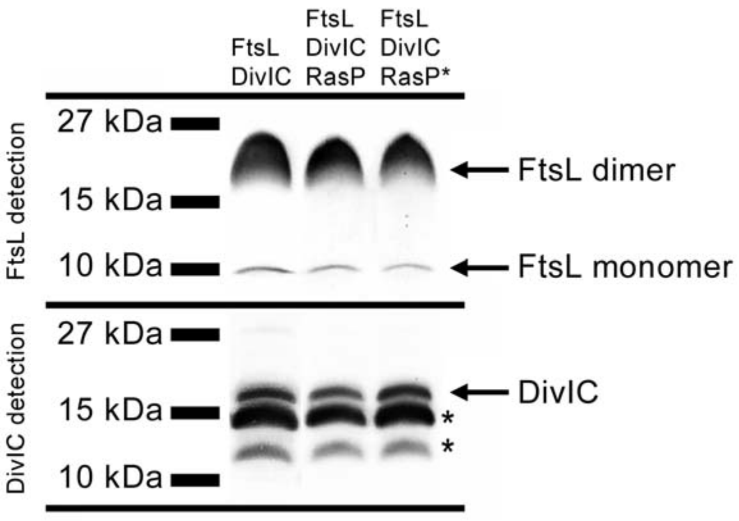

Figure 3.26: Co-expression of FtsL, DivIC and RasP in *E. coli* BL21 (DE3). Shown are immuno-blots of 10% Schaegger SDS-gels. For FtsL detection blots were treated with α-PentaHis and α-Mouse IgG-AP and for DivIC detection with α-DivIC and α-Rabbit IgG-AP. DivIC degradation bands were marked with asteriks. Proteins present in each strain after expression are noted on top. RasP-E21A was abbreviated to RasP*.

As expected from the previous experiments co-expression of FtsL, DivIC and RasP-E21A resulted in FtsL accumulation. The protein was mainly presents as dimers. Co-expression of FtsL, DivIC and active RasP led to the same FtsL concentration. The result showed that DivIC can protect FtsL against RasP cleavage. This indicates that RasP most likely cannot cleave FtsL from the division complex. The tight interaction of FtsL and DivIC should inhibit FtsL proteolysis by RasP as long as the proteins are assembled within the divisome.

3.3.3 Influence of the putative recognition motif on FtsL proteolysis

The fact that DivIC can stabilise FtsL against RasP cleavage raised the question, how this stabilisation is achieved. First hints came from in vivo studies indicating that substrate recognition is essential for FtsL proteolysis. As mentioned under 1.2.2 the N-terminal domain of FtsL bears a putative substrate recognition motif. Truncation or mutation of this motif significantly stabilised FtsL in vivo [Bramkamp et al., 2006]. However, in an in vivo system it was not possible to prove that this stabilising effect was a direct consequence of decreased degradation by RasP. Therefore it was tested whether this motif is required for FtsL degradation by RasP in the heterologous system. Plasmids were constructed to co-express a truncated and a mutated version of FtsL together with RasP or RasP-E21A.

For the truncated FtsL version (FtsL$^{\Delta N}$) 30 amino acids of the N-terminal domain were truncated resulting in a complete loss of the putative recognition motif 25-KKRAS-29. For the mutated FtsL (FtsL25B) the motif was altered to 25-KKAVA-29. Both proteins were expressed with a His-tag fused to the N-terminus. Samples were analysed by SDS-PAGE and immuno-blotting. Unfortunately, the FtsL$^{\Delta N}$ protein was not detectable in immuno-blots (Fig. 3.27 a), suggesting that this version was highly unstable. Only if DivIC was co-expressed the previously observed stabilisation effect led to detection of a FtsL dimer band. The results for the mutated FtsL25B are shown in Figure 3.27 b. Surprisingly, the mutation of the putative recognition motif led to relatively high FtsL25B levels, suggesting that the protein was generally stabilised by the mutation. About 50 % of the protein was present as dimers. As the dimerisation was shown to be concentration dependent (see chapter 3.3.1) it was unclear whether this was an effect of the mutation or caused by the high protein levels.

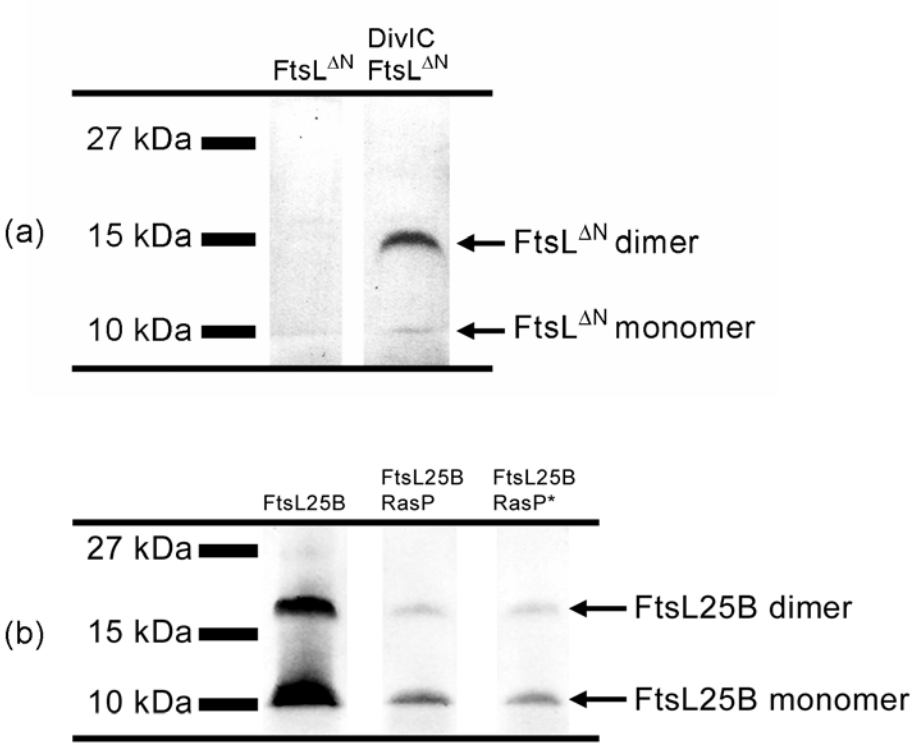

Figure 3.27: The effect of truncation or mutation of the putative recognition motif of FtsL. a) Expression of FtsL$^{\Delta N}$ in *E. coli* BL21 (DE3). b) Co-expression of FtsL25B and RasP in *E. coli* BL21(DE3). Shown are immuno-blots of 10% Schaegger SDS-gels. For FtsL detection blots were treated with α-PentaHis and α-Mouse IgG-AP. Proteins present in each strain after expression are noted on top. RasP-E21A was abbreviated to RasP*.

Additional expression of RasP or RasP-E21A reduced the FtsL25B concentration in general. Co-expression of active RasP led to the same levels of FtsL25B compared to co-expression of RasP-E21A. Obviously the mutation of the recognition motif inhibited degradation, showing that substrate recognition is essential for FtsL proteolysis by RasP. This strongly supported the idea that the stabilising effect observed in vivo [Bramkamp et al., 2006] was caused by inhibition of RasP cleavage.

Inhibiting substrate recognition could abolish FtsL cleavage. It might therefore be possible, that DivIC can stabilise FtsL against proteolysis by blocking recognition. Such a protection would only be possible, if the N-terminal domains of FtsL and DivIC were directly interacting with each other which. In case the N-terminal DivIC domain inhibits substrate recognition of FtsL, co-expression of full length FtsL and an N-terminally truncated DivIC should not result in FtsL stabilisation against RasP. On the other hand it was not clear whether FtsL would be able to form complexes with a truncated DivIC in *E. coli*. For the *E. coli* DivIC homologue, FtsB, it has been shown, that the transmembrane domain and a part of the C-terminal domain are necessary for interaction with FtsL [Gonzalez and Beckwith]. However, *E. coli* FtsB does not posses a cytosolic domain like DivIC from *Bacillus subtilis*. Therefore, it was completely unclear if truncation of this domain would influence the protein-protein interaction. To this end interactions of full-length and truncated versions of FtsL and DivIC were studied using a bacterial two-hybrid system.

3.3.4 Influence of the N-terminal domains of FtsL and DivIC on the protein-protein interactions

The bacterial two-hybrid assay is based on the complementation of adenylate cyclase activity. The adenylate cyclase from *Bordetella pertussis* can be separated into two parts, named the T18 and the T25 fragment after their molecular size. If both parts are brought into near vicinity of each other they interact and activity is restored. To study the protein interactions either the T18 or the T25 part of the adenylate cyclase was fused to the N-terminus of FtsL and DivIC and co-expressed in *E. coli* BHT101 cells. In addition the interactions of truncated FtsL (FtsL$^{\Delta N}$) and truncated DivIC (DivIC$^{\Delta N}$) without their respective N-terminal domains were investigated. Though the FtsL$^{\Delta N}$ protein had proved to be unstable in the *E. coli* BL21

(DE3) cells, fusion of the stable parts of the adenylate cyclase to its N-terminus should hopefully enhance stability.

As negative control the T18 and T25 part of the adenylate cyclase alone were expressed. As positive control the parts were fused to the leucine zipper of GCN4. Cells were grown on LB plates containing X-gal as described under 2.6.2. Blue colour indicated direct interaction of the fusion proteins. An overview over all combinations tested is shown in Fig. 3.28.

The FtsL self interaction was indicated by a strong signal (Fig. 3.28, A1). This was in accordance to older data [Daniel et al., 2006]. Surprisingly this self interaction was lost upon truncation of the N-terminal FtsL domain (Fig. 3.28, B2). It could not be ruled out, that this was due to reduced stability of the truncated protein in *E. coli* which was observed during the co-expression experiments (chapter 3.3.3, Fig. 3.27 a).

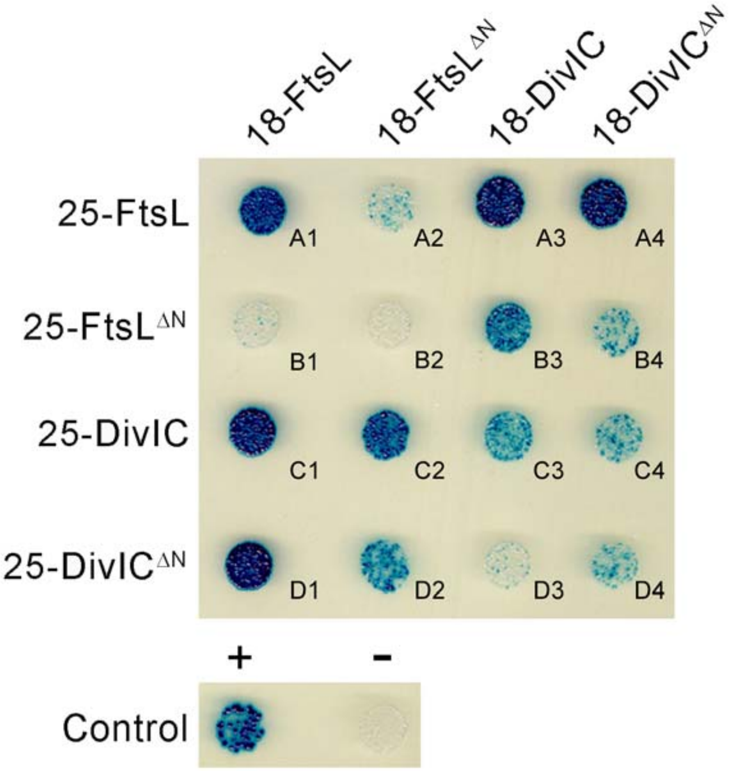

Figure 3.28: Protein-protein interactions of FtsL and DivIC in full-length and N-terminally truncated forms (FtsL$^{\Delta N}$ and DivIC$^{\Delta N}$) shown by a bacterial two hybrid assay. The fusion proteins with the T18 part of CyaA are noted on top and the fusion proteins with the T25 part are noted on the left. Blue colonies indicate direct protein-protein interaction, white colonies indicate no interaction.

DivIC showed self interaction in this system as well (Fig. 3.28, C3), although for previous bacterial two-hybrid studies this has not been reported [Daniel et al., 2006]. The interaction signal was not as strong as seen for FtsL self interaction, but clearly visible. Truncation of the N-terminal DivIC domain had no significant effect on self-interaction (Fig. 3.28, D4).

The FtsL self interaction was indicated by a strong signal (Fig. 3.28, A1). This was in accordance to older data [Daniel et al., 2006]. Surprisingly this self interaction was lost upon truncation of the N-terminal FtsL domain (Fig. 3.28, B2). It could not be ruled out, that this was due to reduced stability of the truncated protein in *E. coli* which was observed during the co-expression experiments (chapter 3.3.3, Fig. 3.27 a).

DivIC showed self interaction in this system as well (Fig. 3.28, C3), although for previous bacterial two-hybrid studies this has not been reported [Daniel et al., 2006]. The interaction signal was not as strong as seen for FtsL self interaction, but clearly visible. Truncation of the N-terminal DivIC domain had no significant effect on self-interaction (Fig. 3.28, D4).

In agreement with previous studies on the interactions of *Bacillus subtilis* late cell division proteins [Daniel et al., 2006], [Robichon et al., 2008] the FtsL-DivIC interaction was by far the strongest interaction (Fig. 3.28, A3 and C1). The blue colour signal of these cells was observed even before the positive control turned blue. The truncated DivIC$^{\Delta N}$ was still able to interact strongly with full length FtsL (Fig. 3.28, A4 and D4). Truncated FtsL$^{\Delta N}$ could interact with full length DivIC, though the interaction was weakened (Fig. 3.28, B3 and C2). An interaction of FtsL$^{\Delta N}$ with DivIC$^{\Delta N}$ was detectable (Fig. 3.28, B4 and D2), but considerably weaker than interaction of the full length proteins. This suggests that the N-terminal domains of FtsL and DivIC do interact and contribute to the protein-protein interaction.

3.3.5 Co-expression of FtsL, DivIC$^{\Delta N}$ and RasP

The bacterial two-hybrid data showed that the N-terminal domain of FtsL and DivIC seem to interact with each other. It also showed that FtsL can still form complexes with DivIC$^{\Delta N}$. Co-expression of FtsL and DivIC$^{\Delta N}$ should therefore lead to complexes with an accessible N-terminal domain of FtsL. It was tested whether DivIC$^{\Delta N}$ could stabilise FtsL against RasP cleavage in these complexes as well (Fig. 3.29).

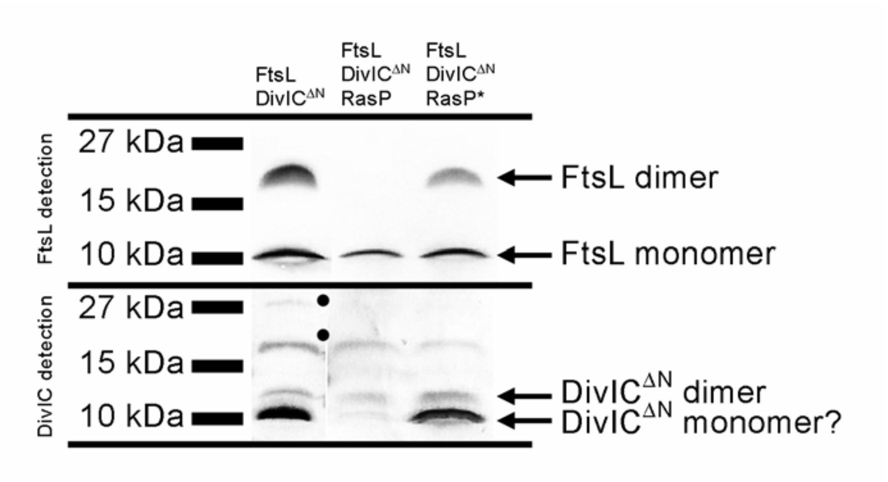

Figure 3.29: Co-expression of FtsL, DivIC$^{\Delta N}$ and RasP in *E. coli* BL21 (DE3). Shown are immuno-blots of 10% Schaegger SDS-gels. For FtsL detection blots were treated with α-PentaHis and α-Mouse IgG-AP and DivIC was detected with α-DivIC and α-Rabbit IgG-AP. Unspecific bands were marked with circles. Proteins present in each strain after expression are noted on top. RasP-E21A was abbreviated to RasP*.

Co-expression of FtsL and DivIC$^{\Delta N}$ led to FtsL dimers, though a monomer band was detected as well. The FtsL levels seemed not as high as in cultures co-expressing both full length proteins. The reason was most likely that the DivIC$^{\Delta N}$ concentration was significantly lower compared to full-length DivIC. Another interesting observation was that the height of the DivIC$^{\Delta N}$ band did not correlate to the size of a monomer, but to a DivIC$^{\Delta N}$ homo dimer. This would suggest that the full-length DivIC most likely was present as dimers as well, which migrated faster into the SDS gel than expected. It is not uncommon for membrane proteins to migrate faster in SDS gels as they are not always completely denatured by SDS. A second DivIC$^{\Delta N}$ band was detected, but it was unclear whether this represented a DivIC$^{\Delta N}$ monomer or a degradation product.

Co-expression of FtsL, DivIC$^{\Delta N}$ and RasP-E21A resulted in the same FtsL dimer and monomer bands as expected. Co-expression of active RasP led to degradation of the FtsL dimers. Obviously RasP can cleave FtsL when its N-terminal domain is not shielded by the N-terminal DivIC domain. The amount of FtsL monomers seemed not decreased by co-expression of RasP. However, this does not necessarily mean that RasP preferably degrades FtsL dimers. It is also possible, that RasP cleavage of the FtsL dimers results in degradation of only one FtsL molecule and simultaneous release of a FtsL monomer. In case RasP degrades FtsL dimers and monomers at the same rate, this would result in more or less constant FtsL monomer levels.

DivIC$^{\Delta N}$ detection revealed that the DivIC$^{\Delta N}$ concentration was reduced when active RasP was co-expressed. As it has been shown that FtsL stabilises DivIC in *E. coli* this could be a side effect of the FtsL degradation by RasP. However, it has never been tested if DivIC is a substrate of RasP. Therefore it was checked whether this effect was really FtsL dependent. The experiment was repeated expressing the mutated FtsL25B instead of FtsL. Because this protein is not degraded by RasP (see chapter 3.3.3) it should be able to stabilise DivIC$^{\Delta N}$ in the presence of RasP. The results are shown in Figure 3.30.

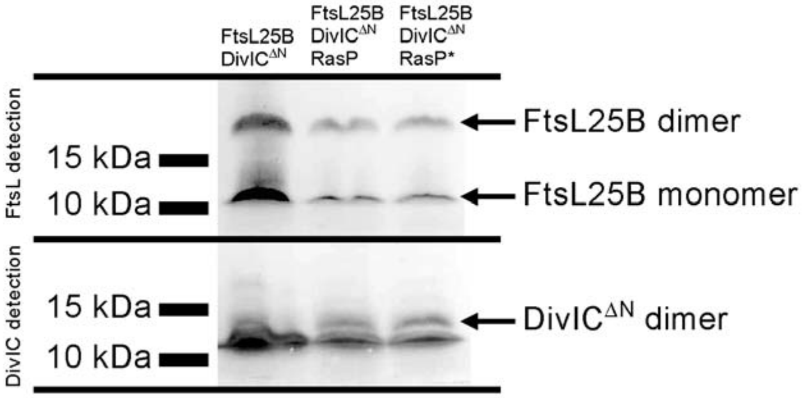

Figure 3.30: Co-expression of FtsL25B, DivIC$^{\Delta N}$ and RasP in *E. coli* BL21 (DE3). Shown are immuno-blots of 10% Schaegger SDS-gels. For FtsL detection blots were treated with α-PentaHis and α-Mouse IgG-AP and for DivIC detection with α-DivIC and α-Rabbit IgG-AP. Proteins present in each strain after expression are noted on top. RasP-E21A was abbreviated to RasP*.

Co-expression of FtsL25B and DivIC$^{\Delta N}$ resulted in FtsL monomers and dimers. As seen before FtsL25B was not degraded by RasP. Consequently, the DivIC$^{\Delta N}$ levels also remained stable in the presence of active RasP. This indicated that the previous decrease of DivIC$^{\Delta N}$ in the presence of RasP seen in Figure 3.29, was indeed due to degradation of FtsL.

4 Discussion

The spatial control of cell division in *Bacillus subtilis* is relatively well understood. The functioning of division site selection systems like the nucleoid occlusion system and the Min system is studied intensively both on a cell biological and a molecular level. In contrast to that nothing is known about temporal control of cell division. Therefore, it was an interesting finding that the intramembrane protease RasP is in involved in degradation of the essential division protein FtsL [Bramkamp et al., 2006]. FtsL was shown to be a rate limiting factor for cell division [Bramkamp et al., 2006] and its degradation could be a possibility to terminate cytokinesis. As the late cell division proteins are interdependent in their assembly and localisation [Errington and Daniel, 2001], [Daniel et al., 2006], [Foster and Popham, 2001] intramembrane cleavage of FtsL by RasP might result in complex disassembly. In the course of this study a possible role of RasP in temporal regulation of cell division was analysed. Since such a function would very likely be linked to disassembly of the membrane part of the divisome, it is important to examine the interactions of FtsL within the divisome.

4.1 FtsL provides a scaffold for cytokinesis

It has been suggested, that the main function of the widely conserved division proteins FtsL, DivIC and DivIB is to provide a scaffold for divisome assembly [Gonzalez et al., 2010]. The synthesis of a new cross cell wall in *Bacillus subtilis* has to be synchronised with constriction of the cytosolic Z-ring. Therefore it seems reasonable that FtsL, DivIC and DivIB could build a complex network with a structural and/or regulatory role for recruitment and positioning of the penicillin binding proteins. Interestingly, previous studies focus mainly on the interactions of FtsL, DivIC and DivIB with each other, but not on self interaction. However, self interaction might be a crucial point in building such a multi-protein complex. In the course of this study several experiments hinted that an oligomerisation ability of FtsL could indeed be an important feature of this protein.

The bacterial two-hybrid assay revealed a relatively strong self interaction of FtsL (chapter 3.3.4, Fig 3.28). When overexpressed in *E. coli* BL21 (DE3) FtsL could form SDS resistant dimers. The formation of SDS resistant dimers has previously also been described for FtsL from *E. coli* [Ghigo and Beckwith, 2000]. However, it seems that the involvement of specific FtsL domains in self interaction differs between FtsL from *Bacillus subtilis* and its *E. coli* homologue. For the *E. coli* protein the periplasmic domain alone is not sufficient to facilitate dimerisation. In contrast to that the purified C-terminal domain of the *Bacillus subtilis* FtsL was present as dimers and tetramers in vitro (chapter 3.2.1, Fig 3.12). This is particularly interesting because the importance of the conserved leucine zipper motif seems to differ as well. Mutating the heptad repeat motif in this domain severely impaired dimer formation, localisation and function in *E. coli* [Ghigo and Beckwith, 2000], but has no obvious effect in *Bacillus subtilis* [Sievers and Errington, 2000].

The existence of tetramers of the periplasmic domain suggested that FtsL is able to form higher complexes. The idea was further supported by the solubilisation experiments. Most of the protein could not be solubilised from *E. coli* membranes, indicating the existence of higher molecular complexes. Fusion to the soluble maltose binding protein drastically enhanced the solubilisation efficiency, probably due to restrained complex formation. Indeed higher molecular FtsL complexes could be seen on SDS gels, when the protein samples were precipidated and thereby concentrated prior to SDS-PAGE analysis. The difference observed for precipitation with TCA or ethanol was interesting. Precipitation with TCA decreased he amount of high molecular weight bands (chapter 3.2.1, Fig 3.11). This could be a hint that there is an ionic component of FtsL self interaction. The fact that FtsL without a MBP tag was best solubilised at high salt concentrations seems to point into the same direction. It should also be noted that the pI value of FtsL is 10.1, which is relatively high. Ionic interactions between FtsL molecules therefore do not seem unlikely.

As the periplasmic domains alone were able to interact, it was surprising that truncation of the N-terminal domain of FtsL from *Bacillus subtilis* seemed to abolish self interaction in the bacterial-two hybrid system. This could be due to a reduced protein concentration. Expression of FtsL$^{\Delta N}$ in *E. coli* BL21 (DE3) showed that the protein was not stable (chapter 3.3.3, Fig. 3.27a). In the bacterial-two hybrid system the stable parts of the adenylate cyclase were fused to the N-terminus of FtsL$^{\Delta N}$. Though this should hopefully enhance FtsL$^{\Delta N}$ stability, it cannot be ruled out that the lack of a self interaction signal was caused by unspecific degradation of the protein. Unfortunately, there are no FtsL antibodies available to check the FtsL$^{\Delta N}$ levels in these strains. Another hint that FtsL$^{\Delta N}$ is still able to oligomerise came from the co-expression of FtsL$^{\Delta N}$ and DivIC. Co-expression of DivIC resulted in a FtsL$^{\Delta N}$ dimer. This definitely argues against a total loss of self interaction upon truncation of the N-terminal domain. On the other hand mutation of the cytosolic recognition motif from 25-KKRAS-29 to 25-KKAVA-29 seemed to result in a relatively high FtsL dimer formation (chapter 3.3.3, Fig. 3.27b). This would support the idea that the N-terminal domain at least contributes to self interaction of FtsL. In general it is difficult to compare the oligomerisation of the concentrated periplasmic domains in vitro to the relatively moderate overexpression in the bacterial two-hybrid system. To clarify which domains are involved in FtsL self interaction additional experiments would be necessary. Certain FtsL domains could be exchanged with domains of an unrelated protein and the bacterial two-hybrid assay could then be repeated with those constructs. This might avoid protein stability issues.

It was very interesting to observe that DivIC and DivIB obviously had an effect on the FtsL oligomerisation. Co-expression of FtsL and DivIC drastically increased the formation of FtsL dimers. Though co-expression experiments at low induction levels revealed that this dimerisation was strongly dependent on the FtsL concentration (chapter 3.3.1, Fig. 3.25), a DivIC specific effect was still observed. A weak dimer band was only detectable when DivIC was co-expressed. Also, truncated FtsL$^{\Delta N}$ was present as dimers when co-expressed with DivIC, even though the proptein concentration was rather low due to the FtsL$^{\Delta N}$ instability in *E. coli*. Moreover only in the presence of DivIC the amount of FtsL dimers exceeded the amount of monomers. For example this was not observed when FtsL was highly expressed in *E. coli* BL21 (DE3) for purification (chapter 3.2.1, Fig. 3.10 and Fig. 3.11). Still, it is difficult to judge how much the DivIC specific effect exactly contributes to FtsL dimerisation compared to the concentration dependent effect. Also, it was not clear whether DivIC actively facilitated dimerisation or simply stabilised FtsL-FtsL interaction.

A direct interaction of FtsL and DivIB in the absence of other division proteins has been controversially discussed [Daniel et al., 2006], [Robichon et al., 2008]. However, co-expression of FtsL and DivIB in *E. coli* BL21 (DE3) showed that the proteins obviously are capable of direct interaction as DivIB had an effect on FtsL dimerisation as well (chapter 3.3.1, Fig. 3.24). In agreement with in vivo data [Daniel et al., 2006] DivIB did not seem to stabilise FtsL in *E. coli*. The overall FtsL level was not significantly increased upon co-expression of DivIB, ruling out a concentration dependent effect on FtsL dimerisation. The fact that DivIC and DivIB influence FtsL oligomerisation, further supports the idea of a structural network build by these proteins.

DivIC does not only influence FtsL dimerisation, but also protein stability. A general stabilisation of FtsL and DivIC by each other has previously been shown in *Bacillus subtilis*

[Daniel et al., 2006] and in a heterologous *E. coli* system [Robichon et al., 2008]. In accordance to that a general stabilisation of full length FtsL as well as FtsL$^{\Delta N}$ by DivIC was observed during the co-expression experiments (chapter 3.3.2, Fig. 3.26 and Fig. 3.27). The concentration of full length DivIC was not influenced by FtsL in this system. The reason might be the relatively high expression level of DivIC. Expression of DivIC$^{\Delta N}$ resulted in much lower protein levels and in this case a stabilisation effect of FtsL on DivIC$^{\Delta N}$ became more significant (chapter 3.3.5, Fig 3.30). The results show that this stabilisation apparently is mediated by interaction of the periplasmic and/or transmembrane domains as the truncated proteins are stabilised as well.

It is not known yet, which domains are involved in FtsL-DivIC interaction in *Bacillus subtilis*. Previous studies concentrated on the interaction of the C-terminal domains in vitro with contradicting results [Sievers and Errington, 2000], [Robson et al., 2002]. The results of the bacterial two-hybrid assay (chapter 3.3.4, Fig 3.28) suggested that the N-terminal domains of FtsL and DivIC contribute to the interaction as well. In addition the N-terminal domain of DivIC was able inhibit substrate recognition of FtsL by RasP, which will be further discussed in chapter 4.3.3. This showed that a direct interaction between the cytosolic domains is very likely.

In *E. coli* the transmembrane domain and a part of the C-terminal domain of the DivIC homologue FtsB are necessary for interaction with FtsL [Gonzalez and Beckwith, 2009]. However, FtsB does not posses a cytosolic N-terminal domain like DivIC. To study the contribution of different domains to the FtsL-DivIC interaction in more detail, it would be interesting to exchange specific with domains with those of unrelated proteins.

4.2 A possible function of FtsL oligomerisation during complex assembly

Despite their small size FtsL, DivIc and DivIB seem to display various interaction sites. FtsL can independently interact with DivIC and DivIB. In contrast to other studies [Daniel et al., 2006], [Robichon et al., 2008] the data from the co-expression experiments suggest that DivIC and DivIB are capable of interacting with each other without FtsL present. Also direct interaction of FtsL and DivIB with Pbp2B were previously observed [Daniel et al., 2006], [Robichon et al., 2008]. Yet, it is completely unknown how exactly the membrane part of the divisome is composed. Also the patterns of protein recruitment and complex assembly seem to vary in different organisms. The *E. coli* proteins FtsL, FtsB (DivIC) and FtsQ (DivIB) are able to assemble into a complex without FtsK present, which is necessary for their recruitment to the septum [Buddelmeijer and Beckwith, 2004]. This led to the idea that these proteins pre-assemble into trimeric complexes, which are then recruited to the division site by interaction of FtsQ (DivIB) with FtsK. Such a model does not apply to the situation in *Bacillus subtilis*, because in this organism DivIB is not essential for division at normal growth temperatures [Rowland et al., 1997]. Data from *Streptococcus pneumoniae* show a different pattern as well [Noirclerc-Savoye et al., 2005]. In this case DivIC seems to be the key regulator for localisation of the late division proteins and DivIB and FtsL are co-localized with DivIC only during septation.

These different results show that mere interaction studies will probably not be sufficient to understand the complex network of the membrane division proteins. For the understanding of the cytosolic part of the divisome the discovery of the FtsZ ring as a central structure was crucial. For example the functions of certain proteins like ZapA and SepF are directly linked to FtsZ polymerisation [Gueiros-Filho and Losick, 2002], [Hamoen et al., 2006]. It is unclear, if a similar structure exists in the membrane part of the divisome. While this is a highly speculative concept, it would be very interesting to investigate a possible role of FtsL in the building of such a central structure. FtsL was able to assemble into higher molecular complexes in *E. coli* membranes and the purified C-terminal domains were present as tetramers in vitro. This shows that more than one site for self interaction must exist in this domain. A polymerisation of FtsL into greater networks therefore is theoretically possible. MBP-FtsL could be purified as described under 2.4.7. After removal of the MBP tag by TEV cleavage FtsL might assemble into bigger complexes. It would be interesting to examine whether these FtsL complexes build distinct structures by using electron microscopy. In addition differences in the presence of DivIC and/or DivIB should be investigated.

4.3 The role of FtsL protolysis by RasP during cell division

In order to understand a possible role of RasP in temporal regulation of cell division we wanted to analyse intramembrane cleavage of FtsL on a mechanistic level as well. To this end we tried to establish an in vitro assay.

4.3.1 The intramembrane protease RasP is inactive in vitro

Though the first attempts to establish an in vitro proteolysis assay of FtsL in liposomes looked promising, RasP seems to be inactive under in vitro conditions. The cleavage products observed after incubation of MBP-FtsL with RasP in mixed liposomes did not correspond to a cleavage within the transmembrane domain of FtsL. Instead it seemed that MBP-FtsL was likely cleaved near its cytosolic N-terminus and within the linker region of MBP and FtsL. As the RasP cleavage site is unknown, it cannot be completely ruled out that RasP cleaved FtsL within the cytosolic domain. However, no RasP specific degradation of the control substrate RsiW* was observed in the in vitro assay, while it has previously been demonstrated that RsiW* is a substrate of RasP in vivo [Schöbel et al., 2004]. Taken together this rather indicated that RasP was inactive and MBP-FtsL was cleaved by endogenous *E. coli* proteases (chapter 3.2.4, Fig 3.20).

There are good hints that the protease might be partially denatured. RasP is active in *E. coli* membranes, which was proven by the co-expression experiments. However, it has been reported, that the protein is most likely unstable in detergent solution [personal communication, Jan Löwe]. It was possible to reconstitute RasP into liposomes after purification, which argues against a totally denatured protein. A partial unfolding of certain domains seems more likely.

A hint that this might indeed be the main problem was gained by SDS-PAGE analysis. When samples from the co-expression experiments were analysed by SDS-PAGE and immunoblotting, it showed that RasP migrated faster into the gels as expected for a protein of this size (data not shown). The purified RasP samples did not reveal such an effect. The height of the RasP band in SDS gels perfectly corresponded to the size of the protein. Apparently RasP domains that remained stable against SDS treatment in case of the co-expression experiments were unfolded in case of the purified protein. Of course it is difficult to compare SDS treatment of total cell lysate and of purified protein. Yet these findings support the idea that certain domains of RasP were unfolded during the assay. Also preliminary data from crystal structures suggested unusually high flexibility of domains that most likely should be relatively rigid [Jan Löwe, personal communication].

A different possibility is that domains were not unfolded, but that the conformation relative to each other was changed upon solubilisation. Structural data from other S2P proteases showed that the relative positioning of the transmembrane domains is essential to create characteristic features of the proteins. It is possible that such a conformation is not stable outside the lipid bilayer of the cell membrane. For S2P from *Methanocaldococcus jannaschii* two conformations were observed in crystals, likely representing an open and a closed state of the enzyme [Feng et al., 2007]. However, how these proteases might regulate the switch between those states is completely unknown. Therefore it is also possible that solubilised RasP is somehow trapped in a closed state.

Furthermore, it is not clear if additional factors are necessary for RasP activity. In vivo an effect of the ABC transporter EcsAB on RasP was observed [Heinrich et al., 2008]. In an *ecsA* knockout strain both RasP substrates FtsL and RsiW were stabilised. How RasP activity is modulated by EcsAB is completely unclear though. It is not even known if this is a direct or indirect effect and which other factors might be involved. Therefore it is hard to judge whether RasP could be active in an in vitro assay.

It would be necessary to optimise RasP purification to establish such an assay of FtsL proteolysis by RasP. In the past some intramembrane proteases have been reduced to their transmembrane domains for purification and/or cystralisation. For example this was the case for S2P from *Methanocaldococcus jannaschii* [Feng et al., 2007]. The predicted RasP topology consists of four transmembrane domains and an extracellular PDZ domain. Removing the PDZ domain might be an option to enhance the stability of RasP in solution. However, one problem of the RasP purification was the very low expression level of RasP in *E. coli*. As 70-80 g of cell pellet needed to be used for purification of less than 500 µg of protein, optimising the different purification steps and buffers would be extremely time consuming and cost-intensive. Therefore, the best chance to optimise the RasP purification and the proteolysis assay would be to significantly increase the expression levels of the enzyme. A good strategy might be the fusion of RasP to the transmembrane segment of rabbit cytochrome P450 2B4 (cytTM, residues 1-23). This has been done before to increase the expression of SpoIVFB from *Bacillus subtilis*, another S2P protease [Zhou et al., 2009]. In that case accumulation of SpoIVFB in *E. coli* was increased at least 100-fold.

4.3.2 Substrate recognition is essential for FtsL cleavage by RasP

A central question that we aimed to answer with the in vitro assay was the influence of substrate recognition on FtsL degradation. Sequence alignment of FtsL and the second known RasP substrate RsiW revealed a putative substrate recognition motif within the N-terminal domain of FtsL. In vivo FtsL is significantly stabilised upon mutation or truncation of this putative recognition motif [Bramkamp et al., 2006]. It seemed logical to assume that this was due to decreased FtsL degradation by RasP. Since a functional in vitro assay could not be established, this hypthesis was tested using a heterologous co-expression system. The mutation of the putative recognition motif from 25-KKRAS-29 to 25-KKAVA-29 abolished FtsL degradation by RasP in *E. coli* BL21 (DE3) (chapter 3.3.3, Fig 3.27b). Obviously substrate recognition is essential for FtsL proteolysis and previously described stabilisation in vivo was indeed a direct consequence of impaired RasP cleavage.

The significance of substrate recognition for cleavage by intra-membrane proteases has recently become an important subject of investigation. Structural data indicated that S2P proteases have a conserved position of their active site [Feng et al., 2007]. Still they cleave substrates at different positions within transmembrane domains. Specific recognition sites have been suggested to determine the site of cleavage for each substrate. Indeed such a mechanism has recently been shown for Rhomboid proteases [Strisovsky et al., 2009]. It was demonstrated that specific recognition motifs determine the site of cleavage and are more strictly required than helix destablising residues, which have been discussed in this context before. The essential substrate recognition of FtsL now demonstrates the same principle for RasP. For Rhomboid substrates the cleavage site could be changed by altering the position of the recognition motif using linkers. It would be very interesting to test whether this is possible in the case of FtsL as well.

4.3.3 RasP is involved in preventing divisome re-assembly

As described before a plausible function of RasP in the temporal regulation of cell division was to trigger complex disassembly by removing FtsL from the divisome. Surprisingly, in the presence of DivIC RasP could no longer degrade FtsL (chapter 3.3.2, Fig. 3.26). Obviously DivIC can stabilise FtsL against RasP cleavage. This stabilisation appears to be linked to substrate recognition. The N-terminal domain of DivIC was required for inhibiting FtsL degradation. Most likely the recognition motif is no not accessible in such a FtsL-DivIC complex and therefore RasP cannot degrade FtsL. While general stabilisation of FtsL by DivIC has been shown previously [Daniel et al., 2006], [Robichon et al., 2008] this study provides a first prove of FtsL protection by DivIC against specific degradation by RasP. This strongly questions a role of RasP in divisome disassembly. FtsL tightly interacts with DivIC within the divisome, hence RasP should not be able to cleave FtsL while the complex is still intact.

A different role of RasP in cell division could be to remove FtsL from the membrane after complex disassembly. It has been shown that it is important to prevent re-assembly of the division complex close to a newly formed cell pole [Gregory et al., 2008]. Such re-assembly leads to formation of non viable mini cells. Degradation of FtsL could certainly be a way to prevent the assembly of a mature divisome close to a recent site of division. After cell division is completed and the divisome is disassembled, the N-terminal domain of FtsL could become accessible and substrate recognition would then no longer be impaired. RasP could cleave FtsL and effectively remove it from the membrane. Of course further investigation will be necessary to verify this idea.

The question of pre-assembled FtsL/DivIC/DivIB complexes is of importance in this context. Pre-assembly of such complexes might protect the protein against RasP cleavage before it is recruited to the division site. On the other hand it is also possible that RasP constantly degrades FtsL unless it is incorporated into the divisome. This might indirectly control divisome assembly on a post-tranlational level by restricting the FtsL concentration in the cell. As FtsL is a rate limiting factor for cell division in *Bacillus subtilis* it would make sense to tightly regulate FtsL levels. A third possibility is that RasP is specifically localised and contributes to spatial regulation of division. A polar localisation of RasP could inhibit divisome assembly at the poles by constant degradation of FtsL.

The experiments with the putative cytosolic cleavage product of FtsL support the idea that the main function of FtsL proteolysis by RasP seems to be the removal of the protein from the membrane. Overexpression of the putative degradation product revealed no obvious effect of this peptide. The protein is evenly dispersed throughout the cytosol and rapidly degraded (chapter 3.1.2, Fig. 3.3 and Fig. 3.4). This degradation seems to be unspecific. Mutation of a putative tag for degradation by ClpXP had no effect. This was rather surprising. Obviously there are other degrons despite of the C-terminus. A different possibility is that the domain is unfolded after RasP cleavage and thereby recognised for degradation. Other proteases known for general proteolysis like ClpAP, Lon or FtsH might be involved in this process. FtsL seems to be an unusual substrate of intramembrane proteolysis. In most of cases the cleavage does not take place to simply degrade a protein but rather to release an active product. However, for the γ-secretase a role in general degradation of membrane proteins is discussed as the enzyme seems to cleave a broad spectrum of substrates with poor sequence specificity [De Strooper, 2003].

4.3.4 RasP seems to degrade FtsL without prior site-1-cleavage

An open question in the context of FtsL proteolysis is the possible involvement of a site-1-protease. The experiments rather indicate that no such site-1-cleavage is necessary for degradation of FtsL as the full-length FtsL is degraded in the *E. coli* system. Of course it might be processed by *E. coli* site-1-proteases. The stabilising effect of DivIC co-expression clearly shows that FtsL is degraded by endogenous proteases. However, there are several arguments against site-1-cleavage. In the case of the RasP substrate RsiW most of the extracellular domain needs to be degraded before site-2-cleavage occurs. To mimic this, a C-terminally truncated version of FtsL was expressed in the *E. coli* system. This FtsL$^{\Delta C}$ protein was missing almost all of the extracellular FtsL domain. The protein was not stable in *E. coli* and the concentration was below the detection limit of the immuno-blotting (data not shown). Co-expression of DivIC had no effect on stability, still no FtsL$^{\Delta C}$ was detectable. This shows again, that the general stabilisation by DivIC seems to be mediated by the extracellular domains as discussed under 4.2.1. According to these findings cleavage of the extracellular domain of *Bacillus subtilis* FtsL in *E. coli* would lead to complete degradation of the cleavage product independent of RasP. Co-expression experiments did not support this notion, but instead a clear dependency of FtsL degradation on RasP activity was observed. It therefore seems likely, that RasP is able to cleave full-length FtsL. It cannot be ruled out that site-1-cleavage occurs close to the C-terminus of FtsL. This might not influence the FtsL stability but enable RasP cleavage. On the other hand such cleavage would very likely be sequence specific and the overall FtsL sequence is only poorly conserved.

A second argument against site-1-cleavage is the degradation of FtsL in the presence of DivIC$^{\Delta N}$. Full-length FtsL is generally stabilised by DivIC$^{\Delta N}$ but specifically degraded by RasP (chapter 3.3.5, Fig. 3.29). Obviously FtsL and DivIC$^{\Delta N}$ are able to form complexes and as mentioned above the extracellular domains are stabilised by this interaction. If a site-1-protease from *E. coli* can cleave FtsL within this domain, one would expect that DivIC$^{\Delta N}$ co-expression has an influence on FtsL degradation by RasP. This is not the case, the accessibility of the N-terminal FtsL domain is sufficient to trigger RasP cleavage. Taken together these data strongly question the involvement of other proteases in FtsL degradation.

While degradation of a full length protein by a protease of the S2P family is a novelty, it has been shown for Rhomboid proteases before. Rhomboid-1 from *Drosophila* cleaves full-length Spitz [lee et al., 2001] and the full-length yeast protein cytochrome c peroxidase (Ccp1) is cleaved by the the rhomboid protease Pcp1 [Tatsuta et al., 2007]. In both cases the proteolysis is not regulated by prior cleavage of the substrate. Spitz degradation is controlled by translocation. In the case of Ccp1 membrane dislocation by the m-AAA protease enables Rhomboid cleavage. Both examples show, that temporal regulation of intramembrane proteolysis can be achieved by different ways.

Often intramembrane proteases are involved in signalling cascades across membranes. For example in the case of RsiW substrate degradation is dependent on alkaline stress [Schöbel et al., 2004]. The degradation of the extracellular domain of RsiW is important for passing on information about extracellular conditions. However, in the case of FtsL the C-terminal domain is most likely involved in protein-protein interactions and not in sensing of extracellular conditions. The co-expression experiments showed that RasP cleavage can be controlled be the accessibility of the N-terminal recognition motif. It is conceivable that disassembly of the division complex is the only temporal signal for FtsL proteolysis by RasP. How divisome disassembly is regulated or achieved is unknown. First studies show that the Min-system plays a role in this process [Gregory et al., 2008] [van Baarle and Bramkamp, 2010]. There might be proteolysis involved, but FtsL might not necessarily be the subject of this degradation.

4.4 A new model for FtsL proteolysis by RasP

Based on the results of this study a new model for FtsL proteolysis can be suggested, visualised by Fig. 4.1. When FtsL is expressed in *Bacillus subtilis* it is either constantly degraded by RasP or in the case of preformed FtsL-DivIC complexes it is already stabilised. The protein gets recruited to the division site and is incorporated into the divisome. Within this complex the N-terminal domain of FtsL is probably buried in the cytosolic part of the divisome and it is additionally shielded by direct interaction with the N-terminal domain of DivIC. As substrate recognition is impaired, RasP cannot cleave FtsL from this complex. After division is completed the divisome disassembles upon a yet unknown signal. Thereby, the N-terminal domain of FtsL becomes accessible and RasP can recognise the protein as a substrate. FtsL is cleaved and removed from the membrane. The cytosolic cleavage fragment is then rapidly degraded by general proteolysis. As multiple interactions of FtsL and other late division proteins are necessary for complex assembly, this degradation probably prevents divisome re-assembly.

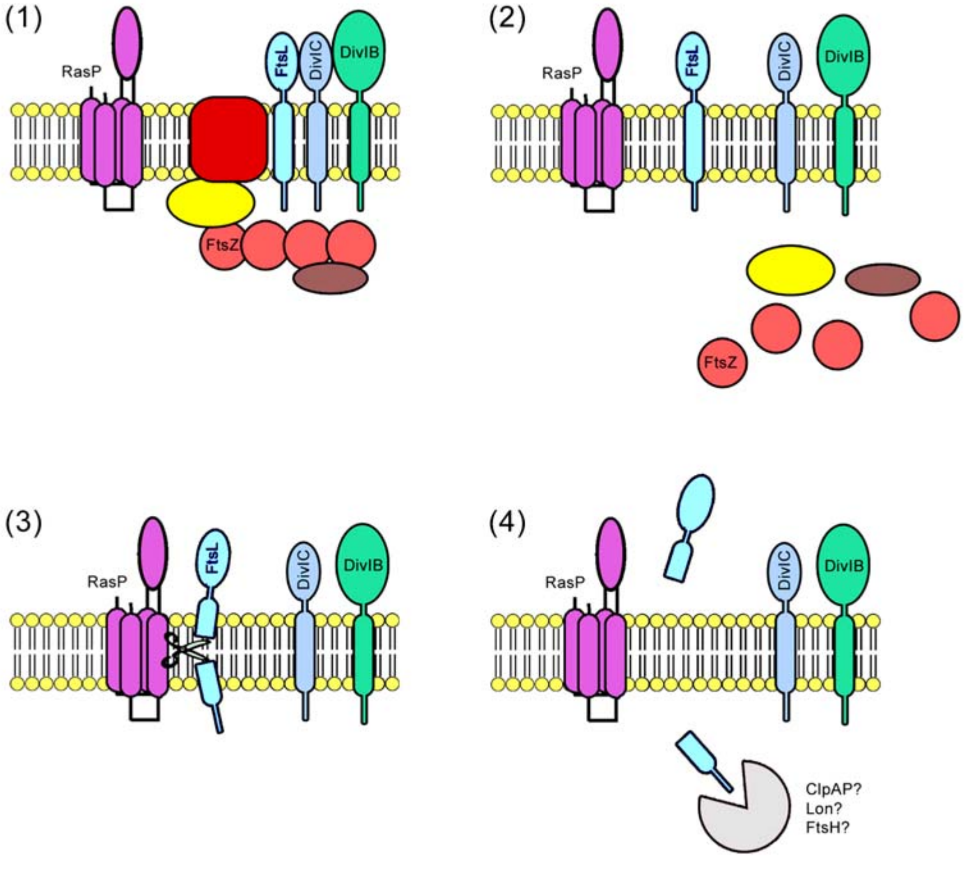

Figure 4.1: New model for FtsL proteolysis by RasP. (1) FtsL is stabilised within the divisome. (2) The divisome disassembles upon a yet unknown signal, (3) RasP cleaves FtsL and thereby removes it from the membrane. (4) The cytoslic cleavage product is degraded by general proteolysis.

5 References

Alba, B.M., **Leeds, J.A.**, **Onufryk, C.**, **Lu, C.Z.**, **Gross, C.A**. 2002. DegS and YaeL participate sequentially in the cleavage of RseA to activate the sigma(E)-dependent extracytoplasmic stress response. Genes Dev. 15;16(16):2156-68.

Akiyama, Y., **Kanehara, K.**, **Ito, K**. 2004. RseP (YaeL), an Escherichia coli RIP protease, cleaves transmembrane sequences. EMBO J. 10;23(22):4434-42.

Arnold, T., **Linke, D**. 2008. The use of detergents to purify membrane proteins. Curr Protoc Protein Sci. 4;4.8.1-4.8.30.

Beall, B., Lutkenhaus, J. 1991. FtsZ in *Bacillus subtilis* is required for vegetative septation and for asymmetric septation during sporulation. Genes Dev. 5(3):447-55.

Bi, E.F., Lutkenhaus, J. 1991. FtsZ ring structure associated with division in *Escherichia coli*. Nature 14;354(6349):161-4.

Blackman, S.A., **Smith, T.J.**, **Foster, S.J**. 1998. The role of autolysins during vegetative growth of *Bacillus subtilis* 168. Microbiology. 144 (Pt 1):73-82.

Bork, P. Sander, C. Valencia, A. 1992. An ATPase domain common to prokaryotic cell cycle proteins, sugar kinases, actin and hsp70 heat shock proteins. Proc. Natl. Acad. Sci. USA 89:7290-7294.

Bramkamp, M., **Emmins, R.**, **Weston, L.**, **Donovan, C.**, **Daniel, R.A.**, **Errington, J** 2008. A novel component of the division-site selection system of *Bacillus subtilis* and a new mode of action for the division inhibitor MinCD. Mol Microbiol. 70(6):1556-69.

Brown, M.S., **Goldstein, J.L**. 1997. The SREBP pathway: regulation of cholesterol metabolism by proteolysis of a membrane-bound transcription factor. Cell. 2;89(3):331-40.

Buddelmeijer, N., **Beckwith, J**. 2004. A complex of the *Escherichia coli* cell division proteins FtsL, FtsB and FtsQ forms independently of its localization to the septal region. Mol Microbiol. 52(5):1315-27.

Bürmann, F. 2007. Cell division in Bacillus subtilis. Internship report

Burton, B.M., **Marquis, K.A.**, **Sullivan, N.L.**, **Rapoport, T.A.**, **Rudner, DZ**. 2007. The ATPase SpoIIIE transports DNA across fused septal membranes during sporulation in *Bacillus subtilis*. Cell. 28;131(7):1301-12.

Campo, N., **Rudner, D.Z**. 2006. A branched pathway governing the activation of a developmental transcription factor by regulated intramembrane proteolysis. Mol Cell. 7;23(1):25-35.

Chen, J.C., **Beckwith, J**. 2001. FtsQ, FtsL and FtsI require FtsK, but not FtsN, for co-localization with FtsZ during *Escherichia coli* cell division. Mol Microbiol. 42(2):395-413.

Daniel, R.A., Harry, E.J., Katis, V.L., Wake, R.G., and Errington, J. 1998. Characterisation of the essential cell division gene *ftsL (yllD)* of *Bacillus subtilis* and its role in the assembly of the division apparatus. Molecular Microbiology 29(2) 593-604.

Daniel, R.A., Noirot-Gros, M.F., Noirot, P., Errington, J. 2006 Multiple interactions between the transmembrane division proteins of *Bacillus subtilis* and the role of FtsL instability in divisome assembly. J Bacteriol. 188(21):7396-404.

De Strooper B. 2003. Aph-1, Pen-2, and Nicastrin with Presenilin generate an active gamma-Secretase complex. Neuron. 10;38(1):9-12.

Din, N. Quardokus, E.M. Sackett, M.J. Brun, Y. 1998. Dominant C-terminal deletins of FtsZ that affect its ability to localize in *Caulobacter* and its interaction with FtsA. Mol. Microbiol. 27:1051-1063.

Duncan, E.A., **Davé, U.P**., **Sakai, J**., **Goldstein, J.L**., **Brown, M.S**. 1998. Second-site cleavage in sterol regulatory element-binding protein occurs at transmembrane junction as determined by cysteine panning. J Biol Chem. 10;273(28):17801-9.

Ellermeier, C.D., **Losick, R**. 2006. Evidence for a novel protease governing regulated intramembrane proteolysis and resistance to antimicrobial peptides in *Bacillus subtilis*. Genes Dev. 15;20(14):1911-22.

Errington, J. Daniel, R.A. 2001. Cell division during growth and sporulation, p.97-109. L. sonenshein, R. Losick, J.A. Hoch, (ed.), *Bacillus subtilis* and its relatives: from genes to cells. American Society for Microbiology, Washington, D.C..

Esser, K., **Tursun, B**., **Ingenhoven, M**., **Michaelis, G**., **Pratje, E**. 2002. A novel two-step mechanism for removal of a mitochondrial signal sequence involves the mAAA complex and the putative rhomboid protease Pcp1. J Mol Biol. 8;323(5):835-43.

Feng, L., **Yan, H**., **Wu, Z**., **Yan, N**., **Wang, Z**., **Jeffrey, P.D**., **Shi, Y**. 2007. Structure of a site-2 protease family intramembrane metalloprotease. Science. 7;318(5856):1608-12.

Foster, S.J., Popham, D.L. 2001. Structure and synthesis of cell wall, spore cortex, teichoic acids, S-layers and capsules, p. 21-41. In L. Sonenshein, R. Losick, and J.A. Hoch (ed.), *Bacillus subtilis* and its relatives: from genes to cells. American Society for Microbiology, Washington D.C..

Ghigo, J.M., **Beckwith, J**. 2000. Cell division in Escherichia coli: role of FtsL domains in septal localization, function, and oligomerization. J Bacteriol. 182(1):116-29.

Goehring, N.W., **Gonzalez, M.D**., **Beckwith, J**. 2006. Premature targeting of cell division proteins to midcell reveals hierarchies of protein interactions involved in divisome assembly. Mol Microbiol. 61(1):33-45.

Goehring, N.W., **Petrovska, I**., **Boyd, D**., **Beckwith, J**. 2007. Mutants, suppressors, and wrinkled colonies: mutant alleles of the cell division gene ftsQ point to functional domains in FtsQ and a role for domain 1C of FtsA in divisome assembly. J Bacteriol. 189(2):633-45.

Gonzalez, M.D., **Beckwith, J**. 2009. Divisome under construction: distinct domains of the small membrane protein FtsB are necessary for interaction with multiple cell division proteins. J Bacteriol. 191(8):2815-25.

Gonzalez, M.D., **Akbay, E.A**., **Boyd, D**., **Beckwith, J**. 2010. Multiple interaction domains in FtsL, a protein component of the widely conserved bacterial FtsLBQ cell division complex. J Bacteriol. 192(11):2757-68.

Goranov, A.I., Katz, L., Breier, A.M., Burge, C.B., Grossmann, A.D. 2005. A transcriptional response to replication status mediated by the conserved bacterial replication protein DnaA. Proc. Natl. Acad. Sci. USA 6;102(36):12932-7.

Gregory, J.A., **Becker, E.C**., **Pogliano, K**. 2008. Bacillus subtilis MinC destabilizes FtsZ-rings at new cell poles and contributes to the timing of cell division. Genes Dev. 15;22(24):3475-88.

Griffith, K.L., **Grossman, A.D**. 2008. Inducible protein degradation in Bacillus subtilis using heterologous peptide tags and adaptor proteins to target substrates to the protease ClpXP. Mol Microbiol. 70(4):1012-25.

Gueiros-Filho, F. J., R. Losick. 2002. A widely conserved bacterial cell division protein that promotes assembly of the tubulin-like protein FtsZ. Genes Dev. 16:2544-2556

Hale, C.A., **de Boer, P.A**. 2002. ZipA is required for recruitment of FtsK, FtsQ, FtsL, and FtsN to the septal ring in Escherichia coli. J Bacteriol. 184(9):2552-6.

Hamoen, L.W. Meile, J-C. de Jong, W. Noirot, P. Errington, J. 2006. SepF, a novel FtsZ-interacting protein required for late step in cell division. Mol. Microbiol. 59(3):989-999.

Heinrich, J., Wiegert, T. 2006. YpdC determines site-1 degradation in regulated intramembrane proteolysis of the RsiW anti-sigma factor of *Bacillus subtilis*. Mol. Microbiol. 62(2):566-79.

Heinrich, J., Lundén, T., Kontinen, V.P., Wiegert, T. 2008. The *Bacillus subtilis* ABC transporter EcsAB influences intramembrane proteolysis through RasP. Microbiology. 154(7)1989-1997.

Heinrich, J., Hein, K., Wigert, T. 2009. Two proteolytic modules are involved in regulated intramembrane proteolysis of Bacillus subtilis RsiW. Mol Microbiol. 74(6):1412-26.

Herlan, M., **Vogel, F**., **Bornhovd, C**., **Neupert, W**., **Reichert, A.S**. 2003. Processing of Mgm1 by the rhomboid-type protease Pcp1 is required for maintenance of mitochondrial morphology and of mitochondrial DNA. J Biol Chem. 25;278(30):27781-8.

Kawai, Y., Ogaswara, N. 2006. *Bacillus subtilis* EzrA and ftsL synergistically regulate FtsZ ring dynamics during cell division. Microbiology 152(4):1129-41.

Lara, B., **Mengin-Lecreulx, D**., **Ayala, J.A**., **van Heijenoort, J**. 2005. Peptidoglycan precursor pools associated with MraY and FtsW deficiencies or antibiotic treatments. FEMS Microbiol Lett. 15;250(2):195-200.

Levin, P.A. Kurtser, I.G. Grossman, A.D. 1999. Identification and characterization of a negative regulator of FtsZ ring formation in *Bacillus subtilis*. Proc. Natl. Acad. Sci. USA. 96:9642-9647.

Li, X., Wang, B., Feng, L., Kang, H., Qi, Y., Wang, J., Shi, Y. 2009. Cleavage of RseA by RseP requires a carboxyl-terminal hydrophobic amino acid following DegS cleavage. Proc. Natl. Acad. Sci. USA 106(36):14837-42.

Little, D., **Weselake, R**., **Pomeroy, K**., **Furukawa-Stoffer, T**., **Bagu, J**. 1994. Solubilization and characterization of diacylglycerol acyltransferase from microspore-derived cultures of oilseed rape. Biochem J. 15;304 (Pt 3):951-8.

Lonetto, M.A., **Brown, K.L**., **Rudd, K.E**., **Buttner, M.J**. 1994. Analysis of the Streptomyces coelicolor sigE gene reveals the existence of a subfamily of eubacterial RNA polymerase sigma factors involved in the regulation of extracytoplasmic functions. Proc Natl Acad Sci U S A. 2;91(16):7573-7.

McQuibban, G.A., **Saurya, S**., **Freeman, M**. 2003. Mitochondrial membrane remodelling regulated by a conserved rhomboid protease. Nature. 29;423(6939):537-41.

Mercer, K.L., **Weiss, D.S**. 2002. The *Escherichia coli* cell division protein FtsW is required to recruit its cognate transpeptidase, FtsI (PBP3), to the division site. J Bacteriol. 184(4):904-12.

Nguyen-Distèche, M., **Fraipont, C**., **Buddelmeijer, N**., **Nanninga, N**. 1998. The structure and function of *Escherichia coli* penicillin-binding protein 3. Cell Mol Life Sci. 54(4):309-16.

Nohturfft, A., **DeBose-Boyd, R.A**., **Scheek, S**., **Goldstein, J.L**., **Brown, M.S**. 1999. Sterols regulate cycling of SREBP cleavage-activating protein (SCAP) between endoplasmic reticulum and Golgi. Proc Natl Acad Sci U S A. 28;96(20):11235-40.

Noirclerc-Savoye, M., **Le Gouëllec, A**., **Morlot, C**., **Dideberg, O**., **Vernet, T**., **Zapun, A**. 2005. In vitro reconstitution of a trimeric complex of DivIB, DivIC and FtsL, and their transient co-localization at the division site in *Streptococcus pneumoniae*. Mol Microbiol. 55(2):413-24.

Patrick, J.E., **Kearns, D.B**. 2008. MinJ (YvjD) is a topological determinant of cell division in *Bacillus subtilis*. Mol Microbiol. 70(5):1166-79.

Pichoff, S., **Lutkenhaus, J**. 2005. Tethering the Z ring to the membrane through a conserved membrane targeting sequence in FtsA. Mol Microbiol. 55(6):1722-34.

Rawson, R.B., **Zelenski, N.G**., **Nijhawan, D**., **Ye, J**., **Sakai, J**., **Hasan, M.T**., **Chang, T.Y**., **Brown, M.S**., **Goldstein, J.L**. 1997. Complementation cloning of S2P, a gene encoding a putative metalloprotease required for intramembrane cleavage of SREBPs. Mol Cell. 1(1):47-57.

Robichon, C., **King, G.F**., **Goehring, N.W**., **Beckwith, J**. 2008. Artificial septal targeting of Bacillus subtilis cell division proteins in Escherichia coli: an interspecies approach to the study of protein-protein interactions in multiprotein complexes. J Bacteriol. 190(18):6048-59.

Robson, S.A., Michie, K.A., Mackay, J.P., Harry, E., King, G.F. 2002. The *Bacillus subtilis* cell division proteins FtsL and DivIC are intrinsically unstable and do not interact with one another in the absence of other septasomal components. Molecular Microbiology 44(3) 663-674.

Rowland, S.L., **Katis, V.L**., **Partridge, S.R**., **Wake, R.G**. 1997. DivIB, FtsZ and cell division in *Bacillus subtilis*. Mol Microbiol. 23(2):295-302.

Rudner, D.Z., **Fawcett, P**., **Losick, R**. 1999. A family of membrane-embedded metalloproteases involved in regulated proteolysis of membrane-associated transcription factors. Proc Natl Acad Sci U S A. 21;96(26):14765-70.

Sakai, J., **Rawson, R.B**., **Espenshade, P.J**., **Cheng, D**., **Seegmiller, A.C**., **Goldstein, J.L**., **Brown, M.S**. 1998. Molecular identification of the sterol-regulated luminal protease that cleaves SREBPs and controls lipid composition of animal cells. Mol Cell. 2(4):505-14.

Schöbel, S., Zellmeier, S., Schumann, W., Wiegert, T. 2004. The *Bacillus subtilis* σ^{W} anti-sigma factor RsiW is degraded by intramembrane prtoteolysis through YluC. Molecular Microbiology. 52(4)1091-1105.

Sievers J. and Errington J. 2000. The *Bacillus subtilis* cell division protein FtsL localizes to sites of septation and interacts with DivIC. Molecular Microbiology 36(4) 846-855.

Sievers, J., **Errington, J**. 2000. Analysis of the essential cell division gene ftsL of Bacillus subtilis by mutagenesis and heterologous complementation. J Bacteriol. 182(19):5572-9.

Strisovsky, K., **Sharpe, H.J**., **Freeman, M**. 2009. Sequence-specific intramembrane proteolysis: identification of a recognition motif in rhomboid substrates. Mol Cell. 25;36(6):1048-59.

Tatsuta, T., **Augustin, S**., **Nolden, M**., **Friedrichs, B**., **Langer, T**. 2007. m-AAA protease-driven membrane dislocation allows intramembrane cleavage by rhomboid in mitochondria. EMBO J. 24;26(2):325-35.

Too, H.P., **Hanley, M.R**. 1988. Solubilization and characterization of substance P-binding sites from chick brain membranes. Biochem J. 1;252(2):545-51.

Urban, S., **Lee, J.R**., **Freeman, M**. 2001. Drosophila rhomboid-1 defines a family of putative intramembrane serine proteases. Cell. 19;107(2):173-82.

Urban, S., **Schlieper, D**., **Freeman, M**. 2002. Conservation of intramembrane proteolytic activity and substrate specificity in prokaryotic and eukaryotic rhomboids. Curr Biol. 3;12(17):1507-12.

Urban, S., **Freeman, M**. 2003. Substrate specificity of rhomboid intramembrane proteases is governed by helix-breaking residues in the substrate transmembrane domain. Mol Cell. 11(6):1425-34.

van Baarle, S., Bramkamp, M. 2010. The MinCDJ system in *Bacillus subtilis* prevents minicell formation by promoting divisome disassembly. PLoS One. 24;5(3):e9850.

van den Ent, F., **Vinkenvleugel, T.M**., **Ind, A**., **West, P**., **Veprintsev, D**., **Nanninga, N**., **den Blaauwen, T**., **Löwe, J**. 2008 Structural and mutational analysis of the cell division protein FtsQ. Mol Microbiol. 68(1):110-23.

Weihofen, A., **Binns, K**., **Lemberg, M.K**., **Ashman, K**., **Martoglio, B**. 2002. Identification of signal peptide peptidase, a presenilin-type aspartic protease. Science. 21;296(5576):2215-8.

Wolfe, M.S., **Xia, W**., **Ostaszewski, B.L**., **Diehl, T.S**., **Kimberly, W.T**., **Selkoe, D.J**. 1999. Two transmembrane aspartates in presenilin-1 required for presenilin endoproteolysis and gamma-secretase activity. Nature. 8;398(6727):513-7.

Wolfe, M.S., **Kopan, R**. 2004. Intramembrane proteolysis: theme and variations. Science. 20;305(5687):1119-23.

Zelenski, N.G., **Rawson, R.B**., **Brown, M.S**., **Goldstein, J.L**. 1999. Membrane topology of S2P, a protein required for intramembranous cleavage of sterol regulatory element-binding proteins. J Biol Chem. 30;274(31):21973-80.

Zellmeier, S., **Schumann, W**., **Wiegert, T**. 2006. Involvement of Clp protease activity in modulating the *Bacillus subtilis* sigmaw stress response. Mol Microbiol. 61(6):1569-82.

Zhou, R., **Cusumano, C**., **Sui, D**., **Garavito, R.M**., **Kroos, L**. 2009. Intramembrane proteolytic cleavage of a membrane-tethered transcription factor by a metalloprotease depends on ATP. Proc Natl Acad Sci U S A. 22;106(38):16174-9.

6 Acknowledgements

I would like to acknowledge the following people:

Prof. Dr. Reinhard Krämer for giving me the opportunity to work in his lab and for his scientific input.

Prof. Dr. Ulrich Baumann for taking the time to be my second referee.

Dr. Jan Löwe for the plasmids and the protocols for MBP-FtsL and RasP purification.

Dr. Marc Bramkamp was the best group leader I could have asked for. The fun and inspirational atmosphere in the cell division lab is simply due to you being the perfect boss. Thanks for all the help, patience and fantastic discussions. I've learned so much about being a scientist from you. I've also learned to be sceptical next time when I hear the phrase "pioneer spirit".

Juri Bach, Joana Mehlmann and Katja Nagler all did their Bacherlor thesis on projects related to mine. Thank you for your hard work and input. I had lots of fun being your supervisor. In theory I should include Frank Bürmann here as well for doing a lab internship on RasP. But hey, we all know I learned more from you then you could have learned from me. Thanks Franky!

My fellow lab members of the cell division group. I would have been lost without you guys. Thank you for all your help and for keeping up with me. Especially when I cursed about the enzyme collection or was the sink police again. Thanks for music, jokes and some really good years. A special shoutout to my "desk mates" Cat and Betty. They kept me sane.

Anja Wittmann and Gabi Sitek for their constant support. What would we do without you?

The complete Krämer lab group for a good working atmosphere, lots of help and lots of fun. I especially have to mention Markus Becker, Sascha Nicklisch and Gerd Seibold here. They were my go-to people for protein biochemistry questions.

Last but certainly not least I have to thank my family. I never ever would have made it without their love and understanding. Mama und Papa, danke für Eure Unterstützung und Euren unerschütterlichen Glauben an mich. Hartmut, danke für all die leckeren Sonntagsdinner und dafür, dass ich jederzeit bei Euch einfallen darf. Maria, Du bist meine Person! Ru, I cannot thank you enough for being there.

7 Addendum

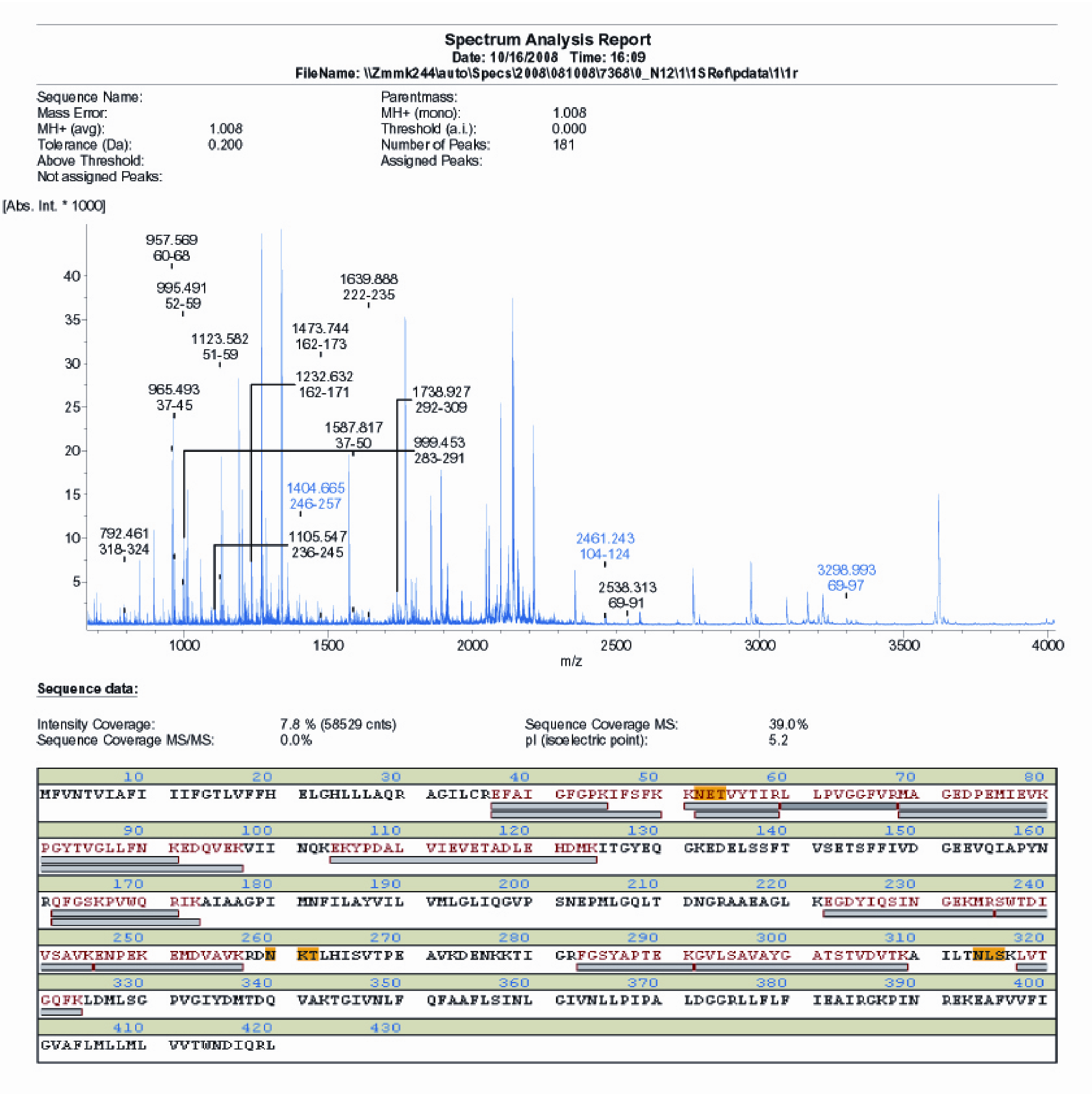

Spectrum Analysis Report
Date: 10/16/2008 Time: 16:09
FileName: \\Zmmk244\auto\Specs\2008\081008\7368\0_N12\1\1SRef\pdata\1\1r

Sequence Name:		Parentmass:	
Mass Error:		MH+ (mono):	1.008
MH+ (avg):	1.008	Threshold (a.i.):	0.000
Tolerance (Da):	0.200	Number of Peaks:	181
Above Threshold:		Assigned Peaks:	
Not assigned Peaks:			

Sequence data:

Intensity Coverage:	7.8 % (58529 cnts)	Sequence Coverage MS:	39.0%
Sequence Coverage MS/MS:	0.0%	pI (isoelectric point):	5.2

10	20	30	40	50	60	70	80
MFVNTVIAFI	IIFGTLVFFH	ELGHLLLAQR	AGILCREFAI	GFGPKIFSFK	KNETVYTIRL	LPVGGFVRMA	GEDPEMIEVK
90	100	110	120	130	140	150	160
PGYTVGLLFN	KEDQVEKVII	NQKEKYPDAL	VIEVETADLE	HDMKITGYEQ	GKEDELSSFT	VSETSFFIVD	GEEVQIAPYN
170	180	190	200	210	220	230	240
RQFGSKPVWQ	RIKAIAAGPI	MNFILAYVIL	VMLGLIQGVP	SNEPMLGQLT	DNGRAAEAGL	KEGDYIQSIN	GEKMRSWTDI
250	260	270	280	290	300	310	320
VSAVKENPEK	EMDVAVKRDN	KTLHISVTPE	AVKDENKKTI	GRFGSYAPTE	KGVLSAVAYG	ATSTVDVTKA	ILTNLSKLVT
330	340	350	360	370	380	390	400
GQFKLDMLSG	PVGIYDMTDQ	VAKTGIVNLF	QFAAFLSINL	GIVNLLPIPA	LDGGRLLFLF	IEAIRGKPIN	REKEAFVVFI
410	420	430					
GVAFLMLLML	VVTWNDIQRL						

Figure S1: Peptide mass fingerprint analysis of the 45 kDa band after in vitro proteolysis of MBP-FtsL$^{\Delta CT}$ by RasP. Shown is the sequence coverage when compared to RasP of *Bacillus subtilis*. RasP seems to be co-migrating with the 45 kDa degradation product.

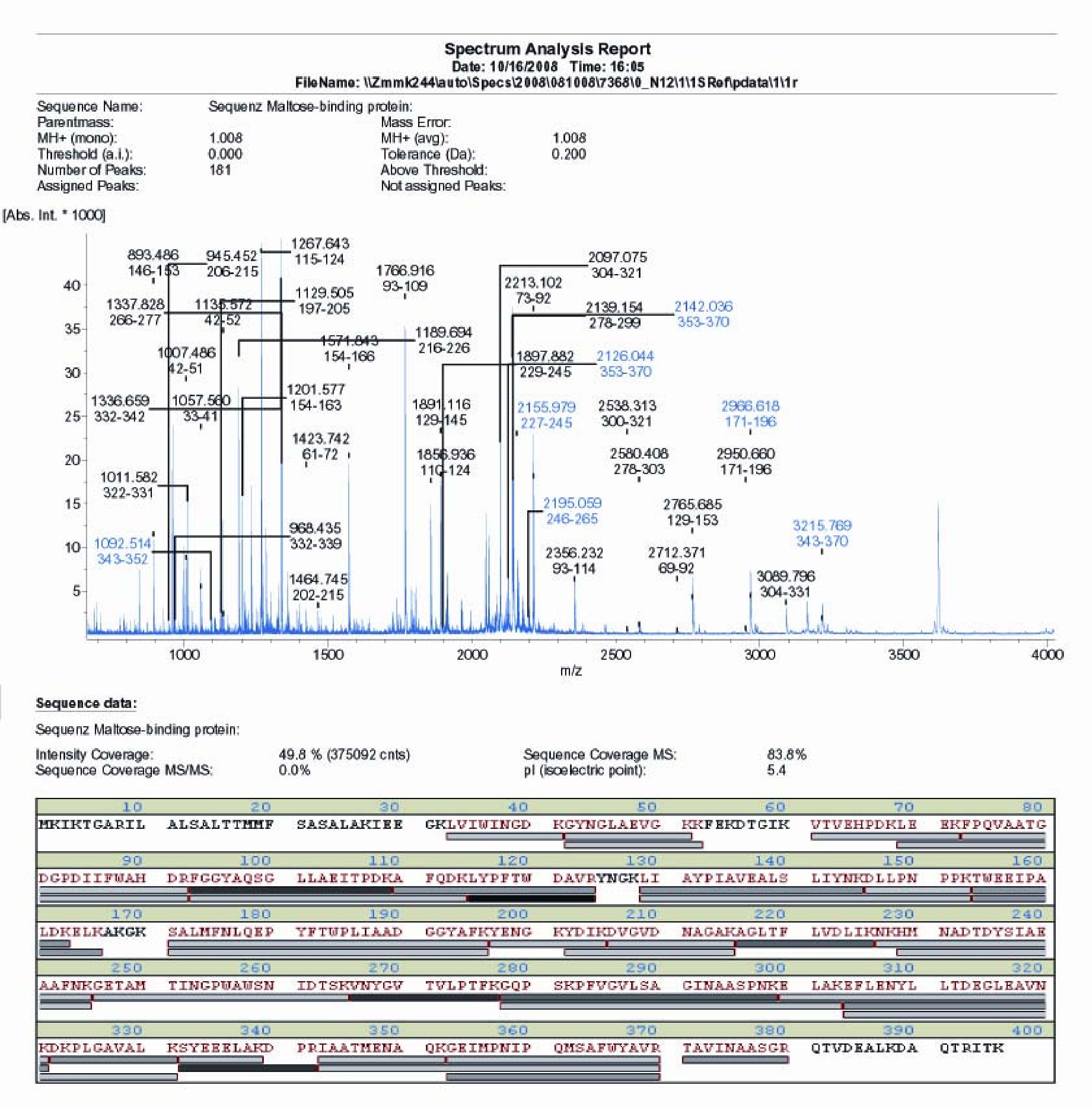

Spectrum Analysis Report

Date: 10/16/2008 Time: 16:05

FileName: \\Zmmk244\auto\Specs\2008\081008\7368\0_N12\1\1SRef\pdata\1\1r

Sequence Name:	Sequenz Maltose-binding protein:		
Parentmass:		Mass Error:	
MH+ (mono):	1.008	MH+ (avg):	1.008
Threshold (a.i.):	0.000	Tolerance (Da):	0.200
Number of Peaks:	181	Above Threshold:	
Assigned Peaks:		Not assigned Peaks:	

Sequence data:

Sequenz Maltose-binding protein:

Intensity Coverage:	49.8 % (375092 cnts)	Sequence Coverage MS:	83.8%
Sequence Coverage MS/MS:	0.0%	pI (isoelectric point):	5.4

10	20	30	40	50	60	70	80
MKIKTGARIL	ALSALTTMMF	SASALAKIEE	GKLVIWINGD	KGYNGLAEVG	KKFEKDTGIK	VTVEHPDKLE	EKFPQVAATG
90	**100**	**110**	**120**	**130**	**140**	**150**	**160**
DGPDIIFWAH	DRFGGYAQSG	LLAEITPDKA	FQDKLYPFTW	DAVRYNGKLI	AYPIAVEALS	LIYNKDLLPN	PPKTWEEIPA
170	**180**	**190**	**200**	**210**	**220**	**230**	**240**
LDKELKAKGK	SALMFNLQEP	YFTWPLIAAD	GGYAFKYENG	KYDIKDVGVD	NAGAKAGLTF	LVDLIKNKHM	NADTDYSIAE
250	**260**	**270**	**280**	**290**	**300**	**310**	**320**
AAFNKGETAM	TINGPWAWSN	IDTSKVNYGV	TVLPTFKGQP	SKPFVGVLSA	GINAASPNKE	LAKEFLENYL	LTDEGLEAVN
330	**340**	**350**	**360**	**370**	**380**	**390**	**400**
KDKPLGAVAL	KSYEEELAKD	PRIAATMENA	QKGEIMPNIP	QMSAFWYAVR	TAVINAASGR	QTVDEALKDA	QTRITK

Figure S2: Peptide mass fingerprint analysis of the 45 kDa band after in vitro proteolysis of MBP-FtsL$^{\Delta CT}$ by RasP. Shown is the sequence coverage when compared to maltose binding protein. MBP was detected in the 45 kDa band, but no Ftsl fragments were detectable.

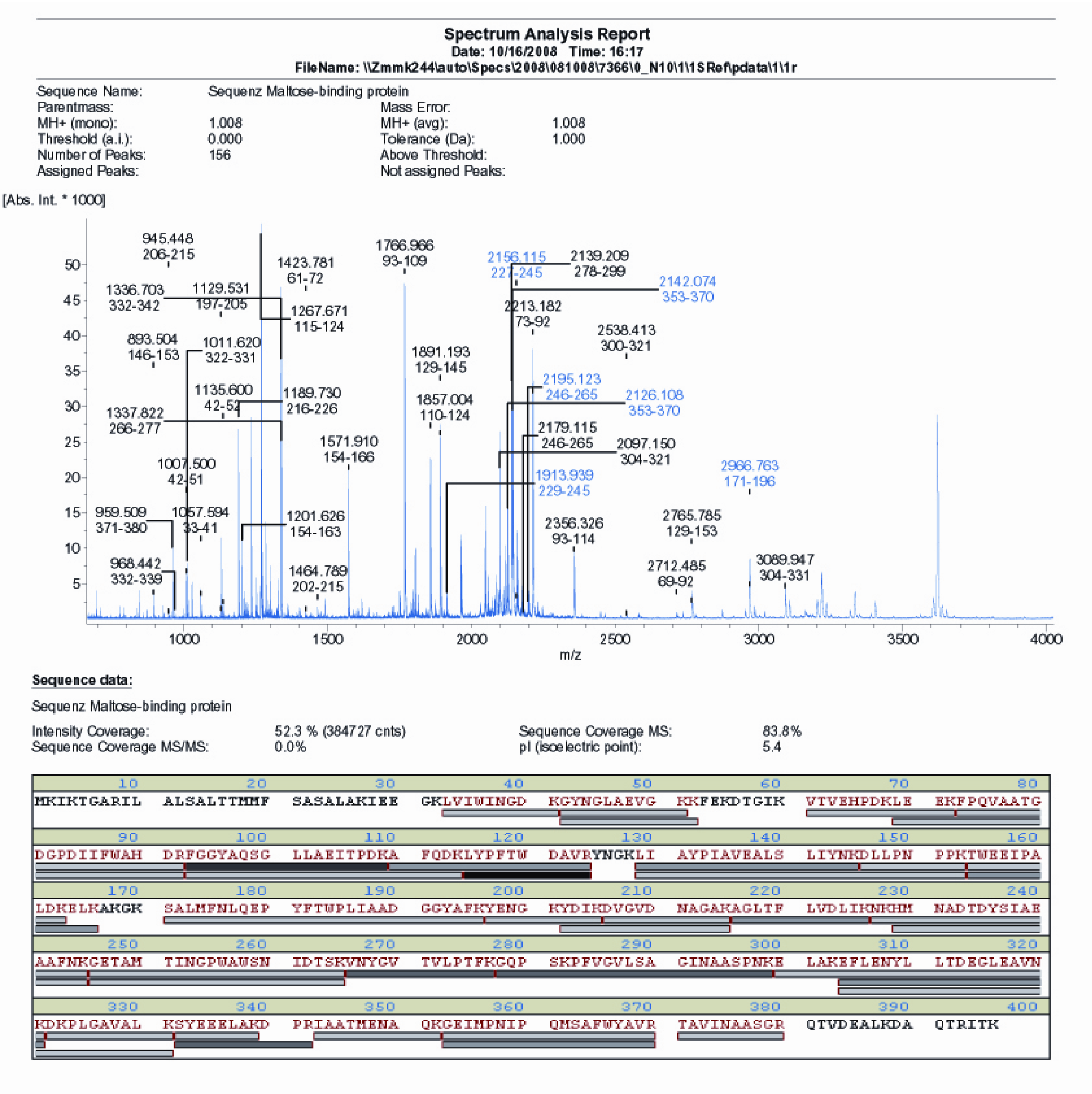

Spectrum Analysis Report

Date: 10/16/2008 Time: 16:17

FileName: \\Zmmk244\auto\Specs\2008\081008\7366\0_N10\1\1SRef\pdata\1\1r

Sequence Name:	Sequenz Maltose-binding protein		
Parentmass:		Mass Error:	
MH+ (mono):	1.008	MH+ (avg):	1.008
Threshold (a.i.):	0.000	Tolerance (Da):	1.000
Number of Peaks:	156	Above Threshold:	
Assigned Peaks:		Not assigned Peaks:	

[Abs. Int. * 1000]
50
45
40
35
30
25
20
15
10
5
945.448
206-215
1336.703
332-342
1129.531
197-205
893.504
146-153
1011.620
322-331
1135.600
42-52
1337.822
266-277
1007.500
42-51
959.509
371-380
1057.594
33-41
968.442
332-339
1423.781
61-72
1267.671
115-124
1189.730
216-226
1201.626
154-163
1464.789
202-215
1571.910
154-166
1766.966
93-109
1891.193
129-145
1857.004
110-124
2156.115
221-245
2139.209
278-299
2142.074
353-370
2213.182
73-92
2538.413
300-321
2195.123
246-265
2126.108
353-370
2179.115
246-265
2097.150
304-321
1913.939
229-245
2356.326
93-114
2966.763
171-196
2765.785
129-153
2712.485
69-92
3089.947
304-331
1000
1500
2000
2500
3000
3500
4000
m/z

Sequence data:

Sequenz Maltose-binding protein

Intensity Coverage:	52.3 % (384727 cnts)	Sequence Coverage MS:	83.8%
Sequence Coverage MS/MS:	0.0%	pI (isoelectric point):	5.4

10	20	30	40	50	60	70	80
MKIKTGARIL	ALSALTTMMF	SASALAKIEE	GKLVIWINGD	KGYNGLAEVG	KKFEKDTGIK	VTVEHPDKLE	EKFPQVAATG
90	100	110	120	130	140	150	160
DGPDIIFWAH	DRFGGYAQSG	LLAEITPDKA	FQDKLYPFTW	DAVRYNGKLI	AYPIAVEALS	LIYNKDLLPN	PPKTWEEIPA
170	180	190	200	210	220	230	240
LDKELKAKGK	SALMFNLQEP	YFTWPLIAAD	GGYAFKYENG	KYDIKDVGVD	NAGAKAGLTF	LVDLIKNKHM	NADTDYSIAE
250	260	270	280	290	300	310	320
AAFNKGETAM	TINGPWAWSN	IDTSKVNYGV	TVLPTFKGQP	SKPFVGVLSA	GINAASPNKE	LAKEFLENYL	LTDEGLEAVN
330	340	350	360	370	380	390	400
KDKPLGAVAL	KSYEEELAKD	PRIAATMENA	QKGEIMPNIP	QMSAFWYAVR	TAVINAASGR	QTVDEALKDA	QTRITK

Figure S3: Peptide mass fingerprint analysis of the 42 kDa band after in vitro proteolysis of MBP-FtsL$^{\Delta CT}$ by RasP. Shown is the sequence coverage when compared to maltose binding protein. MBP was detected in the 42 kDa band, but no Ftsl fragments were detectable.

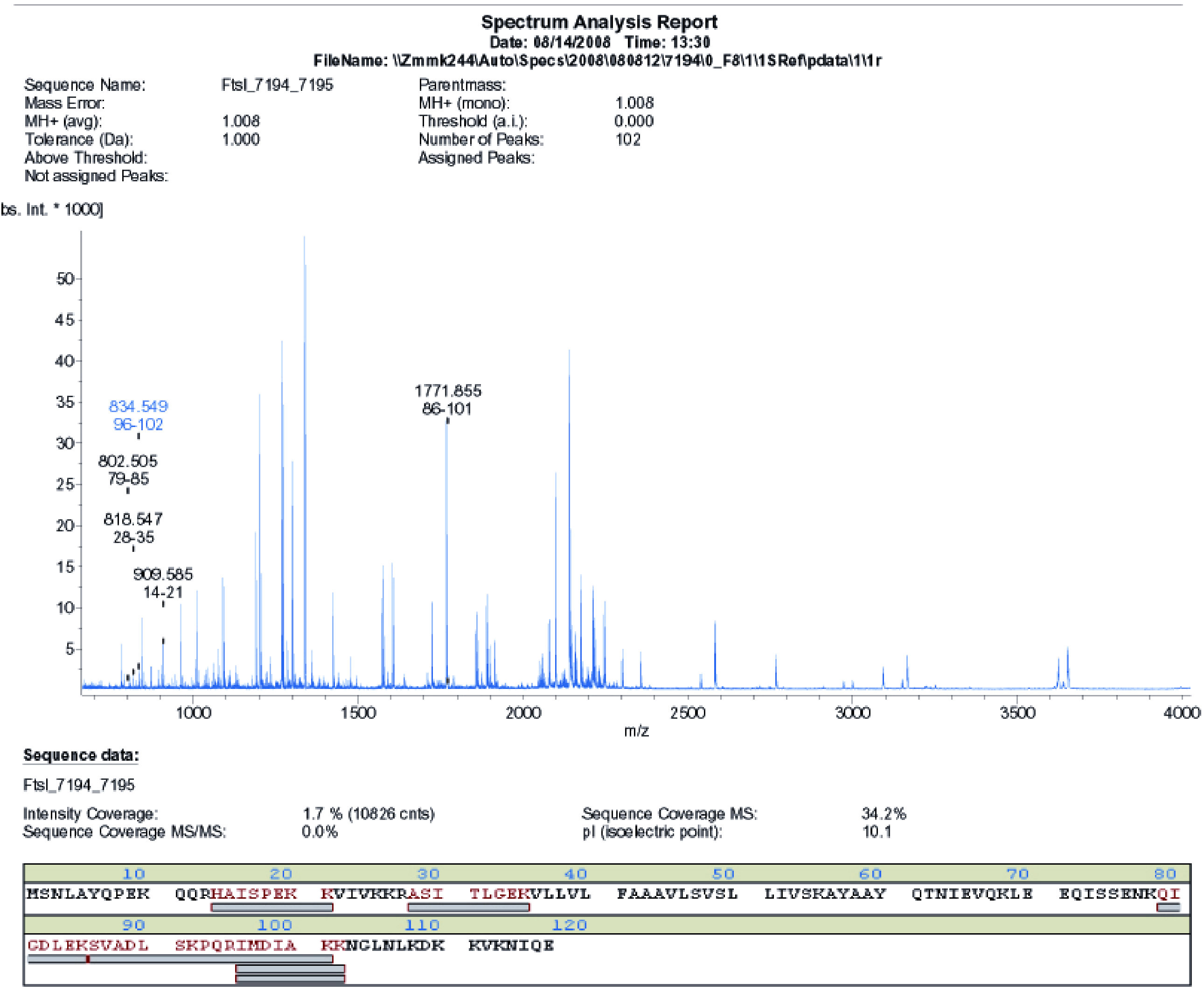

Spectrum Analysis Report
Date: 08/14/2008 Time: 13:30
FileName: \\Zmmk244\Auto\Specs\2008\080812\7194\0_F8\1\1SRef\pdata\1\1r

Sequence Name:	Ftsl_7194_7195	Parentmass:	
Mass Error:		MH+ (mono):	1.008
MH+ (avg):	1.008	Threshold (a.i.):	0.000
Tolerance (Da):	1.000	Number of Peaks:	102
Above Threshold:		Assigned Peaks:	
Not assigned Peaks:			

Sequence data:

Ftsl_7194_7195

Intensity Coverage:	1.7 % (10826 cnts)	Sequence Coverage MS:	34.2%
Sequence Coverage MS/MS:	0.0%	pI (isoelectric point):	10.1

10	20	30	40	50	60	70	80
MSNLAYQPEK	QQRHAISPEK	KVIVKKRASI	TLGEKVLLVL	FAAAVLSVSL	LIVSKAYAAY	QTNIEVQKLE	EQISSENKQI
90	100	110	120				
GDLEKSVADL	SKPQRIMDIA	KKNGLNLKDK	KVKNIQE				

Figure S4: Peptide mass fingerprint analysis of the 14 kDa band after in vitro proteolysis of MBP-FtsL$^{\Delta CT}$ by RasP. Shown is the sequence coverage when compared to FtsL of *Bacillus subtilis*. The 14 kDa band seems to consist of FtsL$^{\Delta CT}$.

8 Affirmation

Hereby, I declare to have prepared the present dissertation autonomously without illegitimated assistance. No other supplemental material or references have been used than those, which are annotated.

Köln, August 2010

(Inga Wadenpohl)

9 Curricilum Vitae

Name: Wadenpohl
Vorname: Inga
Adresse: Opladner Straße 126, 40764 Langenfeld
Geburtsdatum: 12.12.1979
Geburtsort: Leverkusen

Schullaufbahn

1986-1990	Don Bosco Grundschule Langenfeld
1990-1999	Werner Heisenberg Gymnasium Leverkusen

Hochschullaufbahn

1999-2002	Universität Köln (Abschluss: Vordimplom)
2002-2006	Albert Ludwigs Universität Freiburg (Abschluss: Diplom)
ab 2007	Universität Köln (Promotionsstudium)